PETTERI PARKKILA

BIOINTERACTION ASSESSMENTS OF LIPID MEMBRANES IN RELATION TO DRUG ACTION
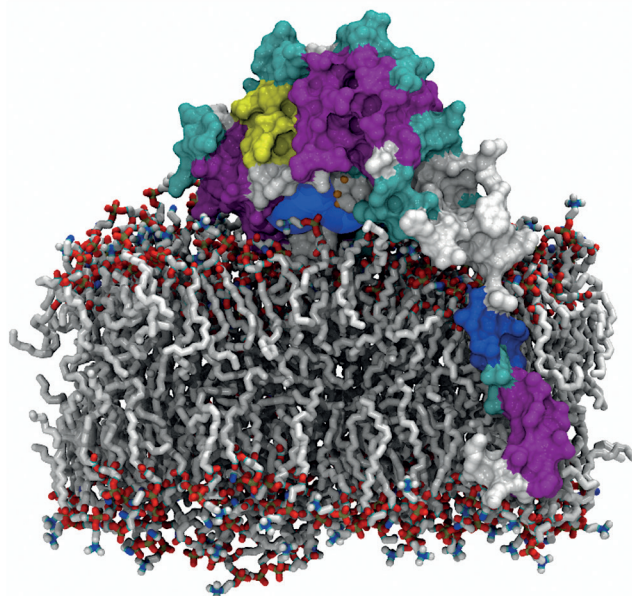
DRUG RESEARCH PROGRAM
DIVISION OF PHARMACEUTICAL BIOSCIENCES
FACULTY OF PHARMACY
DOCTORAL PROGRAMME IN MATERIALS RESEARCH AND NANOSCIENCES
UNIVERSITY OF HELSINKI

Drug Research Program
Division of Pharmaceutical Biosciences
Faculty of Pharmacy
University of Helsinki
Finland

Doctoral Programme in Materials Research
and Nanosciences (MATRENA)

BIOINTERACTION ASSESSMENTS OF LIPID MEMBRANES IN RELATION TO DRUG ACTION

Petteri Parkkila

ACADEMIC DISSERTATION

Doctoral thesis, to be presented for public examination with the permission of the Faculty of Pharmacy of the University of Helsinki, in lecture hall 110, Forest Sciences Building, on the 14th of October, 2020 at 13 o'clock.

Helsinki, 2020

Supervisors: Dr. Tapani Viitala
                      Division of Pharmaceutical Chemistry and Technology
                      Faculty of Pharmacy
                      University of Helsinki
                      Finland

                      Dr. Alex Bunker
                      Division of Pharmaceutical Biosciences
                      Faculty of Pharmacy
                      University of Helsinki
                      Finland

Pre-examiners: Prof. Lukasz Cwiklik
                      J. Heyrovský Institute of Physical Chemistry
                      Czech Academy of Sciences
                      Czech Republic

                      Prof. Lasse Murtomäki
                      Department of Chemistry and Materials Science
                      School of Chemical Engineering
                      Aalto University
                      Finland

Opponent: Prof. Fredrik Höök
                      Department of Physics
                      Chalmers University of Technology
                      Sweden

Custos: Prof. Marjo Yliperttula
                      Division of Pharmaceutical Biosciences
                      Faculty of Pharmacy
                      University of Helsinki
                      Finland

ABSTRACT

Lipids self-assemble into lipid bilayers, which divide bodily tissues into cells and into functionally specified compartments. Imbalances in the lipid composition and metabolism take part in severe neurodegenerative diseases such as Alzheimer's and Parkinson's disease. These conditions are currently only symptomatically treated, and the functional insight into the effects of the drugs in different stages of the conditions is lacking. In the field of pharmacy, the current drug design protocols rely on the separate evaluation of the binding affinity between target protein and drug and the extent of lipid bilayer permeation, which dictates how likely the drug is to reach its target. For example, the direct treatment of the central nervous system requires the drug to cross the blood-brain barrier. Most of the drug target proteins are, however, permanently attached to the lipid membranes. This thesis hypothesizes that lipids and proteins can act together in relation to drug action, which chemical variations in the membrane constituents can profoundly affect.

Oxidative stress induces peroxidation of unsaturated fatty acids, modulating the membrane properties, such as the permeability to water. It is of importance to understand how lipid peroxidation influences the extent of segregation of the domains in the lipid membrane. Although the functionality of the domains *in vivo* is elusive, they may be associated with a myriad of cellular functions, such as the attachment of the actin cytoskeleton. By measuring lateral diffusion of lipids in Langmuir monolayers, we showed that the presence of oxidized lipids could irreversibly modulate the miscibility of the segregated microscale domains. This may affect the action of proteins, drugs and other molecules that interact with such structures.

Since biological membranes are incredibly complex, consisting of thousands of molecules, they are challenging to study. Therefore, model lipid membranes are used in membrane research. In this thesis, these model systems were characterized using label-free surface-sensitive analytical techniques. Using the membrane models, we showed that the membrane-bound catechol-*O*-methyltransferase (COMT) is able to function at the membrane-water interface, suggesting that the membrane partitioning and orientation of its substrates and inhibitors influences the drug efficacy. Inhibition of membrane-bound COMT is desirable in Parkinson's disease since it elevates dopamine levels in the brain. Also, the inhibition prevents the methylation of levodopa, a dopamine precursor that is currently the primary therapeutic agent. Therefore, we studied the partitioning of dopamine and different catechol compounds to model lipid membranes. Partitioning to the membranes, where the existence of nanoscale domains is proposed, was limited. The partitioning also seemed to be modulated by the charge, lipophilicity and hydrogen-bonding capacity of the compounds and surface charge of the membrane. These factors also affect the orientation of the compounds in the lipid membrane, which can define the probability of the

to-be-catalyzed moieties to reach the catalytic site of the protein. To conclude, the results of this thesis demonstrate that the lipid environment can modulate drug action, which may have consequences for the design of novel therapeutics for neuropathological conditions.

ACKNOWLEDGEMENTS

From individuals who have influenced my career profoundly, first, I must thank the late Prof. Paavo Kinnunen. Without the opportunity to work in his lab, starting way back during my second year at Aalto University, I would probably not be writing this text now. A Bachelor student coming to the lab would immediately become integrated into the scientific culture in the form of attending discussions in meetings and conferences. This is what truly motivated me as a young scientist, and perhaps in some different environments, that motivation would have died right from the start. Specifically, I want to thank Drs. Vladimir Zamotin and Roberto Tejera-Garcia for their supervision during that time and Chris, Ajay, Sanjeev, Riku, Tuuli and Sakari for fantastic banter in and out of the lab. For their hospitality during my visit to Prague, I thank my co-authors Prof. Martin Hof, Dr. Martin Štefl and Dr. Agnieszka Olżyńska. Their in-depth knowledge of lipid biophysics and fluorescence methodologies made an impact on me and inspired me to learn more.

I thank my supervisors Dr. Tapani Viitala and Dr. Alex Bunker, for their guidance and trust for an unknown engineer who wanted desperately to do a PhD. Dr. Viitala's immense knowledge and support during up and down moments of the research have been invaluable. The help from Dr. Bunker with manuscript writing and his insight into the physics of lipid membranes has helped tremendously in carrying out the thesis work. Custos, Prof. Marjo Yliperttula helped profoundly in guiding the last stages of the thesis project. Prof. Fredrik Höök is thanked for serving as my opponent, and Profs. Lukasz Cwiklik and Lasse Murtomäki are thanked for the pre-examination. For all the help and exciting collaborations, I specifically thank Dr. Artturi Koivuniemi, M.Sc. Jaakko Itkonen, M.Sc. Otto Kari, Dr. Tatu Lajunen, Dr. Aniket

CONTENTS

LIST OF ORIGINAL PUBLICATIONS

This thesis is based on the following publications:

I **Parkkila, P.***, Štefl, M.*, Olżyńska, A., Hof, M. & Kinnunen, K. J. Phospholipid lateral diffusion in phosphatidylcholine-sphingomyelin-cholesterol monolayers; Effects of oxidatively truncated phosphatidylcholines. Biochimica et Biophysica Acta (BBA) - Biomembranes, 2015. 1848(1): 167–173.
(*equal contribution to this work)

II **Parkkila, P.**, Elderdfi, M., Bunker, A. & Viitala, T. Biophysical Characterization of Supported Lipid Bilayers Using Parallel Dual-Wavelength Surface Plasmon Resonance and Quartz Crystal Microbalance Measurements. Langmuir, 2018. 34(27): 8081–8091.

III Magarkar, A., **Parkkila, P.**, Viitala, T., Lajunen, T., Mobarak, E., Licari, G., Cramariuc, O., Vauthey, E., Róg, T. & Bunker, A. Membrane bound COMT isoform is an interfacial enzyme: General mechanism and new drug design paradigm. Chemical Communications, 2018. 54(28): 3440–3443.

IV **Parkkila, P.**, & Viitala, T. Partitioning of Catechol Derivatives in Lipid Membranes: Implications for Substrate Specificity to Catechol-*O*-methyltransferase. ACS Chemical Neuroscience, 2020. 11(6): 969–978

The publications are referred to in the text by their **Roman numerals**.

AUTHOR'S CONTRIBUTIONS

Publication I:
The author contributed to the study design and performed the experiments together with M.Sc. (later Dr.) Martin Štefl and Dr. Agnieszka Olżyńska. The author wrote the first draft of the manuscript and revised it together with the co-authors.

Publication II:
The author designed the study with the co-authors. The author performed the experiments and data analysis. The author wrote the first draft of the manuscript and revised it based on the comments of the co-authors. The author served as a corresponding author.

Publication III:
The author performed the surface plasmon resonance experiments and assisted Dr. Tatu Lajunen with the isothermal titration calorimetry experiments. The author wrote and revised the experimental part of the manuscript, together with the co-authors.

Publication IV:
The author designed the study with Dr. Tapani Viitala. The author performed the experiments and data analysis. The author wrote the first draft of the manuscript and revised it based on the comments of the co-author. The author served as a corresponding author.

ABBREVIATIONS

AD	Alzheimer's disease
$\beta_2 AR$	β_2 adrenoreceptor
3-MT	3-methoxytyramine
AdoMet	*S*-adenosyl-L-methonine
BBB	blood-brain barrier
CNS	central nervous system
Chol	cholesterol
COMT	catechol-*O*-methyltransferase
Cryo-EM	cryogenic electron microscopy
DAG	diacylglycerol
DOPC	1,2-dioleoyl-*sn*-glycero-3-phosphocholine
DOPE	1,2-dioleoyl-*sn*-glycero-3-phosphoethanolamine
DOPS	1,2-dioleoyl-*sn*-glycero-3-phospho-L-serine
DPPC	1,2-dipalmitoyl-*sn*-glycero3-phosphocholine
DSC	differential scanning calorimetry
ER	endoplasmic reticulum
EV	extracellular vesicle
FCS	fluorescence correlation spectroscopy
FRAP	fluorescence recovery after photobleaching
FRET	fluorescence resonance energy transfer
GPI	glycophosphatidylinositol
GPCR	G-protein coupled receptor
GPMV	giant plasma membrane vesicles
GUV	giant unilamellar vesicle
IMP	integral membrane protein
ITC	isothermal titration calorimetry
L_α	liquid crystalline phase
L_β	gel phase
L_d	liquid-disordered phase
L_o	liquid-ordered phase
LUV	large unilamellar vesicle
MB-COMT	membrane-bound catechol-*O*-methyltransferase
MD	molecular dynamics simulations
MP-SPR	multi-parametric surface plasmon resonance
MUFA	monounsaturated fatty acid
OxPL	oxidized phospholipids
PA	phosphatidic acid
PazePC	1-palmitoyl-2-azelaoyl-*sn*-glycero-3-phosphocholine
PI	phosphatidylinositol
PD	Parkinson's disease
POPC	1-palmitoyl-2-oleoyl-*sn*-glycero-3-phosphocholine
PoxnoPC	1-palmitoyl-2-(9'-oxononanoyl)-*sn*-glycero-3-phosphocholine
PUFA	polyunsaturated fatty acid
QCM	quartz crystal microbalance
QCM-Z	impedance-based quartz crystal microbalance

ROS	reactive oxygen species
S-COMT	soluble catechol-*O*-methyltransferase
SEM	scanning electron microscopy
SiO$_2$	silicon dioxide
SLB	supported lipid bilayer
SM	sphingomyelin
SPB	supported phospholipid bilayer
SPR	surface plasmon resonance
STED	stimulated emission depletion microscopy
SUV	small unilamellar vesicle
SVL	supported vesicular layer
TAG	triacylglycerol
TEM	transmission electron microscopy
TIR	total internal reflection
TIRF	total internal reflection fluorescence
TMD	transmembrane domain
WFM	wide-field microscopy

1 INTRODUCTION

The lipid membranes of the mammalian cells are immensely complex structures consisting of over a thousand different lipid species (van Meer, 2005). Changes in the lipid composition and metabolism, or alterations in the chemical structures of lipids, have connections to severe neuropathological conditions such as Alzheimer's disease (AD) (Lane & Farlow, 2005; Volinsky & Kinnunen, 2013), Parkinson's disease (PD) (Dexter et al., 1989; Fabelo et al., 2011) and lipidosis-induced dystrophies (Powers et al., 1987). The inability of cells to repair these impairments implicates disruption in the lipid homeostasis, which is under delicate regulation by the cellular machinery (Grimm et al., 2007; Vance & Vance, 2009). The current view is that the organization of lipids varies across vast spatiotemporal scales, contributing to the essential cellular functions through protein-protein and lipid-protein interactions (Jacobson et al., 2007; Kinnunen, 1991; Levental et al., 2020; Nicolson, 2014; Simons & Ikonen, 1997).

During the past few decades, biophysical and biochemical studies of lipid membranes have become intertwined with the efforts in medical sciences. Notably, diseases of the central nervous system (CNS), mostly present in the aging populations, have driven scientists to look for molecular-level hallmarks specific for individual pathologies. For example, increasing evidence exists that α-synuclein aggregation in PD triggers lipid dyshomeostasis affecting lipid-related neuronal functions such as synaptic vesicle trafficking (Fanning et al., 2020). Or, as suggested by Fanning et al., is the interplay between proteins and lipids bidirectional? The question is crucial for the novel treatment strategies, which have, at the moment, mainly considered PD as a proteinopathy (Fields et al., 2019).

Attempts in pharmaceutical sciences to study drug action concerning the physics of the lipid membranes have been limited. For developing new drugs for the treatment of CNS diseases, there are two main motivations to adopt a more lipid-centric approach. First, for a drug to be effective, it must permeate the blood-brain barrier (BBB) in quantities that result in a therapeutic effect (Pardridge, 2007). Secondly, the drug should reach its desirable target, which often is a receptor or an enzyme embedded in a lipid bilayer. Besides, the drug could need to overcome additional lipid barriers, sometimes via facilitated or active transport by membrane-bound proteins. While both lipophilicity of the drug, or interactions with the lipids, and affinity to the target protein, have both been recognized to contribute to its therapeutic effect (Lipinski et al., 1997; Ma et al., 2014), relationships between the two remain elusive (Peetla et al., 2011; Seddon et al., 2009; Yin & Flynn, 2016). Therefore, the view that drug action is merely a manifestation of separate drug-lipid and drug-protein interactions, i.e. obeying the lock-and-key paradigm of computational drug design (Conrad, 1992), should be revisited. This different viewpoint has implications for the evaluation of the drug-target networks, which currently

focus on the identification of all relevant protein targets for individual drugs, without the focus on the lipid environment of the targets (Cheng et al., 2012; Yıldırım et al., 2007).

This thesis pursues to elucidate the role of lipids and lipid-embedded proteins in the modulation of drug action. First, the existing literature is reviewed, with the focus on what were the crucial subjects and issues that motivated to conduct the research presented in this thesis. Then, the aims of the study are formulated and results discussed considering the current knowledge. Finally, the future endeavors of drug and biomembrane research are discussed. The advancements in structural biophysics, lipidomics, biophotonics and *in silico* methods, should remain as the drivers of the research during the current decade.

2 REVIEW OF THE LITERATURE

2.1 BIOLOGICAL MEMBRANES

Biological membranes (Fig. 2.1), or *biomembranes*, are responsible for cellular *compartmentalization*, which allows specific compartments in the biological environment to perform their essential functions. The fundamental component of the biological membrane is the *lipid bilayer*. The lipid composition of the membranes forming cellular barriers differs drastically from that of subcellular organelles, for example. Logically, evolution has adopted lipids to serve this function since they self-assemble to closed structures due to the minimization of free energy. This review is not in the scope to discuss every intricacy of biological membranes in detail, such as membrane fusion, albeit a significant phenomenon and widely studied in recent years (London, 2015; Petrany & Millay, 2019). The purpose is to give an illustrative insight into the biological complexity of biomembranes, which supports the aims of this thesis. Later in this review, membranes are discussed in the context of how they can be modeled and studied.

2.1.1 LIPIDS

By the general definition, *lipid* "is a loosely defined term for substances of biological origin that are soluble in nonpolar solvents" (McNaught & Wilkinson, 1997). The hydrophobic effect drives the aggregation of lipids in water, i.e. the water has an entropic tendency to minimize its interfacial area. Weak interactions, electrostatic in nature, take part in stabilizing the aggregates. Therefore, lipids can adopt different phase structures based on the physical geometry of the lipids depicted by their chemical structures. The biologically most relevant form of the lipid aggregates is the *lamellar phase*, which in cells manifests as a single lipid bilayer. In the bilayer, nonpolar lipid *acyl chains* of the two leaflets face each other, and the hydrophilic polar *headgroups* are exposed to water.

Lipids provide the structure of the membrane and functional environment for membrane proteins. Also, they participate in signal transduction, cell growth and reproduction and trafficking of substances in vesicles (van Meer et al., 2008). Most lipids include *fatty acids*, carboxyl acids with an aliphatic hydrocarbon chain. Triacylglycerols (TAGs), with three acyl chains, are stored in the fat cells, while most lipids forming cellular membranes are *glycerophospholipids*. Diacylglycerol (DAG), with two hydrocarbon chains attached to glycerol via ester linkages, is connected to phosphate with a headgroup moiety. In practice, however, the entire structure excluding the hydrocarbon chains is referred to as the *lipid headgroup* since the chemical

groups present in the whole moiety dictate its properties such as net charge. Various nomenclatures related to lipids are presented in Fig. 2.1.

Although the localization of the lipids with different headgroups varies between tissues and cellular compartments, some general remarks about their relative abundancies can be made. Phosphatidylcholines (PCs), having a cylindrical shape, are the primary component of all biomembranes. Phosphatidylethanolamines (PEs), largely present in the intracellular membranes, induce negative membrane curvature due to their conical shape, which drives the formation of nonlamellar structures on their own. Similarly to PE, anionic phosphatidylserine (PS) is mostly present in the inner leaflet of the *plasma membrane*, the primary boundary of the cells (Fadok et al., 1998). The relative amount of PE and PS in the outer leaflet of the plasma membrane is kept low by the P4-ATPase enzymes (van Meer et al., 2008). Some minor lipid species include phosphatidylinositol (PI), phosphatidic acid (PA) and cardiolipin, which have their specific functions in their prevailing compartments. Sphingomyelin (SM), with a hydrophobic ceramide backbone, and cholesterol (Chol), are essential to the structure of the outer plasma membrane leaflet and have unique properties in contributing to synaptic
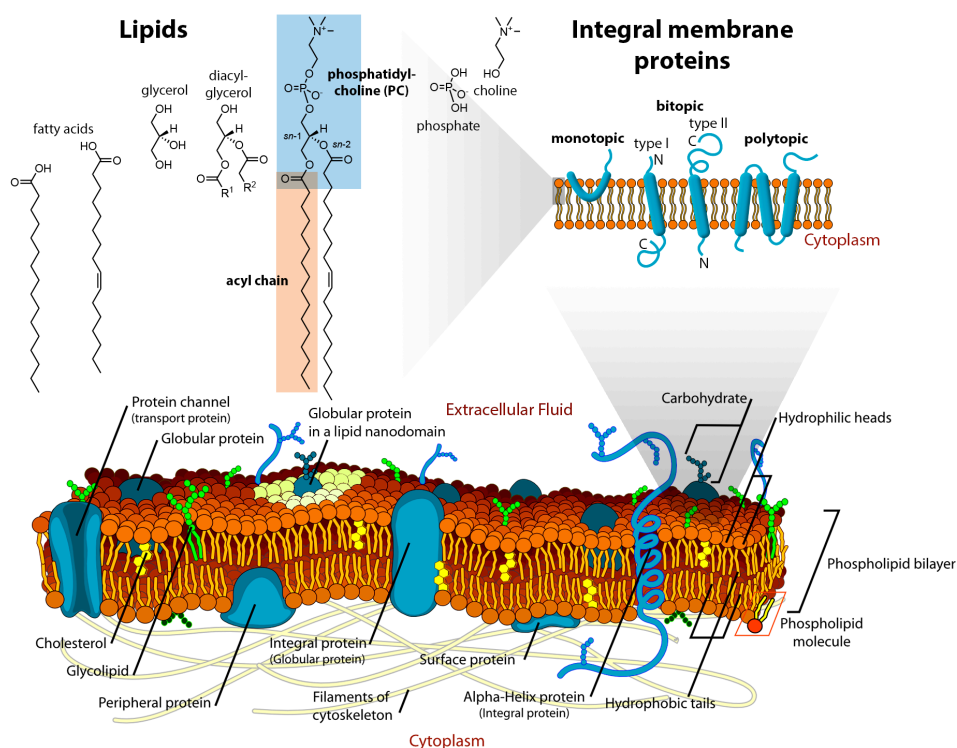
Figure 2.1 Simplified depiction of a biological membrane and its components. Adapted with permission from https://pixabay.com/vectors/biology-cell-diagram-science-41522/ (by Clker-Free-Vector-Images from Pixabay, accessed 4.6.2020)

function (Hussain et al., 2019). They may also modulate lateral order in the plasma membranes (Simons & Ikonen, 1997).

Unsaturation, i.e. the presence of double bonds in the lipid acyl chains, is the main contributor to increased membrane fluidity and decreased bending rigidity (Rawicz et al., 2000), due to the double-bond-enabled chain flexibility. Acyl chain length and the degree of unsaturation are closely related to the lamellar gel-liquid crystalline (L_β-L_α) transition temperature (T_m). For a phase mixing to happen, the entropy of mixing has to overcome the favorable interactions between the lipid components at a critical set of thermodynamic variables. These phase boundaries with changing lipid composition are presented in phase diagrams. The liquid crystalline phase is the most relevant at physiological temperatures of mammals. Most membrane lipids are composed of monounsaturated fatty acids (MUFAs) with a single double-bond in one or both of the acyl chains of the glycerol backbone. Polyunsaturated fatty acids (PUFAs) are mostly present in the lipid membranes of brain tissues and are prone to lipid peroxidation (Dexter et al., 1989; Liu et al., 2015). Since PUFAs cannot be produced endogenously, they are absorbed as nutrients from the foods consumed in the diet and transported through the blood-brain barrier via facilitated and passive diffusion mechanisms (Liu et al., 2015). While unsaturated lipids are in the majority, some lipids in the biomembranes are saturated, such as sphingomyelins.

2.1.2   MEMBRANE PROTEINS

Integral membrane proteins (IMPs) are permanently residing in the lipid membrane and therefore integral to the membrane structure (Singer & Nicolson, 1972). IMPs have multiple classes based on the number of their transmembrane domains (TMDs) and topology, i.e. the orientation of the domains (Fig. 2.1). Many IMPs are also glycosylated, containing branched polysaccharide structures. Traditionally, the complexity of their purification has hindered the progress in the structural biology of IMPs. Specific solubilization protocols using detergents and possible reconstitution of the purified protein to a model membrane system are needed (Seddon et al., 2004). The presence of co-purified lipids in the x-ray crystal structures of IMPs implicates that the lipids have a role in maintaining protein integrity via tight interactions or specific binding sites (Hanson et al., 2008; Marius et al., 2005; Palsdottir & Hunte, 2004). Incorporation of lipids, such as cholesterol, in the detergent-solubilized membrane proteins, has shown to be essential to catalytic IMP activity and successful crystallization (Hunte & Richers, 2008). The use of lipid cubic phases, where different shapes of lipids are present to offer a stable environment for the proteins, seems to help with retaining the IMP activity (de Kruijff, 1997). The relation between protein-lipid interfacial tension and the energetics of the rhodopsin signal transduction (Brown, 1994; Wiedmann et al., 1988) has exemplified the importance of physical membrane properties in maintaining IMP functionality.

Human G-protein-coupled receptors (GPCRs) are important signal transducers sensitive for drugs, hormones and neurotransmitters. For long, their successful crystallization was impeded by the low relative quantities of functional receptors during protein expression (Zhao & Wu, 2012). The loss of electron density in the vicinity of the ligand-binding site of the β_2 adrenoreceptor (β_2AR) close to the lipid-water interface suggested that lipids have an ordering effect on the TMDs (Cherezov et al., 2007; Rasmussen et al., 2007). The impact of lipids on the agonistic action of catecholamines (Swaminath et al., 2005) is not adequately understood (Jafurulla & Chattopadhyay, 2012); nevertheless, the fact that membrane-perturbations affect adrenoreceptor functionality is well known from early biochemical studies (Cerione et al., 1983; Limbird & Lefkowitz, 1976).

Both rhodopsin and β_2AR are *polytopic* membrane proteins with several TMDs. Perhaps surprisingly, structural studies of polytopic proteins are more frequent than *monotopic* and *bitopic* proteins having one transmembrane segment, passing the membrane only partially (monotopic) or fully (bitopic). The first available crystal structure for a full bitopic protein (CYP51 from *Saccharomyces cerevisiae*) suggests that the transmembrane helix may contribute to the function of the enzyme by orienting the catalytic domain relative to the lipid bilayer (Monk et al., 2014). Before that, molecular dynamics simulations were used to investigate the 24-residue trans-membrane α-helix of the bitopic enzyme membrane-bound catechol-*O*-methyltransferase (MB-COMT) together with its 26-residue linker fragment (Orłowski et al., 2011). This fragment connects the transmembrane part to the soluble part bearing the catalytic domain. The soluble part is identical with the soluble COMT isoform (S-COMT). In simulations, an ion pair formed between the oppositely charged arginine and glutamic acid of the MB-COMT linker fragment, which indicated a stabilizing effect of the formed loop structure at the lipid-water interface. MB-COMT has a crucial metabolic function in the brain, i.e. catalyzing the addition of methyl group to the 3-*O* and 4-*O* (to a lesser extent) hydroxyl groups of catecholamines dopamine and noradrenaline. Recovery of the enzyme activity during detergent purification has been modest (Pedro et al., 2015). Interestingly, preference of catecholamines towards MB-COMT versus S-COMT is roughly 100-fold higher, but the difference ceases to exist after the introduction of a detergent Triton-X (Jeffery & Roth, 1984). These factors suggest that the lipid membrane may contribute significantly on the enzyme functionality.

In addition to the absence of structural and functional insight, topological features of MB-COMT have been under debate (Chen et al., 2011; Schott et al., 2010). Considering that calcium, an inhibitor of MB-COMT, is a prevalent cation in the synaptic cleft (Higley & Sabatini, 2012), intracellular localization of MB-COMT in the cytosolic side of ER membrane seems plausible (Myöhänen & Männistö, 2010). Now it is widely agreed that MB-COMT resides in the rough endoplasmic reticulum (rough ER) (Männistö & Kaakkola, 1999). This would make MB-COMT a type I IMP with the *N*-terminus of the TMD facing the ER lumen, although uniprot.org (The

Uniprot Consortium, 2020) still lists it as a type II topology based on the study by Chen et al. (2011). Nevertheless, the studies have not excluded the possibility of additional isoforms of COMT exhibiting extracellular action (Schott et al., 2010).

An intriguing quality of the lipid membrane is the reduction of dimensionality, primarily recognized for *peripheral membrane proteins* that operate in both lipid and water environments (Berg et al., 1991). For this reason, kinetic process rates are influenced by the exchange of the enzyme, ligands and cofactors between the two- and three-dimensional spaces (Berg et al., 2001). These exchange rates may differ drastically from the catalysis rates, complicating the experiments and the subsequent analysis. For IMPs, the distinction between enzyme activation in the interface and the water phase is even more troublesome since the activity of the enzyme cannot be measured without the membrane (Gelb et al., 2000). Still, interfacial catalysis performed by an integral membrane protein has been described by Ullrich et al. (2011) for a lipid-catalyzing enzyme DAG kinase from *Escherichia coli*. For IMPs with nonlipid substrates, such action is yet to be construed.

2.1.3   INTERACTIONS IN MEMBRANES

Although covalent bonds between lipids, proteins and carbohydrates are prominent in membranes, noncovalent interactions described below govern most of the membrane structure:

- *Electrostatic interactions*, as such, are often referred to as repulsive or attractive interactions between anions, cations and chemical groups with a formal charge.

- *Hydrogen bonds*, by the name, form between a hydrogen atom and a more electronegative atom or moiety.

- *Steric repulsions* exist due to the overlap of electron clouds of the atoms in the lipid hydrocarbon chains, for example.

- *Dipolar interactions* are a combination of all interactions where an electrical dipole formed by partial charges takes part. For example, "van der Waals" attractions occur between the lipid hydrocarbon chains, contributing to the chain order.

Hydrophobic effect, although not an interaction *per se*, contributes to the insertion of lipidated proteins (Erwin et al., 2016) and secondary structures of IMPs (Yonkunas & Kurnikova, 2015). Also, a *salt bridge* is a term used for a combination of electrostatic interaction and hydrogen bond, typically formed between the charged amine and carboxyl functional groups. Chemical moieties of the membrane constituents define the extents of these interactions, which in turn regulate the physical properties of the membrane such as lateral pressure (Cantor, 1999; Marsh, 1996) and membrane curvature (McMahon & Gallop, 2005). In addition to the properties of the lipids

themselves, variations in the chemical environment of the lipid-water interface take part in defining the local membrane structure. Interfacial hydration (Jurkiewicz et al., 2012), local pH gradients (Cherepanov et al., 2004) and concentrations of osmolytes (Söderlund et al., 2003) are particularly important.

2.1.4   STRUCTURE OF BIOLOGICAL MEMBRANES

The structural intricacies of biological membranes were long unknown; nevertheless, the effects of electrolytes on biological membranes were studied for decades before any currently used techniques existed (Danielli, 1944; Kedem & Katchalsky, 1958). The famous fluid-mosaic model by Singer & Nicolson (1972) presented the idea of the membrane as a mosaic where the lipid bilayer forms the matrix of the biological membrane with sparsely floating IMPs (Singer & Nicolson, 1972). The model incited increasing interest in lipid-protein interactions; for example, it was demonstrated that the physicochemical properties of membranes affect the enzymatic activity of phospholipase A2 (Verger et al., 1973) and membrane thickness and the composition of the annular lipid shell regulate the activity of adenosine triphosphatase (East & Lee, 1982). Notably, while the fluid-mosaic model argued against a long-range ordering of the integral membrane proteins, it did not exclude the possibility of short-range order and lateral organization in general. The thermodynamical reasonings of the fluid-mosaic model are still relevant, and the model has been since revised by the original authors and other contributors to account for, e.g. the dynamical nature of membrane components and nonrandom long-range order maintained by cytoskeletal systems (Nicolson, 2014).

Lateral organization in biological membranes is perhaps the most discussed and controversial topic in biomembrane research. Since cells have different ordered compartments, why should there not be order in the membranes as well? After the model presented by Singer & Nicolson, distinct phase separation in binary lipid mixtures led to consider that such behavior could also exist in biological membranes (Binder et al., 2003). Indeed, the plate-model of Jain & White (1977) proposed that the biomembrane would have "relatively rigid plates or patches that are in relative motion with respect to each other." Later, the idea that biomembranes structure their tasks via functional "*rafts*" (Simons & Ikonen, 1997) was viewed as a solution to the problem of how proteins and lipids cooperate in the chaotic environment driven by thermal fluctuations. In model membranes, lipid-lipid interactions drive the segregation of sphingomyelin, a high-T_m lipid, and cholesterol, to *liquid-ordered* (L_o) phases, or rafts, while unsaturated phospholipids with low T_m stay in the *liquid-disordered* (L_d, equal to L_α) phase. The L_o phase is fundamentally different from the gel (L_β) phase in terms of less restricted translational and rotational freedom. Theoretically, the L_o-L_d phase coexistence depends on the balance between line tension, dipole density

difference and mixing entropy (Lee et al., 2011). The term "*domain*" is traditionally reserved for any lateral assembly in a lipid membrane, while the raft is a detergent-extracted fraction enriched in sphingomyelin, cholesterol and proteins attached to glycophosphatidylinositols (GPIs) (Binder et al., 2003). Therefore, in practice, the term raft is reserved for the proposed SM-Chol assemblies in biological membranes.

Even though phase-separation prevails in synthetic membranes, the implications of such action *in vivo* remain elusive. Foremost, domains studied in model systems have sizes in micrometers. Possible evidence for rafts in cells came from a pioneering study by Baumgart et al. (2003), who showed that in cell-derived GUVs (giant plasma membrane vesicles, GPMVs), under specific conditions, membrane curvature can drive lateral segregation to distinct L_o-L_d phases. Later, advances in super-resolution microscopy allowed the detection of nanoscale L_o-L_d segregation (Eggeling et al., 2009). Conflicting results came when the specific trapping of sphingomyelin probes was concluded not to be related to the formation of L_o-L_d domains (Honigmann et al., 2014), calling the previous findings of "rafts" into question. Thus, the dynamical coexistence of raft domains has not been captured as initially proposed. The inherent difficulty of detecting rafts seems to come from the fact that the existence of domains is highly dynamic. Even single-phase lipids form short-lived nanoscopic entities arising from a myriad of lipid-lipid and lipid-protein interactions (Jacobson et al., 2007). The domains could be under near-critical fluctuations (Veatch et al., 2008), which modulate the lateral diffusion of the lipids over vast time-scales (Ehrig et al., 2011). Therefore, while the biological consequences of the raft hypothesis need clarification, the general scientific consensus is that lateral organization is fundamental to the membrane architecture (Levental & Levental, 2015; Nicolson, 2014).

An intriguing property of the L_o-L_d boundaries *in vitro* is their role in facilitating membrane fusion. The boundaries could serve as interaction sites for viral peptide-mediated entry (Yang et al., 2015). Another foundational characteristic of the biological membranes, asymmetry in the lipid bilayer, is not currently well understood, although its existence has been known for multiple decades (Rothman et al., 1976). In fact, the dominant presence of PE, prone to form nonlamellar phases, in the inner leaflet, while the outer leaflet contains sphingomyelin and cholesterol driving lateral segregation in model systems, raises the question how can plasma membrane even exist as a bilayer at all (Ackerman & Feigenson, 2015). A final major conundrum unresolved in the membrane structure is how cells maintain lipid homeostasis. The superlattice model (Somerharju et al., 2009), in particular, has proposed an answer with physical reasoning. Briefly, imbalances in the superlattice, i.e. the states of free energy minimum the lipid membrane naturally adopts, could drive the action of the relevant enzymes responsible for maintaining optimal lipid composition (Hermansson et al., 2011).

Finally, the enormous degree of molecular crowding present in the biological environment should be acknowledged. While the essence of biological processes is speculated from relatively simple physicochemical

foundations, i.e. the building blocks of the system, the complexity of the real *in vivo* environment of cells is mostly beyond comprehension. For example, the estimated range of macromolecule concentrations in cells, 80–400 mg/mL (Homouz et al., 2008), translates into 2-10 millimoles per liter, using an average protein molecular weight of 40 kDa. Since this range corresponds to the concentrations of different divalent cations in biological compartments, macromolecular crowding contributes to the osmotic pressure of the compartments, and therefore, cellular signaling events and endocytosis (Miermont et al., 2013; Rauch & Farge, 2000). Similarly, assuming there are approximately 30,000 proteins per μm² in a biological membrane (Guigas & Weiss, 2016), approximately half of the membrane is occupied by proteins. In this estimate, however, the fraction of protein inside the lipid bilayer and above the membrane surface is not considered.

2.2   LIPID MEMBRANE MODELS

Because of the complexity of biological membranes, membrane models (Fig. 2.2) are used to allow a finite amount of physical system parameters, controlled by the specific design of the experiment. This section reviews the most widely adopted lipid membrane model systems, which are suited for *in vitro* studies of both synthetic membranes and biological membranes isolated from their native cellular environment. From the model systems not discussed in detail, lipid nanodiscs are emerging as platforms to study integral membrane proteins in native-like conditions (Parmar et al., 2018).
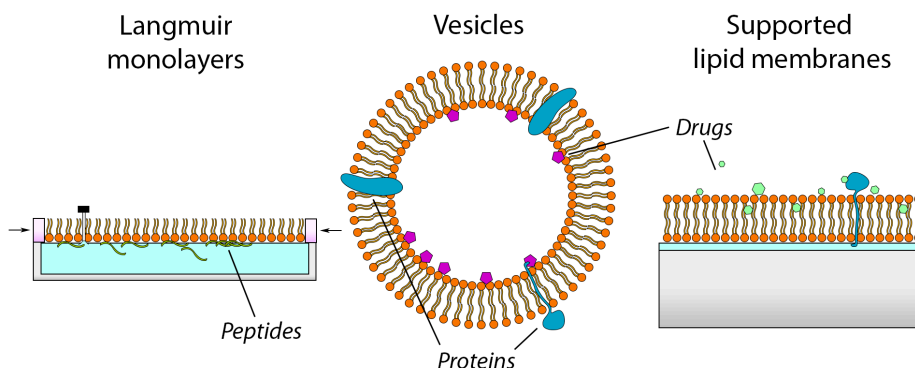
Figure 2.2   Representation of the common lipid membrane model systems. Peptides, proteins and drugs, for example, can be embedded or encapsulated in these systems.

2.2.1   LANGMUIR MONOLAYERS

While a self-assembled monolayer at an air-water interface does not fully embody the characteristics of a lipid bilayer, Langmuir monolayers have a fundamental place in biomembrane research. The areal compression and expansion of the monolayer allow for the direct investigation of phase changes in a monomolecular film. The uses of Langmuir monolayers in biologically-relevant applications are numerous. Lipid-nanoparticle interactions (Hernandez-Borrell et al., 1990), lung surfactant behavior under compression (Kulovesi et al., 2010) and interfacial binding of therapeutic or transmembrane peptides (Posada et al., 2014) have been studied, for example.

A *Langmuir-Blodgett trough* controls the monolayer area, and it can be combined with a temperature controller or complementary extensions such as microscopes and light scattering devices. The basis of the instrument is the lowering of surface tension of water upon the introduction of surface-active species, measured using a plate or a wire subjected to a force proportional to the surface tension. The surface pressure, $\Pi = \gamma_0 - \gamma$ is the difference between the air-water interfacial tension without ($\gamma_0 \approx 72$ mN/m) and with the monolayer present at the interface. The correspondence between the surface pressure measured in the Langmuir monolayer experiments and lipid bilayers has been suggested to occur at the range of high surface pressures (30−35 mN/m), corresponding to the hydrophobic free energy density resulting from the integration over the interfacial lateral pressure profile (Marsh, 1996).

2.2.2   LIPID VESICLES

Vesicles are closed lipid structures. They are ubiquitous in human tissues, serving as vehicles for cells to transfer substances intra- and extracellularly (Calafat et al., 1993; van der Pol et al., 2012). *Unilamellar vesicles* consist of only one lipid bilayer, while *multilamellar vesicles* (MLVs) can have multiple bilayers. Further classification is roughly based on the vesicle size: *small unilamellar vesicles* (SUVs, <100 nm), *large unilamellar vesicles* (LUVs, 100−1000 nm) and *giant unilamellar vesicles* (GUVs, >1000 nm). Vesicles designed for pharmaceutical drug delivery are often called *liposomes* (Bunker et al., 2016), which can function as carriers of therapeutic agents (Maherani et al., 2013) and gases (Sakai et al., 2009), for example.

SUVs and LUVs are prepared using various methods, most commonly by sonication, extrusion, or reverse-phase evaporation (Szoka Jr. & Papahadjopoulos, 1980). The preparation of GUVs requires specific protocols different from the SUV and LUV preparations. Since the sizes of SUVs and LUVs are at most few times the diffraction limit of light, GUVs are usually used in fluorescence imaging and lateral diffusion studies, while SUVs and LUVs are used in calorimetric and fluorescence spectroscopy studies. Supported vesicular layers (SVLs) on the solid supports are formed via noncovalent adsorption of the vesicles modulated by the chemical properties

of the surfaces or as *tethered* vesicles via covalent linkage of lipids or intermediate linkers to the surface (Ye et al., 2009).

2.2.3   SUPPORTED LIPID MEMBRANES

Lipid bilayers may be created directly on top of solid supports (e.g. on mica or SiO_2) as freely-floating membranes (Keller & Kasemo, 1998; Salamon et al., 1996), or as tethered membranes (Atanasov et al., 2005; Giess et al., 2004; Heyse et al., 1995). Also, monolayers can be formed on hydrophobic supports. The bilayers on solid supports are called supported lipid bilayers (SLBs) or supported phospholipid bilayers (SPBs) (Tamm & McConnell, 1985). Although Langmuir-Blodgett transfer can be applied to form bilayers, allowing asymmetric lipid distribution, the most versatile protocol for freely-floating SLB formation is perhaps the vesicle rupture approach. While the details of the process were not known during the early studies, it was generally accepted that favorable interactions of vesicles with the solid support lead to accumulation of vesicles on the surface, leading to a critical vesicle density-induced vesicle rupture (Keller et al., 2000; Keller & Kasemo, 1998). Anderson et al. (2009) confirmed the role of strong adhesion energy between vesicles and negatively-charged silicon dioxide (SiO_2) in initiating the vesicle accumulation process in high salt conditions. Chemical properties of the solid substrate can, therefore, facilitate the SLB formation (Granqvist et al., 2014; Reimhult et al., 2007), along with the physical properties of the vesicles and experimental conditions, such as osmotic pressure (Jackman et al., 2013). A study by Andrecka et al. (2013) using interferometric scattering microscopy refuted the contribution of vesicle fusion, and instead, demonstrated the interplay between the energetics of the surface-vesicle interactions and the subsequent spreading of the nanoscale bilayer patches.

Morphologically stable SLBs, in principle, have an advantage over supported vesicle systems that they avoid nonspecific surface interactions, differences in vesicle coverage and contributions from the vesicle polydispersity and curvature to the interactions. Incorporation of IMPs to the membranes makes SLBs a versatile platform to study biological interactions between IMPs and their ligands in a membrane environment (Salamon et al., 1996). Membranes extracted from cells can be sonicated together with synthetic vesicles to form vesicles that rupture more easily on solid supports (Dodd et al., 2009; Lee et al., 2010) to create natural membrane mimic platforms. Also, peptides can facilitate the formation of the supported bilayer (Cho et al., 2009; Hardy et al., 2012), although it is unclear to what extent the peptide influences the membrane properties.

Significant concern about the applications of SLBs has been the possible hindrances to lipid mobility and protein denaturation due to the proximity of the solid support. Indeed, diffusion coefficients in SLBs can be approximately half to those measured in vesicle systems (Pincet et al., 2016; Przybylo et al., 2006). Incorporation of polymer supports acting as spacers can address these

concerns by ensuring IMP stability (Pace et al., 2015; Ye et al., 2009). The preparation process of vesicles does not seem to impact the fluidity of the SLBs (Lapinski et al., 2007), but is rather controlled by the interactions of the SLBs with the solid support (Seu et al., 2007).

2.3 EXPERIMENTAL METHODS FOR STUDYING LIPID MEMBRANES

This section briefly describes the standard experimental methods suited for the research of model membranes and biological membranes (Fig. 2.3). Many methods that have provided essential insight into the membrane physics and architecture are not discussed. For example, electrochemical methods provide useful information on the electrical properties of the membranes, such as resistance and capacitance. Important microscopy techniques, not further discussed, include scanning electron microscopy (SEM), transmission electron microscopy (TEM) and cryogenic electron microscopy (cryo-EM). Atomic force microscopy (AFM) is also not discussed even though it is widely used in the characterization of supported lipid bilayer morphology in combination with the surface-sensitive methodologies (Richter & Brisson, 2005).

2.3.1 THERMODYNAMICAL METHODS

Like all structures of matter, lipid membranes obey the laws of thermodynamics, and thus thermodynamical methods suit well for lipid membrane studies. Differential scanning calorimetry (DSC) was used in many pioneering works before more advanced technologies existed and is still the method-of-choice for the studies on membrane thermal phase behavior. The thermodynamic parameters of the phase transitions can be derived directly from the heat capacity measurements. Isothermal titration calorimetry (ITC), capable of resolving the relevant thermodynamical quantities of binding processes, has been particularly useful for studying the interaction of drugs with vesicles (Ikonen et al., 2010; Osanai et al., 2013) and conformational changes of peptides upon membrane binding (Seelig, 2004); however, there is uncertainty regarding the effect of vesicle size on the measured enthalpy and entropy changes (Seelig, 2004).

2.3.2 FLUORESCENCE METHODS

Fluorescence methods have been, and still are, most widely adopted in studies of both model membrane systems and biomembranes of living cells. Their applications are numerous and only briefly discussed here. Intrinsic tryptophan fluorescence is a powerful method to study peptide and protein insertion to membranes and conformational changes (Christiaens et al.,
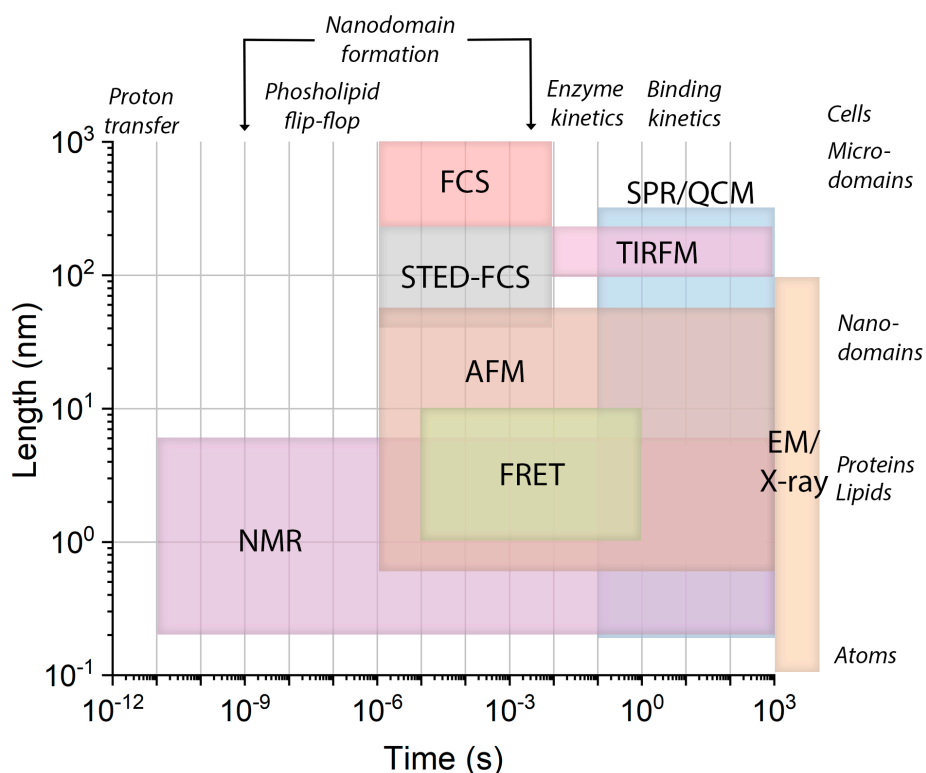
Figure 2.3 Approximate spatiotemporal scales at which different techniques and instruments are used to study lipid membranes (Chiu & Leake, 2011; Dror et al., 2012; Sezgin et al., 2019). For SPR & QCM, the length scale represents the sensitivity to changes in the vicinity of the sensor surface, not the lateral resolution.

2002). Fluorescent labeling of proteins and lipids in GUVs has allowed determining the partitioning of proteins in L_o-domains (Levental & Levental, 2015). Fluorescent sterols can quantify the kinetics of sterol esterification (Homan et al., 2012), and the fluorescence resonance energy transfer is a sensitive approach to detect the nanoscale proximity of probes or intrinsic residues in membranes in relation to nanoscale segregation (Pathak & London, 2011), or peptide-lipid interactions (Matos et al., 2010), for example.

Diffusion is a ubiquitous property of matter, suited for characterizing the degree of lateral or rotational constraints directed to the membrane constituents. For that purpose, fluorescence correlation spectroscopy (FCS) allows measuring the fluorescence fluctuations arising from the fluorophore entering and leaving a focused confocal laser beam. FCS has been combined with super-resolution microscopy techniques such as stimulated emission depletion microscopy (STED) (Honigmann et al., 2014). Also, pyrene-labeled lipids can probe the lateral mobility in the membranes. This has provided

insight into the lipid peroxidation in the membrane (Borst et al., 2000) and superlattice membrane ordering (Kinnunen, 1991). Diffusion can also be measured using fluorescence recovery after photobleaching (FRAP), although control experiments regarding intrinsic photobleaching of fluorophores and anomalous diffusion are needed (Pincet et al., 2016). Of single-molecule microscopy techniques, total internal reflection fluorescence (TIRF) microscopy has superior capabilities for optical sectioning, and outside of the traditional imaging applications, it has been used in, e.g. single-molecule drug binding assays (Gunnarsson et al., 2015) and size calculations for individual glass-tethered vesicles (Olsson et al., 2015).

While fluorescence methods are powerful tools in biomembrane research that no label-free methodology can currently match in spatiotemporal resolution, their use requires careful consideration of the possible interferences. Generally, the fact that only a minimal relative amount of fluorophore resides in the membrane does not exclude the possibility that interactions of the probe with the studied molecules interfere with the studied phenomena. Fluorophores can partition between different phases depending on the lipid composition (Chan & Boxer, 2007). Fluorescence quenching of amino acids present in proteins, generally tryptophans, is often incorrectly used in ligand binding studies to extract binding stoichiometry on an assumption of a single quenching mechanism (van de Weert & Stella, 2011). Also, photophysics of the used fluorophores (Amaro et al., 2016) and possible false positives in drug assays based on fluorescence (Simeonov & Davis, 2015), should be acknowledged.

2.3.3 SCATTERING METHODS AND NUCLEAR MAGNETIC RESONANCE

Small-angle neutron and x-ray scattering are used in studying structural membrane properties. Since x-rays scatter from electrons and neutrons from atomic nuclei, they provide slightly different information. X-rays resolve the distance between electron density maxima of the lipid headgroups, while neutron scattering provides the total bilayer thickness due to the high deuterated water-lipid contrast (Kučerka et al., 2015). Area-per-lipid-molecule, for example, can be then calculated using specific modeling approaches. Also, volume probabilities are obtained, allowing comparisons with density calculations from molecular dynamics (MD) simulations (Pan et al., 2015). Although not belonging to the category of scattering techniques, nuclear magnetic resonance (NMR), solid-state NMR in particular, is sensitive for subnanometer dynamics in the membranes, allowing the studies of a myriad of membrane-related properties. These include ligand binding to membrane proteins (Watts, 2005), enzyme kinetics in membranes (Ullrich et al., 2011), membrane hydration (Petrache et al., 2004) and lipid-ion interactions (Roux & Bloom, 2005). Order parameters

from solid-state NMR are often used to validate the results from MD simulations (Ferreira et al., 2013).

2.3.4   OPTICAL SURFACE-SENSITIVE METHODS

Optical surface-sensitive techniques are label-free and are able to resolve changes in the dielectric permittivity of the material due to the exchange of molecules in the vicinity of the optical sensor surface. In essence, together with fluorescence techniques, they are *biophotonic* methodologies. Surface plasmon resonance (SPR), based on the light-induced surface plasmon resonance phenomenon, is sensitive to the interfacial binding events on the metal sensor surface. It has been an industry-standard in biosensor applications such as ligand-protein binding studies for screening new drug candidates (Huber & Mueller, 2006; Lee et al., 2015; Olaru et al., 2015). Vesicles and lipid bilayers (Abdiche & Myszka, 2004; Heyse et al., 1995; Keller et al., 2000), also with incorporated membrane proteins (Salamon et al., 1999, 1996) and living cells (Abadian et al., 2014), have been studied extensively using SPR. While the traditional Biacore (General Electric Healthcare, Chicago, IL, USA) instruments use the detection of narrow ranges of incidence angles of *p*-polarized light, some other devices, such as the multi-parametric SPR instrument (MP-SPR) from Bionavis (Tampere, Finland), enable to measure the full range of incidence angles, including the angle of total internal reflection (TIR). MP-SPR allows for inline correction for changes in bulk liquid refractive index, without the need for laborious reference measurements with an empty sensor; however, procedures for performing and analyzing drug-lipid interactions exploiting the benefits of the MP-SPR instrumentation need further elaboration.

Flow channel-based instruments such as SPR introduce the possibility to mimic flow conditions in the bloodstream. Also, the flow of liquid over the sensor surface establishes a constant flow of analyte molecules from and into the flow channel of the instrument, ensuring that the kinetic equations governing the interaction do not contain time dependencies for analyte concentration. This condition fulfills if the assay conditions are not dependent on the mass transport to the surface, i.e. the liquid flow over the surface balances the effect of molecular diffusion perpendicular to the surface. Mass depletion over time is problematic for *in vitro* enzymatic studies, for example, since the approximations made in the Michaelis-Menten kinetics may not hold under these conditions (Rusu, 1998).

Disadvantages of SPR include the somewhat limited throughput, inability to resolve the mode and location of binding respective to the sensor surface and insensitivity to anisotropic events such as changes in the orientation of the membrane-bound species (Lee et al., 2015). Ellipsometry (Howland et al., 2007), coupled plasmon-waveguide resonance (Salamon & Tollin, 2001), dual-polarization interferometry (Mashaghi et al., 2008; Swann et al., 2004) and optical waveguide lightmode spectroscopy (Reimhult et al., 2007) can

reveal these properties. The orientation of molecules in lipid membranes may also be studied using infrared spectroscopy, linear dichroism (Lopes & Castanho, 2005) and vibrational sum frequency spectroscopy techniques (Tang & Allen, 2009). Although not a light-based method, quartz crystal microbalance provides complementary information on lipid membrane models such as changes in viscoelasticity and hydration of the membrane (Cho et al., 2010). Care is needed, however, when comparing results obtained using instruments with different means of model membrane formation. The acquired physical properties of the membranes, e.g. diffusion, thickness and hydration, are primarily dependent on the type of membrane model, preparation of the membrane and the used methodology. Instead of seeing a particular method as superior to another, one should appreciate advantages and disadvantages of each method and interpret the results in the context of the current information.

2.4 NEURODEGENERATION: FROM LIPIDOPATHY TO THERAPEUTICS

This section briefly reviews neurodegeneration in relation to dysfunction in the lipid homeostasis, which manifests as changes in the membrane lipid composition and protein functionality. Lastly, the current treatment for Parkinson's disease using L-dopa administration and adjunct COMT inhibitors is discussed. While only Alzheimer's disease and Parkinson's disease are focused on, a multitude of other neurodegenerative diseases are also associated with disruptions in lipid metabolism (Grimm et al., 2007).

2.4.1 LIPIDS IN NEURODEGENERATIVE DISEASES

The foundational insight from early chromatographic studies showed that the lipid composition in the brain is linked to disease states (Fillerup & Mead, 1967; O'Brien & Sampson, 1965; Rouser et al., 1965). The dry weight of lipids of total brain mass varies from around 40 to 70 % in white and gray matter to approximately 80 % in myelin sheaths (O'Brien & Sampson, 1965). Procedures for postmortem subcellular fractionation (Swanson et al., 1973) allowed to study lipid and protein compositions of individual cell types and cellular fractions (Ayola et al., 1988; Fabelo et al., 2011) and to assess the role of mineral imbalances present in the pathological conditions (Wenstrup et al., 1990), for example.

Alzheimer's disease

Alzheimer's disease (AD), the most common neurodegenerative disorder, is characterized by gradually advancing degeneration of neurons (Fig.2.4) in
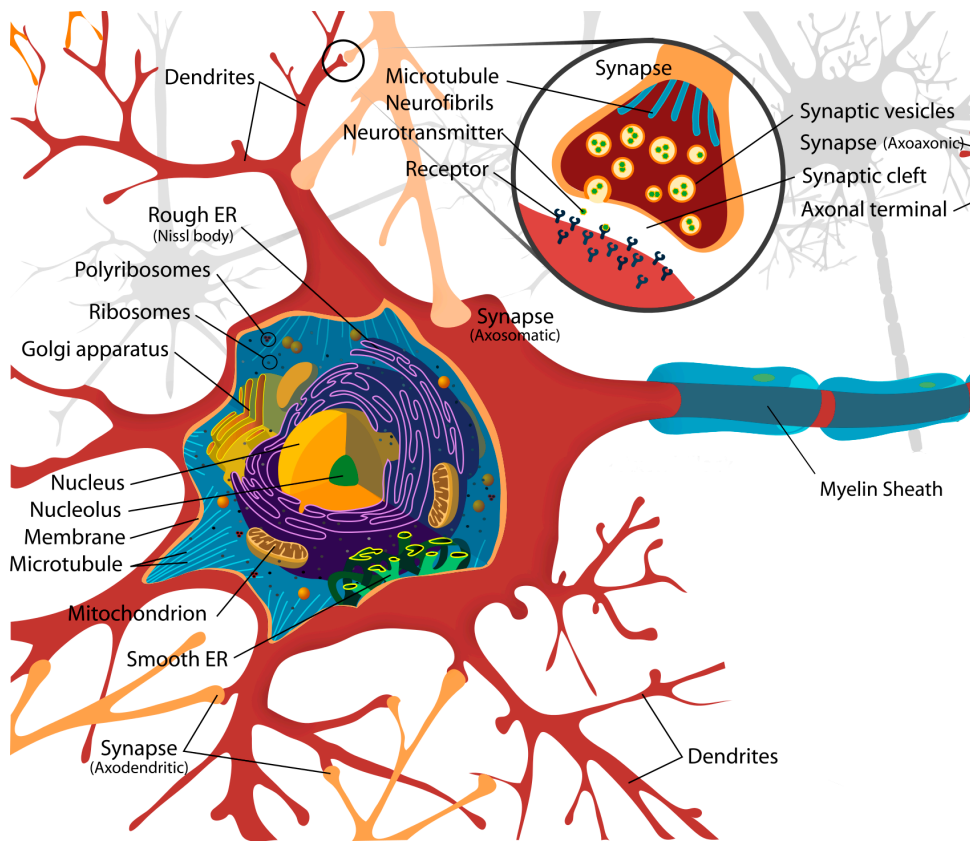
Figure 2.4 Representation of a neuronal soma (cell body) and its surroundings. Adapted with permission from https://pixabay.com/illustrations/drawing-nerve-cell-neurone-732830/ (by Gerd Altmann from Pixabay, accessed 4.6.2020)

various areas of the brain, such as the hippocampus and cerebral cortex. This leads to cognitive and motor dysfunction, dementia and, eventually, death. A decrease in total lipid mass was first quantified in the brains of two AD patients (Rouser et al., 1965). Later, specific loss of PE plasmalogens (Ellison et al., 1987) and sulfatides (Han et al., 2002) has been demonstrated. The loss of sulfatides, a class of sphingolipids, is present in myelin, which is crucial for effective nerve signaling. On the other hand, no decrease in brain sphingomyelin has been observed, but higher SM in plasma could indicate a deceleration in the advancement of the disease (Wood, 2012). The decrease in PE plasmalogens, on the other hand, indicates dysfunction in peroxisomal lipid metabolism (Wood, 2012). The β-amyloid (Aβ) peptide aggregation to senile plaques is the prevailing theory for the cause of AD, and the production of these peptides by the secretase IMPs is regulated by lipids such as cholesterol, sphingolipids, PIs and PAs (Di Paolo & Kim, 2011; Grimm et al., 2007). γ-secretase could also be associated with lipid rafts (Di Paolo & Kim,

2011). Since Aβ is also a regulator of lipid metabolism, Aβ aggregation can lead to lipid dyshomeostasis due to the disruption in this regulatory cycle (Di Paolo & Kim, 2011; Grimm et al., 2007). Also, apolipoprotein E isoforms have been suggested to traffick Aβ and lipids with different efficiencies, which links dietary considerations to the AD pathologies (Lane & Farlow, 2005). Finally, negatively-charged lipids such as PS seem to enhance amyloid fibril formation in model membrane systems (Gorbenko & Kinnunen, 2006).

Parkinson's disease

In Parkinson's disease (PD), dopaminergic neurons are lost in the nigrostriatal pathway. The symptoms of tremors, rigidity and slowness usually appear after 60 % of the nigral cells have died (Bonifácio et al., 2007). The disease arises from α-Synuclein (α-Syn) aggregation and misfolding to Lewy bodies inside presynaptic terminals (Barchet & Amiji, 2009). Therefore, inhibition of α-Syn aggregation is the target for novel therapeutic strategies (Svarcbahs et al., 2016). α-Syn binds to the lipid headgroups of model lipid membranes via its amphipathic α-helix, leading to a subsequent membrane remodeling dependent on the presence of curvature-inducing lipids such as PE (Ouberai et al., 2013). Specifically, binding of α-Syn to the lipid membrane simultaneously with a chaperone complex regulates presynaptic vesicle fusion, suggesting the synaptic vesicle exocytosis may be hampered in PD (Burré et al., 2010). Ineffective cholesterol transport in the brain by apolipoproteins can also induce excessive interactions of α-Syn with Chol-containing membranes, highlighting the importance of functioning cholesterol homeostasis in the brain (Emamzadeh, 2017). These factors can cooperate with various protein dysfunctions, such as tubulins responsible for the cytoskeletal function, thus promoting microglia-aggravated neuroinflammation present even in the early stages of the disease (Chung et al., 2009). PUFAs have been shown to possibly promote the solubilization of α-Syn to oligomers (Sharon et al., 2003).

Lipid peroxidation

Reactive oxygen species (ROS) exist naturally as products of oxygen metabolism, but their amount can increase under stress. Susceptible locations for lipid peroxidation are mitochondria and pulmonary alveoli, where unsaturated lipids comprise the lung surfactant (Khabiri et al., 2012). Acyl chains are prone to degradation at their double-bonds, producing carboxylic acid and aldehyde derivatives, oxidized phospholipids (oxPLs). Therefore, PUFAs are highly susceptible to lipid peroxidation, which can modulate protein-lipid interactions in disease states associated with fibril formation (Kinnunen et al., 2012). Specifically, lipid peroxidation can induce the formation of Aβ fibril aggregates and mitochondrial dysfunction in PD due to the prominent interactions of α-Syn with oxPLs (Auluck et al., 2010;

Kinnunen et al., 2012; Ruipérez et al., 2010). These findings highlight the importance of studying oxidative stress-induced changes in the physical state of lipid membranes.

Biophysical studies on model membrane systems using stable oxPLs have elucidated the disruptive role of lipid peroxidation in modulating the physical membrane properties. First, oxPLs induce lateral expansion and membrane thinning (Mason et al., 1997; Wong-ekkabut et al., 2007) due to the reversal of the truncated *sn*-2 acyl chains (Beranova et al., 2010), which also makes them susceptible for macrophage recognition (Greenberg et al., 2008). As anesthetics can modulate the miscibility transition temperature of the L_o-L_d coexistence (Gray et al., 2013), oxPLs can stabilize the domain separation. In Langmuir monolayers, the acyl chain reversal leads to the increase in line tension induced by the hydrophobic height-mismatch in the L_o-L_d domain boundaries (Lee et al., 2011; Volinsky et al., 2012). Also, oxidation products disrupt membrane asymmetry in SUVs and LUVs by inducing transbilayer diffusion, i.e. flip-flop, of PS to the outer plasma membrane leaflet (Volinsky et al., 2011). Lateral diffusion in SLBs has been shown to increase slightly upon the presence of oxidated lipid species (Beranova et al., 2010). For cholesterol, intriguing properties have been suggested, such as protection from free radical attack, oxPL-induced increased water permeability (Mosca et al., 2011) and structural disorder (Štefl et al., 2014). This draws a parallel to the function of tocopherols (vitamin E) which have been suggested to interact with specific proteins, lipids and membrane phases to scavenge free radicals (Atkinson et al., 2008; Wang & Quinn, 2000), but the insight into this action has been hindered by the same experimental problems concerning the lipid raft paradigm. To conclude, while the mechanistic picture of oxPLs acting in model systems together with various membrane components has become more detailed, the connection of lipid peroxidation to dynamical nanoscale events such as phase separation needs further inspection.

2.4.2   PARKINSON'S DISEASE THERAPEUTICS

For noninvasive treatment of CNS diseases, there are two options. Either the drug or drug carrier crosses the blood-brain barrier and reaches its target directly, or the drug acts in the periphery. The latter can cause an indirect effect in the CNS via signaling cascades or treat the adverse symptoms of another treatment in the CNS or periphery. No new viable treatments for AD have emerged after 2003 (Hung & Fu, 2017). The current therapeutics mostly focus on symptomatic treatment using acetylcholinesterase inhibitors and the inhibition of excess glutamate activity, which would otherwise be neurotoxic (Hung & Fu, 2017). In PD, COMT is targeted to compensate for the dopaminergic neuronal loss. The next sections discuss this strategy in detail.

COMT in dopamine metabolism

Dopamine has two major metabolic pathways in the postsynaptic neurons, and dysfunction in these routes can lead to excessive neurotransmitter buildup. Monoamine oxidases (MAO, types A, and B), located in the outer leaflet of mitochondrial membranes, catalyze the reaction of the amine groups of the dopamine molecules to aldehydes. Of the two COMT isoforms, MB-COMT performs 3-*O*-methylation of dopamine with lower capacity but has a ten- to hundred-fold higher affinity for dopamine than S-COMT (Jeffery & Roth, 1984; Lotta et al., 1995). Thus, it is believed that MB-COMT is the primary isoform in brain, and S-COMT has a secondary role. COMT activity is found in all brain areas, especially in microglial cells (Myöhänen & Männistö, 2010), and MB-COMT is found in the postsynaptic neurons of the striatum (Francis et al., 1987). Both isoforms are coded by the same gene and require *S*-adenosyl-ʟ-methionine (AdoMet) and Mg^{2+} as cofactors, in that order (Lotta et al., 1995). Val158Met polymorphism of COMT has been linked to an increased risk of schizophrenia (Egan et al., 2001), involuntary movements (dyskinesias) during PD treatment (de Lau et al., 2012) and PD-related cognitive disabilities (Williams-Gray et al., 2008). The mutation has also been found to diminish the activity (Cotton et al., 2004) and thermostability (Rutherford et al., 2008) of the enzyme *in vitro*. Also, 3-methoxytyramine (3-MT), the 3-*O*-methylated metabolite of dopamine, has been recognized as a neuromodulator associated with involuntary movements in mice, elucidating its role in the dyskinesia developed during ʟ-dopa treatment (Sotnikova et al., 2010). The main interest in 3-MT has been in its use as a biomarker (Peitzsch et al., 2013), and not much is known about its biological functions.

COMT as drug target

Unfortunately, only symptomatic treatment of PD is currently possible. It focuses on elevating the dopamine levels in the striatum, where administration of ʟ-dopa (levodopa), an endogenous precursor of dopamine, is the primary treatment. Since no effective therapeutics have emerged for the last 50 years, ʟ-dopa remains as the "gold standard" (Hornykiewicz, 2010). ʟ-dopa should cross the BBB via active transport by ʟ-type amino acid transporters (del Amo et al., 2008), albeit in minimal quantities (Bonifácio et al., 2007). It is known that BBB starts to restructure during aging (Patel & Patel, 2017); however, a study using a PD rat model did not conclude notable changes in the BBB functionality, which would affect the efficacy of ʟ-dopa treatment in the late stages of the disease (Ravenstijn et al., 2012). Dyskinesias, resulting from the loss of synaptic plasticity in the corticostriatal pathway (Picconi et al., 2003), are common in long-term ʟ-dopa treatment.

Since ʟ-dopa is a COMT substrate, it is prone to methylation in the periphery, reducing its bioavailability and elimination half-life (Ma et al., 2014). Also, aromatic amino acid decarboxylase (AADC) effectively metabolizes ʟ-dopa to dopamine in the periphery. Therefore, supplementing

L-dopa with COMT, AADC and MAO inhibitors in the treatment of PD as adjuncts is customary. Unfortunately, AADC inhibitors, such as carbidopa, lead to pulsating dopamine levels, and subsequently, motor impairment (Müller, 2015). While the first-generation COMT inhibitors were somewhat toxic, second-generation nitrocatechol compounds developed in the late '80s were more promising (Männistö & Kaakkola, 1999). The nitro group in the catechol ring acts as an electron-withdrawing moiety, inducing a pK_a shift and subsequent deprotonation of the reactive hydroxyl groups (Bonifácio et al., 2007). As a consequence, nitrocatechols are reversible and competitive tight-binding inhibitors acting at low nanomolar concentrations (Lotta et al., 1995), although noncompetitive inhibition has also been suggested (Borges et al., 1997). Due to their tight-binding nature, nitrocatechols show slow association and dissociation, which makes the incubation time another variable in the studies of the enzyme kinetics (Borges et al., 1997).

The main second-generation COMT inhibitors are nitecapone, entacapone and tolcapone. Their adverse effects include dyskinesia, nausea and dizziness (Bonifácio et al., 2007). Still, tolcapone was approved in 1997, since it showed enhanced motor function in PD patients, along with an increase in elimination half-time and the area under the curve during L-dopa treatment (Olanow & Watkins, 2007). The methylation to 3-*O*-methyltolcapone is not a major metabolic route, and instead, tolcapone is largely excreted to urine via other routes (Jorga et al., 1999). As a lipophilic compound, tolcapone enters to CNS and also inhibits striatal COMT, while entacapone acts mainly peripherally (Nissinen et al., 1992). Entacapone seemed to inhibit rat striatal COMT better with intrastriatal administration (Forsberg et al., 2005), while nitecapone does not suppress striatal COMT activity (Männistö & Kaakkola, 1999). Tolcapone, although still prescribed in some countries, was primarily withdrawn due to its hepatotoxicity, while entacapone as a liver-safe drug is still largely in use (Bonifácio et al., 2007; Olanow & Watkins, 2007). The toxicity of tolcapone has been attributed to patient-specific mitochondrial dysfunction (Longo et al., 2016). Tolcapone was recently shown to induce cell apoptosis *in vitro* and to inhibit the growth of neuroblastoma tumors in a mouse model, introducing it as a potential treatment for these pathologies (Maser et al., 2017).

Attributing to the lack of 3D structure for MB-COMT, physicochemical factors that would enable to develop drugs with the inhibition of MB-COMT in mind, are not known. Silva et al. (2016) showed promising results for novel nitrocatechol compounds with prominent BBB permeability and the ability to differentiate between total rat liver and brain COMT. Robinson et al. (2012) performed a comprehensive analysis of non-nitrocatechol inhibitors for the inhibition of human and rat COMT isoforms. A peculiar detail in the experimental details of the study was the use of a detergent Fos-Choline-12 in the preparations of the enzymes for *in vitro* studies. Although it is a lipid-like detergent, and some success has been found in retaining the MB-COMT activity using long-chain ionic detergents (Pedro et al., 2018), the effects of the individual detergents with varying concentrations should be carefully

investigated. As discussed, if the presence of the lipid membrane is essential to the catalytic function of MB-COMT isoform, detergent-extraction can result in a vast underestimation of the inhibitory potential for the compounds towards the membrane-bound isoform.

3 AIMS OF THE STUDY

Based on the existing literature, chemical diversity of lipids and alterations in the lipid membrane composition influence the physical properties of the membranes and, consequently, cellular functionality. Using model lipid membranes, the hypothesis of this thesis was to show whether the lipids and their physicochemical diversity can regulate biointeractions between membrane proteins, endogenous catechol compounds and pharmaceuticals. This hypothesis has potential implications for the role of lipid membranes in modulating drug action, and thus the treatment of (neuro)pathological conditions where the simple protein-centric paradigm for pharmacological targeting may not be sufficient. In order to test the hypothesis, the specific intermediate aims were to:

1. Investigate how the biophysical properties of model membranes are dependent on the chemical diversity of the lipid species (**I**, **II**) and, specifically, how the chemical modifications (lipid peroxidation) can alter the lateral organization in model membranes (**I**).

2. Study how a prominent catecholamine-metabolizing enzyme, membrane-bound catechol-*O*-methyltransferase (MB-COMT), functions at the lipid-water interface (**III**).

3. Assess the role of the lipid membrane in regulating the MB-COMT enzyme-substrate activity by investigating the interactions between catechols and model membranes (**III**, **IV**).

4 MATERIALS AND METHODS

This chapter describes the materials and methods used in the thesis to study lipid membrane systems. The detailed experimental procedures are specified in the original publications **I-IV**. Table 4.1 outlines the used methods and the physical properties that were studied. Later in the chapter, the term *analyte* refers to any chemical entity of interest that is studied using the biophysical methods. The experiments were performed at 24 °C (**I**) or 20 °C (**II, III, IV**).

Table 4.1 Summary of the experimental methods adopted.

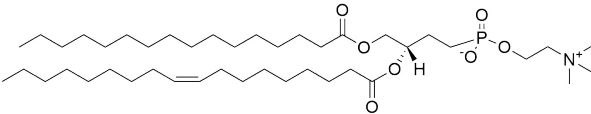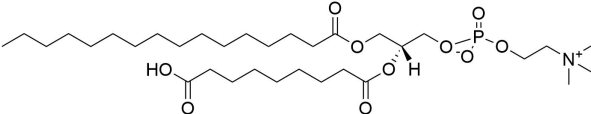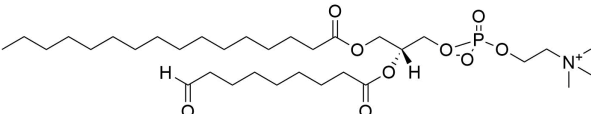| Method	Properties studied	Publication
Fluorescence correlation spectroscopy (FCS)	Lateral diffusion time (τ_D), Miscibility transition pressure (Π_m)	**I**
Isothermal titration calorimetry (ITC)	Changes in enthalpy (ΔH), entropy (ΔS) and free energy (ΔG), Mole ratio distribution coefficient (binding constant, K)	**III**
Langmuir monolayers	Area-per-lipid-molecule (a) Surface pressure (Π)	**I**
Surface plasmon resonance (SPR)	Area-per-lipid-molecule (a), "Dry" surface-mass density (Γ_{dry}), Membrane distribution coefficient (D_m) Binding constant (K), Number of binding sites (n), Refractive index (n_l), Refractive index increment ($\mathrm{d}n/\mathrm{d}C_*$), Optical thickness ($d_l$) "Dry" thickness ($d_{\mathrm{dry}}$)	**II, III, IV**
Quartz crystal micro-balance (QCM)	Effective thickness (d_l) or density (ρ_l), "Wet" surface-mass density (Γ_{wet})	**II, III, IV**
Wide-field microscopy (WFM)	Visualization of lipid domains	**I**

4.1 MATERIALS AND SAMPLE PREPARATION

Table 4.2 shows the lipids used in the experiments of this thesis, along with the corresponding chemical structures and the publications where the lipids were used. All lipids were from Avanti Polar Lipids (Alabaster, AL, USA), except DOPS used in publication **IV**, which was obtained from Larodan AB (Solna,

Sweden). In study **I**, POPC and its oxidated analogs were studied. Lipids with two monounsaturated oleoyl chains were used in the later studies. While these lipids are prone to oxidative degradation in air (Khabiri et al., 2012), notable peroxidation-induced changes in membrane properties have not been observed in SUVs (Borst et al., 2000). Lipids were mixed in chloroform (0.15 mg/mL total lipid) from their respective chloroform stock solutions. The preparation of SUVs had minor variations between the studies, but the basic principles are as follows:
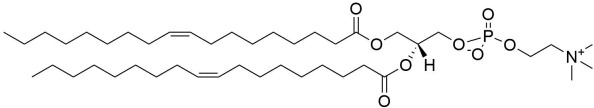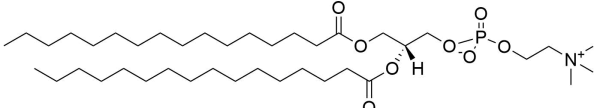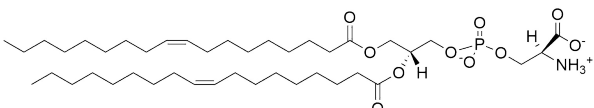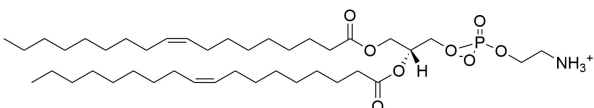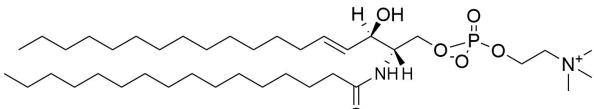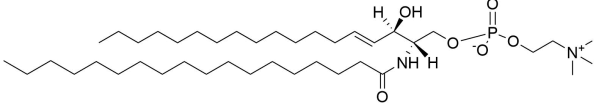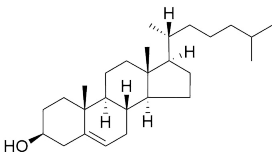
1. Chloroform was evaporated using a rotary vacuum system (**II**, **III**) or a nitrogen stream (**IV**, partly in **II**) to form a thin film at the bottom of the glass vial.

2. Thin-film hydration was performed by vigorous shaking of the lipids dissolved in HEPES-buffered saline (20 mM HEPES, 150 mM NaCl at pH 7.4).

3. Multilamellar vesicles were down-sized using extrusion protocols with a final extrusion through a 50 nm filter membrane (**II**, **III**), or by bath sonication (**IV**). After all protocols, the measured mean particle size was less than 70 nm, measured using dynamic light scattering.

Supported lipid bilayers were formed from the SUVs on SiO_2-coated proprietary SPR sensor chips and QCM crystals using the vesicle rupture approach, described in more detail in the publications of the thesis.

Table 4.2 Different lipids used in the publications of the thesis.

Abbreviation	Full name & chemical structure	Publ.
POPC 16:0-18:1 PC	1-palmitoyl-2-oleoyl-*sn*-glycero-3-phosphocholine	**I, II**
PazePC	1-palmitoyl-2-azelaoyl-*sn*-glycero-3-phosphocholine	**I**
PoxnoPC	1-palmitoyl-2-(9'-oxononanoyl)-*sn*-glycero-3-phosphocholine	**I**

Table 4.2 (continued)

Abbreviation	Full name & chemical structure	Publ.
DOPC 18:1 (Δ9-Cis) PC	1,2-dioleoyl-*sn*-glycero-3-phosphocholine	**II**, **III**, **IV**
DPPC 16:0 PC	1,2-dipalmitoyl-*sn*-glycero3-phosphocholine	**II**
DOPS 18:1 (Δ9-Cis) PS	1,2-dioleoyl-*sn*-glycero-3-phospho-L-serine	**II**, **III**, **IV**
DOPE 18:1 (Δ9-Cis) PE	1,2-dioleoyl-*sn*-glycero-3-phosphoethanolamine	**III**, **IV**
SM, Sphingomyelin (Egg, Chicken)	N-(hexadecanoyl)-sphing-4-enine-1-phosphocholine	**II**, **IV**
SM, Sphingomyelin (Brain, Porcine)	N-(octadecanoyl)-sphing-4-enine-1-phosphocholine	**I**
Chol, Cholesterol		**I**, **II**, **IV**

4.2 FLUORESCENCE CORRELATION SPECTROSCOPY (FCS)

Fluorescence correlation spectroscopy (FCS) measurements were performed by combining a Langmuir trough (μtrough XS; Kibron, Helsinki) with a custom inverted confocal microscopy setup based on Olympus IX 71 (Olympus, Hamburg, Germany). The focusing of the microscope in the direction of the monolayer normal (optical path, z) was established using a z-scan setup (Humpolíčková et al., 2006). In FCS, the intensity fluctuations from the excited diffusing fluorophores are analyzed using an autocorrelation function. This function describes the self-similarity of a signal with a time-lag τ. The general form of the autocorrelation function for the experiments can be written by considering the ergodicity property of Brownian motion. In other words, some fraction T of fluorophores have a lifetime τ_T in the triplet excited state (Enderlein et al., 2005; Widengren et al., 1995),

$$G(\tau) = \frac{\langle F(t)F(t+\tau)\rangle_t}{\langle F(t)\rangle_t^2} = 1 + \frac{1 - T + Te^{-\tau/\tau_T}}{c\,(1-T)(4\pi D_T\tau)} \frac{\int \Theta(\mathbf{r}')\,\Theta(\mathbf{r})\,e^{-\frac{|\mathbf{r}-\mathbf{r}'|^2}{4D_T\tau}}\,d\mathbf{r}\,d\mathbf{r}'}{\left(\int \Theta(\mathbf{r})\,d\mathbf{r}\right)^2}, \quad (4.1)$$

where c is the mean concentration of particles in the focal area, D_T is the translational diffusion coefficient, and $\Theta(\mathbf{r}) \sim e^{-2|\mathbf{r}|^2/w(z)^2}w(0)^2/w(z)^2$ is the molecule detection function approximated as a Lorentzian-Gaussian function with an effective beam diameter $w(z)$ in the direction of the optical path. The autocorrelation function can be simplified knowing that the lateral diffusion time, i.e. the average time the fluorophore diffuses through the focal area, is $\tau_D = w(z)^2/4D_T$ (Humpolíčková et al., 2006):

$$G(\tau, z) = 1 + \left(1 - T + Te^{-\tau/\tau_T}\right) \frac{1}{N(z)\,(1-T)} \frac{1}{1 + \tau/\tau_D(z)}, \quad (4.2)$$

which can be fitted to the autocorrelation functions obtained from the experiments at different positions z. The minima for τ_D and N, the average number of particles, are calculated considering a parabolic dependence on z. In study **I**, a two-component extension of Eq. 4.2 was used to account for domain migration at the air-water interface. In addition to FCS, a wide-field microscopy setup was utilized to study the morphology of the segregated L_o-domains during the miscibility transition process.

4.3 SURFACE PLASMON RESONANCE (SPR)

SPR experiments in this thesis were conducted using dual-wavelength (670 and 785 nm), multi-parametric SPR instruments from BioNavis, Tampere, Finland (MP-SPR Navi 200 and 200A). Supported lipid bilayers, formed *in situ* on sensors coated with SiO_2, were used in all publications. Also,

supported vesicular layers were used in study **II**. The characterization of the lipid model membranes in study **II** was conducted using Fresnel-layer matrix formalism (in a proprietary software LayerSolver, BioNavis, Tampere, Finland) utilizing the full reflection spectra as a function of incidence angle, a characteristic feature of the multi-parametric SPR instrumentation. In publication **III**, SPR was only used in the qualitative assessment of the extent of protein interaction with the model membrane. Study **IV** relies on Jung formalism (Jung et al., 1998), where only the changes in the SPR peak minimum angle and the angle of total internal reflection (TIR) are used in the analysis. Jung formalism allows to quantify the addition of analyte mass due to the interactions with the membrane.

4.3.1   FRESNEL-LAYER MATRIX FORMALISM

Fresnel-layer matrix formalism is the basis for the theoretical description of the reflectance of light from the optical SPR system in a Kretschmann configuration. A prism (p) is used to couple p-polarized light in a way that excites surface plasmons at the metal-bulk medium interface at a specific resonance angle, SPR peak minimum angle (θ_{SPR}). The resonance requires matching of the wave vector components of the incident light and surface plasmons, parallel to the sensor surface. In the vicinity of the metal boundary, perturbations in the refractive index induce shifts in the SPR peak minimum angle due to a change in the resonance condition. The addition of molecules is modeled by an additional homogeneous film layer between the metal and bulk medium (b), which can be gaseous or liquid. The Fresnel reflection coefficient for p-polarized light is written as (Johnston et al., 1995; Kooyman, 2008, p. 28):

$$r_p(\theta) = \frac{(M_{(1,1)} + M_{(1,2)}Q_b)\,Q_p - (M_{(2,1)} + M_{(2,2)}Q_b)}{(M_{(1,1)} + M_{(1,2)}Q_b)\,Q_p + (M_{(2,1)} + M_{(2,2)}Q_b)}, \qquad (4.3\mathrm{a})$$

$$Q_x = (1/n_x^2)\sqrt{n_x^2 - n_p^2\sin^2\theta}, \quad x = p, b\,, \qquad (4.3\mathrm{b})$$

where (i, j) are the elements of a matrix $M = M_1 \cdot \ldots \cdot M_N$. The individual matrices M_k represent the layer $k = 1,\ldots,N$ between the prism and bulk medium and depend on the angle of incidence for the laser light (θ), the wavelength of the light in vacuum (λ_0), optical thickness (d_k), refractive indices of the layer (n_k) and the prism (n_p). Since the measured reflectance curve without the bilayer (l) is first used to find the unknown system-dependent parameters, only d_l and n_l, i.e. the physical properties of the bilayer, are left to solve; however, a continuum of possible solutions for d_l and n_l exists for one measurement with specific experimental conditions. In contrast, the use of two different bulk media in two measurements, preferably air and liquid, results in two sets of reflectance curves; this allows for the determination of an exact, analytical, solution (Granqvist et al., 2013). Alternatively, multiple wavelengths may be used, given that the dispersive characteristics of the bilayer are known, i.e. the wavelength-dependence of the refractive index $n_l(\lambda)$

(Peterlinz & Georgiadis, 1996; Zhou et al., 2001). In practice, a linear relationship (constant $dn/d\lambda$) between the refractive indices is assumed.

In principle, solving both d_l and n_l would give useful information about the structural changes in the membrane, i.e. the net changes in both the optical membrane thickness and concentration of molecules; however, uncertainties in the bulk refractive index, n_b, introduces additional problems regarding the determination of the solutions for d_l and n_l using dual-wavelength analysis. In study **II**, this challenge was addressed by varying n_b for the other wavelength until an acceptable range was established for d_l and the linear dispersion coefficient $dn/d\lambda$. Due to the sensitivity of the instrument to the changes in n_b, it was not further pursued to resolve both optical thickness and refractive index after a binding event for an analyte. Therefore, the simpler Jung formalism was later adopted.

4.3.2   JUNG FORMALISM

The formalism developed by Jung et al. (1998) relates the change in the SPR peak angle minimum to the wavelength-dependent optical properties of the adsorbed film (n_l, d_l) and two system-related parameters, sensitivity coefficient (S) and decay length (δ) of the evanescent electric field perpendicular to the sensor normal:

$$\Delta\theta_{\text{SPR}} = R = S\,(n_l - n_b)\left(1 - e^{-d_l/\delta}\right) \approx S\,(n_l - n_b)\frac{d_l}{\delta} \qquad (4.4)$$

where R is the *response* of the SPR instrument in the limit $d_l \ll \delta$, which approximately holds for a lipid bilayer. From now on, the response is assumed to have been corrected for the bulk effect, i.e. variations in n_b during the measurement (Fig. 4.1). This is achieved by measuring the sensitivity of the instrument for the changes in the bulk refractive index using a noninteracting solute. Since the refractive index of a liquid with dissolved analyte has an approximately linear dependency on the bulk concentration of the analyte, Jung model is rewritten as follows:

$$R = S\,(dn/dC_*)\frac{\Gamma_{\text{dry}}}{\delta}, \qquad (4.5)$$

where (dn/dC_*) is the refractive index increment in reference to the bulk concentration C_*, and $\Gamma_{\text{dry}} = c_l d_l$ denotes the surface-mass density (mass per unit area) of the bilayer which is the product of the lipid concentration and optical bilayer thickness. Surface-mass density is referred to as "dry" mass, since in SPR, the surface-mass density does not vary with different amounts of coupled water associated with the bilayer.

The refractive index increment can be derived from literature, or alternatively, measured using the surface plasmon resonance instrument by calculating the change in the bulk refractive index ($\Delta n_b \sim \Delta\theta_{\text{TIR}}$) as a function of the molar analyte concentration (Liang et al., 2010). (dn/dC_*) for lipid dispersions is not necessarily applicable for a lipid bilayer, thus it does not
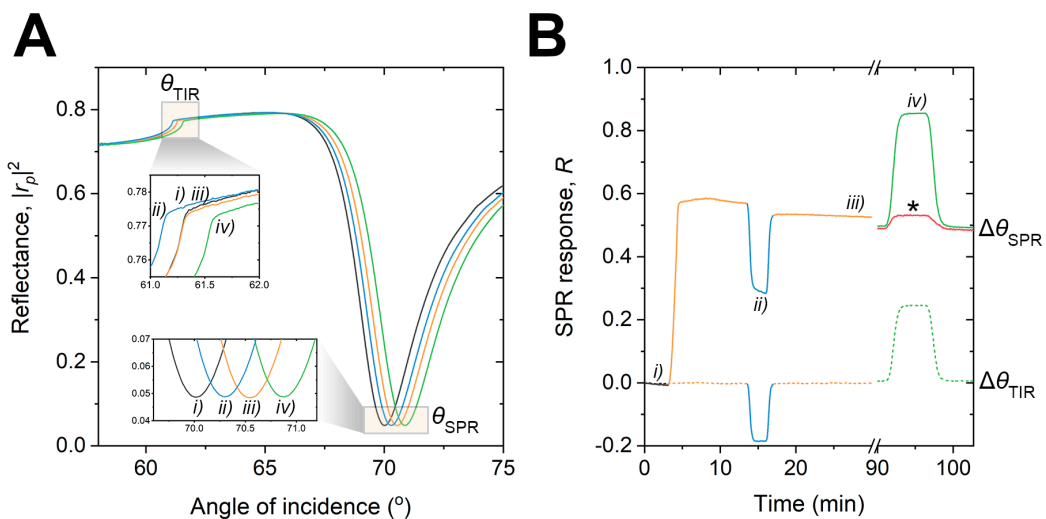
Figure 4.1 A) Reflectance of *p*-polarized light ($|r_p(\theta)|^2$) vs. angle of incidence (θ) in the MP-SPR setup based on the Kretschmann configuration. *i*) baseline, *ii*) water injection after SLB formation, *iii*) after SLB formation, *iv*) interaction with an SLB. B) The corresponding SPR response ($R = \Delta\theta_{SPR}$) (solid lines) and the change in TIR angle ($\Delta\theta_{TIR}$) vs. time. Asterisk marks the SPR response corrected for the bulk effect from $\Delta\theta_{TIR}$.

allow the calculation of surface-mass density directly from Eq. 4.5. The ($\mathrm{d}n/\mathrm{d}C_*$) for a lipid bilayer is, therefore, not a bulk parameter *per se* in Eq. 4.5, but a conversion factor. For the estimation of ($\mathrm{d}n/\mathrm{d}C_*$) for hydrated adsorbed molecules, such as lipids, the nonlinear equation based on the Lorenz-Lorentz relation can be used instead:

$$\mathrm{d}n/\mathrm{d}C_* = \frac{(n_{iso}^2 + 2)\left(r\,(n_b^2 + 2) - v(n_b^2 - 1)\right)}{3(n_{iso} + n_b)}, \tag{4.6}$$

where n_{iso} is the isotropic refractive index of the adsorbed film, r is the ratio of molar refractivity and molecular weight, and v is the inverse of the density of the pure film constituent (Cuypers et al., 1983; Reimhult et al., 2004; Salamon & Tollin, 2001). For lipids, the density of $\rho_l \approx 1.05\,\mathrm{g\,cm^{-3}}$ is assumed throughout this study (Mashaghi et al., 2008). From Γ_{dry}, the "dry" thickness can be estimated as

$$d_{dry} = v_l \Gamma_{dry}. \tag{4.7}$$

The reason for the use of isotropic refractive indices in calculating $\mathrm{d}n/\mathrm{d}C_*$ lies in the birefringence of lipid bilayers. Surface plasmon resonance instrumentation relying only on a plasmon excitation with *p*-polarized incident light does not resolve both ordinary and extraordinary refractive index components. For lipid bilayers exhibiting uniaxial birefringence, the measured values of n_l are closer to the refractive index of the extraordinary wave, which is approximately parallel to the lipid chains and the membrane

normal (Salamon et al., 1999). A coupled waveguide spectroscopy extension can provide the perpendicular component of the refractive index, or the isotropic refractive index could be estimated from the measurements (Mashaghi et al., 2008; Salamon & Tollin, 2001).

After the conversion of the measured response to surface-mass density, kinetics and partitioning of the analytes interacting with the supported lipid membrane can be described. The logarithm of the partition coefficient ($\log P$, for undissociated analyte species) and distribution coefficient ($\log D$, for all species at specific pH) are important descriptors in the pharmaceutical drug design process in predicting the extent of passive diffusion through membranes. Assuming that the binding follows kinetics where one analyte molecule binds to one binding site on the membrane (Figueira et al., 2017), the distribution coefficient is defined as follows (*kinetic model*):

$$D_m = \frac{\Gamma_a^{max}}{M_a d_l} K, \tag{4.8}$$

where Γ_a^{max} is the maximal surface-mass density capacity for the analyte binding to the membrane, K is the mole ratio distribution coefficient or the binding constant, and M_a is the molecular weight of the analyte. Maximal binding capacity is also related to the number of binding sites,

$$n = \frac{\Gamma_a^{max}}{\gamma \Gamma_{dry}} \frac{M_l}{M_a}, \tag{4.9}$$

where $\gamma \approx 0.5$ for a bilayer (Jodko-Piorecka & Litwinienko, 2013). The binding constant, K, is equivalent to the inverse of the dissociation constant, $K_d = k_d/k_a$, widely used in binding studies of ligands interacting with surface-deposited biomolecules. In the linear range of analyte concentrations, $C_f \ll K^{-1}$ (*linear model*),

$$D_m = \left(\frac{\Delta \Gamma_a}{\Delta C_f}\right) \frac{1}{M_a d_l}, \tag{4.10}$$

which is measured using the linear change in adsorbed surface-mass density (Γ_a) as a function of analyte concentration in bulk (C_f).

4.4   QUARTZ CRYSTAL MICROBALANCE (QCM)

Quartz crystal microbalance (QCM) utilizes piezoelectric properties of a quartz crystal. In the impedance-based QCM instrument (KSV Instruments Ltd, Helsinki, Finland) used, electric impedance is measured as a result of an alternating voltage coupled to a standing acoustical shear-wave above the sensor surface. Equivalent circuit analysis further relates the mechanical surface perturbations to the components of the complex impedance. Using classical Kelvin-Voigt, or viscoelastic modeling, the shift in the complex resonance frequency at different frequency harmonics ($N = 1,3,5,\dots$) in reference to the background shift from liquid (b_0) is modeled as follows

(Nalam et al., 2013; Rodahl & Kasemo, 1996; Voinova et al., 1998):

$$\Delta \tilde{f}_N = \Delta f_N + i \frac{f_0 N}{2} \Delta D_N$$

$$= -\frac{i f_0}{\pi \sqrt{\rho_q \mu_q}} \left[\sqrt{\tilde{\omega}_N} \left(\sqrt{\rho_{b_0} \eta_{b_0}} - \sqrt{\rho_b \eta_b} \right) \right. \tag{4.11}$$

$$\left. - \tilde{\omega}_N d_l \rho_l \left(1 - \frac{\tilde{\omega}_N \rho_l \eta_l}{\rho_l (K_l + \tilde{\omega}_N \eta_l)} \right) \right],$$

where $\tilde{\omega}_N = 2\pi i f_0 N$ is defined as the $2\pi i$-multiples of the fundamental frequency f_0 (4.95 MHz in the impedance-based QCM instrument used; ρ_q = density and μ_q = shear modulus of the quartz). The viscoelastic nature of the adsorbed film with density ρ_l and effective thickness d_l is described by the energy dissipation, ΔD, which depends on the viscosity (η_l) and elastic modulus (K_l) of the layer. The bulk effect due to high analyte concentrations is accounted for by deriving the variation in the product $\rho_b \eta_b$ from the measurements with an empty quartz crystal. In the limits $(\eta_l, K_l) \to \infty$, Eq.4.11 reduces to the linear Sauerbrey equation characterizing a rigid film. Eq. 4.11 was fully used in **IV**, while the Sauerbrey equation was used in **II**. In the SLB formation process, the film layer is initially viscoelastic as the vesicles are adsorbing on the surface, but the SLB, while formed, becomes rigidly coupled with the quartz crystal, seen as vanishing energy dissipation (Keller et al., 2000). Since Eq. 4.11 governs only the product of the effective film thickness and density, the model does not resolve both. The fitting of the data to the equations with different harmonics results in the surface-mass density

$$\Gamma_{\text{wet}} = d_l \rho_l, \tag{4.12}$$

where the surface-mass includes the coupled water, and usually ρ_l is taken from the literature, which leaves the d_l to be a variable. When used in parallel with the SPR instrument, this allows estimating the degree of hydration of the lipid bilayer through equation $\Gamma_{\text{water}} = \Gamma_{\text{wet}} - \Gamma_{\text{dry}}$ (Reimhult et al., 2004, 2006); however, synchronization of the flow in the two instruments is desirable to ensure similar conditions for the SLB formation (Viitala et al., 2012).

5 RESULTS AND DISCUSSION

In this chapter, the main results of the thesis are discussed. First, the effects that chemical modifications and lipid diversity may induce on physical membrane properties are described. Then parallels are drawn between the methodologies developed in the thesis and screening of drug-lipid interactions with experimental and computer-assisted workflows. The chapter concludes with an insight into the interplay between lipids and integral membrane protein catalysis relevant to the catecholamine metabolism and drug action.

5.1 SURFACE-SENSITIVE METHODOLOGIES REVEAL CHANGES IN THE PHYSICAL MEMBRANE PROPERTIES UPON CHEMICAL MODIFICATIONS

5.1.1 LATERAL ORGANIZATION OF THE MEMBRANE IS STABILIZED BY OXIDIZED LIPIDS

Diffusion times in POPC and POPC-PazePC monolayers are linearly proportional to the surface pressure (Fig. 5.1A), highlighting the finding that they mix ideally as a single L_d phase (Grauby-Heywang et al., 2016). While 25 % PazePC induces expansion in the critical area-per-lipid from 0.46 nm² to 0.50 nm², no differences in the diffusion times are seen between POPC and POPC-PazePC monolayers. On the contrary, in ternary raft mixtures (POPC-oxPL-SM-Chol), the disintegration of the distinct L_o domains, miscibility transition, is highlighted by an abrupt increase in the diffusion times of the L_d-partitioning fluorophore (Fig. 5.1B). Quantitatively, this is marked as a position of the maximal slope of the $\tau_D(\Pi)$ curve, giving miscibility transition pressures of 11.7 mN/m (POPC-SM-Chol), 18.7 mN/m (25 % of POPC substituted by PazePC) and 20.4 mN/m (25 % of POPC substituted by PoxnoPC). Interestingly, the compression-expansion cycle performed for domain-forming mixtures with POPC and POPC-PazePC in the L_d-phase showed complete reversibility of the L_o-domain structures when the surface pressure was reduced back to the starting point (Fig. 5.1C). For POPC-PoxnoPC, by contrast, the expansion was first seen as a formation of striped structures and then as morphologically heterogeneous domains not corresponding to the initial structures. While the surface potential was not measured, this leads to the conclusion that the expansion of the monolayer induces a shift in the balance between line tension and dipolar interactions, where the latter drives the formation of the striped domains (Volinsky et al., 2012).
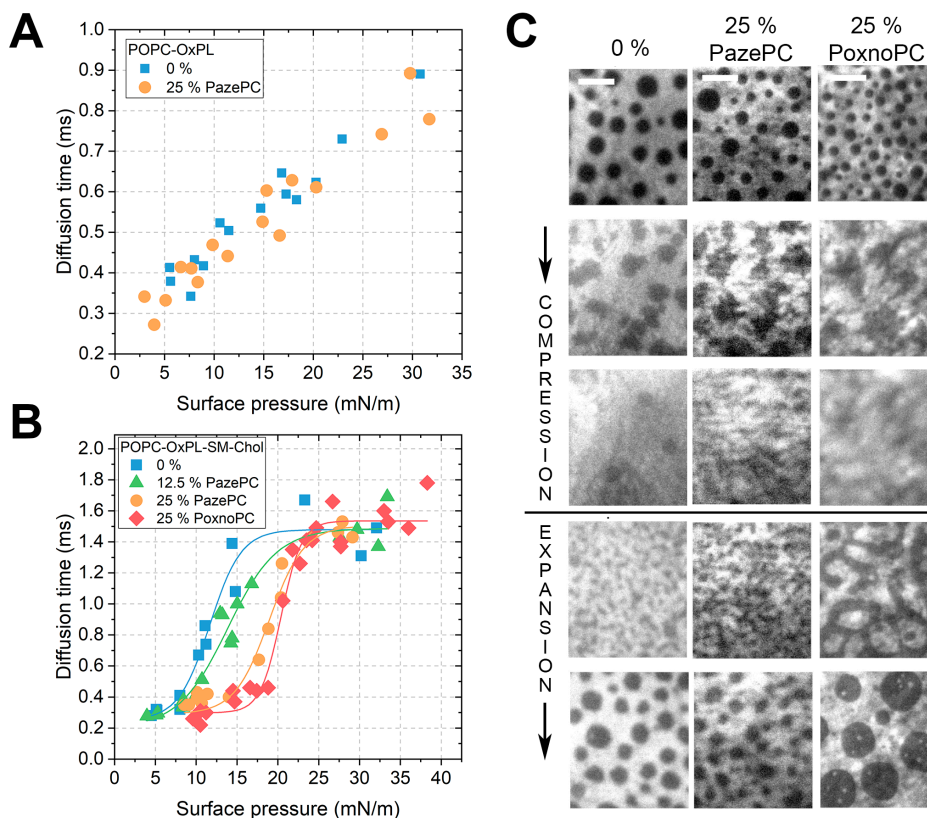
Figure 5.1 Diffusion time (τ_D) vs. surface pressure (Π) for A) POPC monolayers with 0 % or 25 % of POPC substituted by PazePC, B) POPC-SM-Chol (1.5:1.5:1) with 0 %, 12.5 %, or 25 % of the POPC fraction substituted by PazePC/PoxnoPC. C) Wide-field imaging of the POPC-SM-Chol mixtures with 0 or 25 % of the POPC fraction substituted by PazePC / PoxnoPC. Adapted from **I** (Figs. 2, 3, 5), with permission from Elsevier (see details on page **??**).

A previous study using Langmuir monolayers and Brewster angle microscopy highlighted that the prevalent mechanism in the domain stabilization by oxPLs is the modulation of line tension at the L_o-L_d phase boundaries (Volinsky et al., 2012). While the possibility that the domains merely shrink from microscale to nanoscale entities cannot be fully excluded, the sigmoidal shape of the diffusion time as a function of surface pressure suggests that the miscibility transition is genuinely a phase transition. The resemblance to the thermal phase behavior of diffusion coefficients measured for cushioned SLBs is evident (Sterling et al., 2013); however, four-component model membranes have demonstrated the possibility that the transition would be a manifestation of line tension modulating the domain size to a dimension not visible by optical means (Ackerman & Feigenson, 2015). WFM imaging further supports the view that the domains do not merge or change size during the transition as suggested (Volinsky et al., 2012), but rather the

height-mismatch-induced line tension keeping the circular domains intact is abruptly lost at critical surface pressure, resembling a transition to a single phase. The average sizes of the domains for oxPL-containing compositions were the same as for POPC-SM-Chol (**I**, Fig. 4). Therefore, the results do not support the notion that the line tension and dipole density would be able to modulate the domain size continuously (Lee et al., 2011). Nevertheless, nanoscale domains could still exist in the monolayer as dynamical entities that form and disintegrate at very fast timescales. In bilayers, these domains can be interleaflet-coupled (Vinklárek et al., 2019) and function as protein-sorting platforms (Stone et al., 2017), which can be seen as very heterogeneous diffusional behavior (Yamamoto et al., 2017). Indeed, the existence of nanodomains with roughly estimated sizes of 4–15 nm has been demonstrated in vesicles with similar composition than studied here (Pathak & London, 2011).

Regardless of the underlying mechanism of nanodomain regulation, the results suggest that oxPLs can modulate the L_o-L_d phase behavior by shifting the critical transition point. This has importance if the biomembrane exists under near-critical conditions (Cebecauer et al., 2018) with sensitivity to physical changes such as changes in the lateral pressure profile. The differences between PazePC and PoxnoPC can be attributed to the different acyl chain orientations (Beranova et al., 2010; Khandelia & Mouritsen, 2009). The aldehyde moiety in PoxnoPC, inducing chain orientation parallel to the membrane surface, may stabilize the domains via interactions with L_o components, while the more upwards oriented carboxyl moiety in PazePC interacts preferably with the interfacial cations. The partial chain reversal of PoxnoPC can also protect it from the recognition by macrophage scavenger receptors (Beranova et al., 2010; Greenberg et al., 2008). Local membrane thinning can further contribute to the height mismatch at the domain boundaries (Parra-Ortiz et al., 2019), and cholesterol stabilizes the peroxidation-induced perturbations (Štefl et al., 2014).

Although the miscibility transition here is governed by high cooperativity of only a few different lipid components, the enormous amount of different membrane constituents should contribute to the broadening of these transition events in biological membranes, analogous to the temperature phase transitions (Wallgren et al., 2012). As an opposing argument to domain stabilization, Brameshuber et al. (2016) demonstrated that the effect of oxPLs in live cell membranes may be indirectly destructive rather than stabilizing, thus affecting the nanoscale domain disintegration via modulation of sphingomyelinase activity. No physical consequences were associated with domain stability. This discrepancy with the model membrane studies is expected, given the complexity of biological membranes. Then, the fundamental limitations of the used methodologies should be acknowledged when considering the biological relevance of the results. Foremost, the experiments were performed with *i*) monolayers formed on an air-water interface, *ii*) domains with the micrometer size range and *iii*) ranges of miscibility transition pressures that do not correspond to the

currently-assumed equivalence pressures for monolayer-bilayer comparisons, i.e. 30–35 mN/m (Marsh, 1996). While the diffusion coefficients were not calculated due to the uncertainties of the monolayer axial positioning during the experiments, some estimations of the order of magnitude can be made assuming a reasonable beam waist diameter of 250 nm. Diffusion times of ~0.8 and ~1.5 ms at 32 mN/m for the nondomain and domain-forming monolayers would translate into 20 and 10 μm²/s, respectively. The range of 2–5 μm²/s has been measured for SLBs (Humpolíčková et al., 2006; Pincet et al., 2016; Przybylo et al., 2006; Sterling et al., 2013) and 4–8 μm²/s for free-standing bilayers (Pincet et al., 2016; Przybylo et al., 2006); however, quantitative comparisons between different studies are not straightforward, since the lateral diffusion is largely influenced by the used model system and properties of the chosen fluorophores. In live cells, diffusion coefficients are notably lower (Schneider et al., 2017), probably due to the extensive molecular crowding (Guigas & Weiss, 2016). For example, bi-modal distribution of diffusion coefficients with effective values of 0.04 and 0.3 μm²/s was observed in live neurons imaged by super-resolution microscopy (MacGillavry & Blanpied, 2013).

5.1.2 BIOPHYSICAL CHARACTERISTICS OF SUPPORTED LIPID BILAYERS

Morphologies of the vesicle-based model membrane systems depend on many factors, such as vesicle polydispersity and deformation under flow. Since SLBs are formed from these dispersive vesicle solutions, the aim of study **II** was to investigate the quality of the SLBs by evaluating their biophysical properties and to find instrument-specific parameters to differentiate between vesicle and bilayer arrangements on the sensor surface.

The refractive indices of 1.477–1.486 (Fig. 5.2B) obtained for the SLBs agree with both theoretical calculations (Huang & Levitt, 1977) and dual-polarization interferometry measurements where the bilayer was probed with two perpendicular polarization modes (Mashaghi et al., 2008). Although membrane "thickness" (Fig. 5.2A) is always a method-dependent structural quantity, it is of interest to compare the obtained structural data for SLBs with the information gained using the standard methodologies for membrane biophysics, namely x-ray and neutron scattering. The most distinct difference is seen between DOPC and POPC, where the unsaturation in the *sn*-1 chain increases the area-per-molecule (Fig. 5.2B) for DOPC from 0.62 to 0.65 nm². POPC had a higher average thickness (3.90 nm) than DOPC (3.81 nm). Kučerka et al. have measured values of 3.91 nm, 0.643 nm² for POPC (Kučerka et al., 2011), and 3.89 nm, 0.669 nm² at 30 °C (Kučerka et al., 2009). According to the results in study **II**, DOPS might induce lateral compression in the bilayer, as proposed previously (Petrache et al., 2004); however, differences are comparable to errors calculated from the three separate SLB depositions. The observed increase in hydration in DOPC-DOPS bilayers
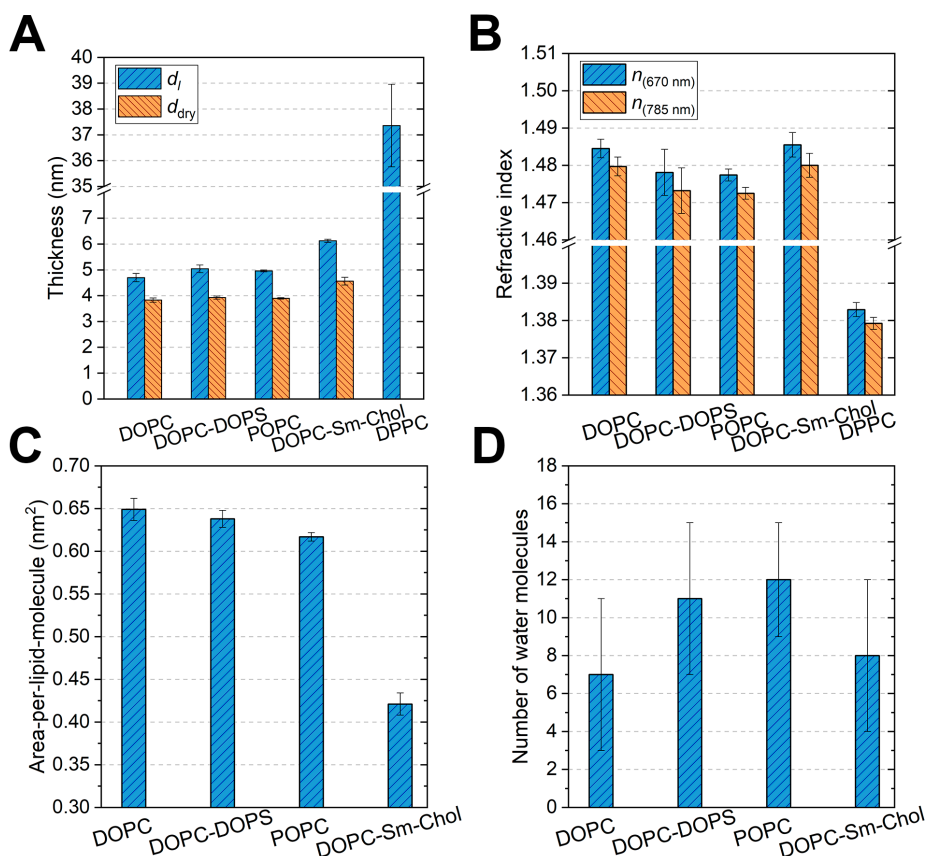
Figure 5.2 A) Modeled optical thickness and "dry" thickness for the SLBs. B) Refractive indices at 670 nm and 785 wavelengths obtained using inverse dual-wavelength modeling. C) Area-per-lipid-molecule of the SLBs. D) The number of water molecules per lipid associated with the SLBs. Molar ratios for lipid mixtures were 7:3 (DOPC-DOPS) and 1:1:1 (DOPC-SM-Chol). Adapted from **II** (Tables 1, 2) with permission from the American Chemical Society (see details on page **??**).

when compared to DOPC can arise from the electrostatic repulsions between the PS headgroups and the negatively-charged SiO_2 surface, or the increased hydration of the headgroups themselves. Approximately 13 water molecules per lipid were obtained for POPC using a similar parallel SPR-QCM approach (Reimhult et al., 2004); however, errors in the hydration calculations in study **II** were rather high due to the use of both SPR and QCM data in the analysis.

Membrane thickness of 4.56 nm and area-per-lipid-molecule of 0.42 nm^2 are close to the values for equimolar raft mixtures studied in atom-scale MD simulations (4.40 nm and 0.41 nm^2), where the latter is attributed to the strong condensing effect by cholesterol (Niemelä et al., 2007). The height difference between L_o and L_d domains can be roughly estimated as a thickness difference between DOPC and DOPC-SM-Chol, i.e. 0.7 nm, agreeing with the value of 0.6 nm found using AFM (Rinia et al., 2001). In conclusion,

biophysical characteristics of the formed DOPC-SM-Chol membranes support their suitability for further studies with membrane-binding ligands.

In addition to SLBs, SVLs composed of gel-phase DPPC vesicles were immobilized via nonspecific adsorption to the SiO_2 surface. Refractive indices for the SVLs, 1.36–1.38, agree with other studies for synthetic vesicle dispersions (Chong & Colbow, 1976) and EVs (Rupert et al., 2018). Layer thicknesses depended on the used procedure for analysis, but the possible values of 37 or 76 nm reflect the effect of partial vesicle coverage (estimated as 71 % in **II**, Table 3) in homogeneous Fresnel-layer modeling.

Optical modeling of the vesicle rupturing event (**II**, Fig. 3A) shows the possibility that, although the effective thickness of the surface-bound layer is increasing due to the vesicle adsorption, the change in refractive index is limited. Thus, the SPR response increases linearly in time; however, the SPR response results from the changes in both variables, and therefore, this homogeneous layer approach does not capture the exact morphological restructuring. Interestingly, it was recently demonstrated that ruptured SLB patches on the surface have accelerating edge fronts, which induce further rupture of the adsorbed vesicles (Mapar et al., 2018). The rupturing process in the optical modeling has a characteristic decrease in the linear dispersion coefficient ($dn/d\lambda$) from the initial value of the bulk ($-0.02 \cdot 10^{-3}$ nm^{-1}) to the values corresponding to the fully-formed lipid bilayer ($-0.04 \cdot 10^{-3}$ nm^{-1}). Since the magnitude of the dispersion coefficient was higher for fully-formed DOPC-SM-Chol SLBs, the decrease in the coefficient may reflect increased membrane order.

Another way to describe the optical dispersion is the ratio between the refractive index increments (Eq. 4.5) at two wavelengths, which is useful in vesicle size and concentration calculations (Rupert et al., 2014, 2016). Transformation of $dn/d\lambda$ using refractive index n (670 nm) = 1.48 results in the ratio of ~1.02, which has been used as a ratio of refractive index increments for the 670 nm and 785 nm wavelengths of the MP-SPR instrument (Rupert et al., 2016). The ratio of SPR responses at the two wavelengths ($R_{(670nm)}/R_{(785nm)}$), on the other hand, allows to qualitatively differentiate between vesicles and bilayer morphologies (~1.8 for SLBs, <1.7 for SVLs). The refractive index increments are also important in calculating the surface-mass densities using Eq. 4.5. The results suggest the ranges of 0.15–0.16 mL/g for SLBs and 0.13–0.15 mL/g for SVLs, depending on the wavelength. Therefore, in principle, the use of a refractive index increment for SVLs, usually 0.135 mL/g (Chong & Colbow, 1976; Ouberai et al., 2013), can lead to a roughly 20 % overestimation of the bilayer surface-mass density.

5.2 IMPLICATIONS FOR SCREENING DRUG-LIPID INTERACTIONS

5.2.1 INLINE MEASUREMENTS OF MEMBRANE DISTRIBUTION COEFFICIENTS

Fresnel-layer analysis performed in study **II** is not particularly useful for high-throughput applications. In study **IV**, the essential parameters describing the binding process were obtained after converting the measured SPR responses (R_a for analyte or drug, R_l for lipid bilayer) to surface-mass densities. If the acquired SPR response (R_a) is linearly proportional to the molar drug concentration in bulk (C), the distribution coefficient can be written to correspond to the formalism of Figueira et al. (2017):

$$D_m = \left(\frac{\Delta R_a}{\Delta C_f} \right) \frac{\mathrm{d}n/\mathrm{d}C_{l,*}}{\mathrm{d}n/\mathrm{d}C_{a,*}} \frac{\rho_l}{R_l M_a}, \tag{5.1}$$

where the lipid density (ρ_l), the molecular weight of the drug (M_a) and refractive index increment for lipids ($\mathrm{d}n/\mathrm{d}C_{l,*} \approx 0.155$ mL/g from **II**) are known, and the remaining refractive index increment of the drug is obtainable from the same SPR measurement inline. The corresponding equation for kinetic titration studies would be
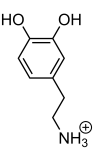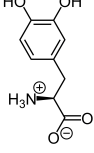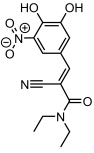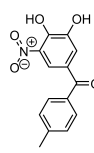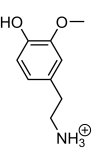
$$D_m = \frac{R_a^{max}}{R_l} \frac{\mathrm{d}n/\mathrm{d}C_{l,*}}{\mathrm{d}n/\mathrm{d}C_{a,*}} \frac{\rho_l K}{M_a}. \tag{5.2}$$

Therefore, analysis protocols in **IV** combined with the above formalisms allow the measurement of the drug distribution coefficients in a single-experiment format with a potential analysis required for saturable binding. The advantage of this approach is also the independence of Eqs. 5.1 and 5.2 from the sensor-dependent parameters, namely S and δ in Eq. 4.4. Since these parameters are sensitive to the wearing of the sensor over time, i.e. the changes in the SiO$_2$ layer thickness (**IV**, Fig. S1), the analysis presented would be suitable for sequential screening of drug candidates binding to the supported lipid bilayer. Current protocols suggest using supported vesicular systems, which involve multiple labor-intensive steps including characterization of vesicle coverage and morphology and numerous separate depositions over a wide range of analyte concentrations (Figueira et al., 2017; Olaru et al., 2015). Therefore, the presented approach suits for high-throughput applications, while sacrificing some advantageous properties of vesicular systems such as increased membrane fluidity when compared to SLBs.

5.2.2 PARALLELS TO LOG $D_{\text{OCT/W}}$

Octanol-water partition coefficient ($\log P_{\text{oct/w}}$) and its pH-dependent extension, distribution coefficient ($\log D_{\text{oct/w}}$), are essential descriptors of

Table 5.1 Data from the experiments for catechol compounds partitioning to the supported lipid bilayers. Molar ratios for lipid mixtures were 8:2 (PC-PS), 11:15:6 (PC-PE-PS) and 1:1:1 (PC-SM-Chol). Binding parameters K and n for L-dopa could not be calculated. The ratios of Michaelis constants, K_m (for substrates), or inhibition constants, K_i (for inhibitors), are calculated from a kinetic study (Lotta et al., 1995) for both isoforms. In the study of Lotta et al., S-COMT and MB-COMT were expressed in *Escherichia coli* and insect Sf9 cells, respectively. Reference values for the octanol-water partition coefficients are from Forsberg et al. (2005) and Mack & Bönisch (1979). Other data are adapted from **IV**, Table 1, with permission from the American Chemical Society (see details on page **??**).

	Dopamine	L-dopa	Entacapone	Tolcapone	3-methoxy-tyramine
Type	substrate	substrate	inhibitor	inhibitor	metabolite
Structure					
D_m					
PC	18	1.4	68	572	53
PC-PS	24	0.2	38	325	67
PC-PE-PS	16	0.6	52	343	47
PC-SM-Chol	10	0.5	28	253	13
$K_{m/i}^{(\text{S–COMT})}/K_{m/i}^{(\text{MB–COMT})}$	13.7	2.3	0.15	0.93	-
$\log D_{\text{oct/w}}^{\text{ref}}$	-2.48[a]	-2.39[a]	0.18[b]	1.03[b]	-2.22[a]
H-bonds	7	10	10	8	6
$\log D_{m,\text{pred}}$	1.66	1.02	2.14	2.94	1.94
$\log D_m$					
PC	1.26	0.14	1.83	2.76	1.72
PC-PS	1.37	-0.82	1.58	2.51	1.83
PC-PE-PS	1.21	-0.20	1.72	2.54	1.67
PC-SM-Chol	1.00	-0.27	1.45	2.40	1.12
K (M^{-1})					
PC	41		471	2754	304
PC-PS	48		384	1712	704
PC-PE-PS	23		406	2267	110
PC-SM-Chol	25		526	3030	243
n					
PC	0.66		0.22	0.31	0.76
PC-PS	0.74		0.15	0.29	0.73
PC-PE-PS	0.96		0.18	0.21	1.21
PC-SM-Chol	0.45		0.06	0.09	0.16

[a](Mack & Bönisch, 1979)
[b](Forsberg et al., 2005)

lipophilicity in drug design applications, particularly in quantitative structure-activity relationship modeling (Mälkiä et al., 2004). Interactions mainly arising from hydrogen bonding and electrostatic interactions with the hydrophilic lipid headgroups are, however, not taken into account by these descriptors. From a purely physicochemical point-of-view, these should be important for the studied catechol compounds in **IV** (Table 5.1). The interaction process can even be biphasic (Raimúndez-Rodríguez et al., 2019), where the molecule first partitions to the membrane-water interface, and subsequently, the more lipophilic moieties are driven inside the membrane. A simple linear model (**IV**, Eq. S15) was established to predict $\log D_m$ from the physicochemical factors (Table 5.1). Notably, the membrane partitioning measured for model membranes by (Osanai et al., 2013) and in **IV**, was characterized using only two descriptors: $\log D_{oct/w}$ and the sum of hydrogen bond donors and acceptors. Although Osanai et al. used ITC in their binding studies, other experimental factors were close to those in study **IV**. The use of more variables, such as polar surface area, or physiological charge, did not result in a better model, quantified with the calculated R^2-values. The result agrees with the evaluation of passive BBB permeability, where more than eight moieties capable of hydrogen-bonding usually does not allow passive permeation through BBB (Pardridge, 2007). Also, $\log D_{oct/w}$ can further reduce or increase partitioning capacity.

5.3 INTERACTION OF DRUGS & ENDOGENOUS CATECHOLS WITH THE LIPID MEMBRANE COULD BE INVOLVED IN THE CATECHOLAMINE METABOLISM

5.3.1 CATALYTIC MECHANISM OF MB-COMT

In molecular dynamics (MD) simulations, the structure of MB-COMT was modeled based on the existing S-COMT crystal structure, with the assumption of an α-helical transmembrane domain together with the putative structure for the flexible linker segment obtained previously (Orłowski et al., 2011). Biophysical techniques were used to investigate the differences in membrane binding of S-COMT with an identical soluble domain with MB-COMT, with (apo) and without (holo) the AdoMet cofactor. Isothermal titration calorimetry (ITC) experiments revealed that although the change in enthalpy is practically zero for S-COMT+AdoMet corresponding to the holo form, notable positive change in entropy can counteract this lack of favorable interactions. Then, the change in Gibbs free energy is slightly more negative for S-COMT+AdoMet when compared to COMT or AdoMet alone; however, as the soluble part of MB-COMT has restricted translational and rotational freedom due to its lipid-anchored extension, the interactions with the membrane may differ from the soluble COMT, which can diffuse freely. In MD

simulations, an initial decrease was seen in the distance between the catalytic domain and membrane-water interface and subsequent increase in hydrogen bonds between the domain and lipid headgroups over 100 nanosecond period (Fig. 5.3A). Thus, initially, the interactions with the membrane may be limited, but the hydrophobic effect upon the change in the catalytic domain conformation due to the binding of AdoMet drives the domain and the entire soluble part closer to the membrane. There, noncovalent interactions with the lipid headgroups may then act as stabilizers of the holo-structure, also supported by the potential of mean force calculations (**III**, Fig. 3). QCM and SPR further showed that holo S-COMT bind irreversibly to the supported lipid bilayer, while the binding of S-COMT and AdoMet alone was barely in the limit of the sensitivities of the instruments (Fig. 5.3C).
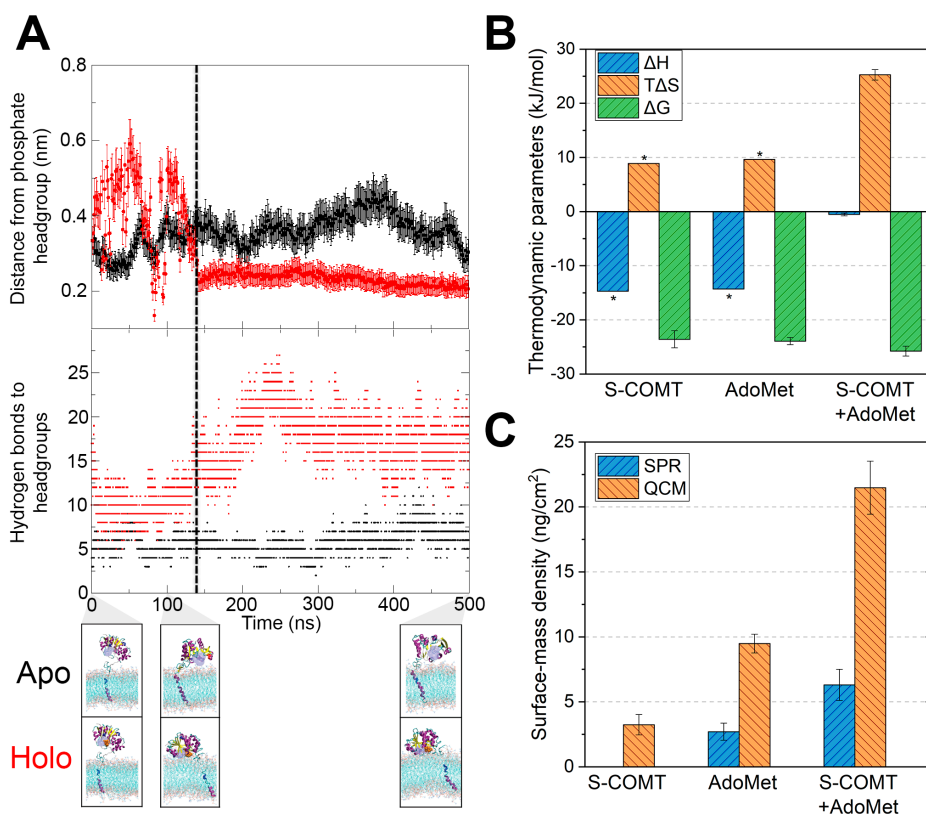
Figure 5.3 A) Distance between the phosphate headgroup and MB-COMT catalytic site and the number of hydrogen bonds formed between the catalytic site and membrane headgroups. Snapshots are shown from the simulation at 0, 100 and 500 ns timepoints. The dashed line marks the time when holo complex becomes attached to the membrane. B) Thermodynamical parameters calculated from ITC experiments. Asterisk marks the parameters with high uncertainty. C) Surface-mass densities calculated using approximative formulas $\Gamma_{SPR} \approx 600\,\Delta\theta_{SPR}$ and $\Gamma_{QCM} \approx 18\,(\Delta f_3/3)$. Adapted from **III** (Figs. 2, S10, & Table S4) with permission from the Royal Society of Chemistry (see details on page **??**).

The above results provide evidence for a membrane-mediated enzyme mechanism, where the holo MB-COMT operates at the membrane-water interface. Therefore, the first requirement for catalysis or inhibition of MB-COMT would be binding of the AdoMet cofactor to its binding site, and then, binding of an interfacial magnesium cation to the catalytic complex. Finally, the requirement for successful drug targeting of MB-COMT isoform, or substrate catalysis of endogenous catechols performed by the enzyme, may be: *i*) the sufficient partitioning of the drug to the lipid membrane and *ii*) the orientation of the hydroxyl moieties in the catechol ring in relation to the catalytic site (**III**, Fig. 1). In the next sections, these partitioning effects are discussed in more detail.

5.3.2   CATECHOL-MEMBRANE INTERACTIONS

Interactions with phosphatidylcholine (PC)

Much of the studies on dopamine-membrane interactions have highlighted the importance of anionic phospholipids in facilitating dopamine accumulation to membrane-water interface. On the other hand, zwitterionic PC has gained less attention due to the limitations of the used instrumentation (Jodko-Piorecka & Litwinienko, 2013; Orłowski et al., 2012). Studying the interaction of neurotransmitters with pure PC membranes is beneficial as a basis, since PC is the most abundant cellular membrane component. In Table 5.1, the membrane distribution coefficient for dopamine in the PC membrane is 18, which is the ratio of the local concentration of dopamine in the membrane and the concentration in bulk (Eqs. 4.10 & 4.8). Surface-mass density at the highest bulk dopamine concentration, $\sim$20 ng/cm^2, translates into $\sim$1.3 nm^2 per molecule, meaning that approximately every other PC molecule is associated with a dopamine molecule at saturation. The same conclusion arises from the kinetic modeling of the SPR data (**IV**, Fig. 1), which gives an estimated number of binding sites, i.e. 0.66 per lipid. Therefore, the interaction mechanism with PC could be primarily governed by the hydrogen bonding between the protonated amine and phosphate group of PC balanced with the electrostatic repulsions between the dopamine molecules and positive interfacial cations competing with the same binding sites. The calculated number of hydrogen bonds between the two moieties in previous MD simulations has been in the range of 0.275–0.805 depending on the membrane composition (Orłowski et al., 2012).

The notable increase in the distribution coefficient of 3-MT compared to dopamine ($\sim$3x) and irreversible binding to the SLB suggest that 3-MT can partition to the membrane interior. Since the binding was irreversible, the data in Table 5.1 presents the calculations of distribution coefficients using the linear equation, Eq. 4.10. The methylation effect may be similar to that of codeine, which has notably higher BBB permeability than morphine, without the additional methyl group (Hillery et al., 2002, p. 329; Oldendorf et al., 1972). Hypothetically, the addition of the methyl group could induce an

orientational shift where the catechol moiety becomes buried in the hydrophobic interior of the membrane. In contrast, the positively charged amine group remains at the membrane-water interface, likely in contact with the phosphate groups. Since the MAO enzyme metabolizes 3-MT in the outer leaflet of the mitochondrial membrane, high lipid affinity could be of importance to the effective disposal of intermediate neurotransmitter metabolites. For drugs, the opposite could be true. Indeed, high lipophilicity of tolcapone, with measured $\log D_m$ of ~2.8 in the PC membrane, can be a contributor to its *in vivo* liver toxicity (Chen et al., 2013).

L-dopa showed little preference towards the PC membrane, while for other model membranes, the partitioning was practically nonexistent. The limited solubility of L-dopa would not allow using higher analyte concentrations. The zwitterionic nature of the molecule with prominent hydrogen bonding capacity would explain the tendency of L-dopa to reside in the water phase. Therefore, physicochemical properties support limited passive permeability through the BBB, and thus active transport of L-dopa is likely needed (del Amo et al., 2008). In contrast, these properties seemed to enhance the membrane binding in the previous studies (Orłowski et al., 2012; Postila et al., 2016); L-dopa seemed to associate strongly with PC-SM-Chol and PC-PE-PS membrane models in Langmuir monolayer experiments and MD simulations.

Interactions with phosphatidylserine (PS)

The result that the addition of PS (20 %) to the PC membrane increases the membrane partitioning by ~30 % (Table 5.1) is in line with the previous findings on dopamine-PS interactions (Jodko-Piorecka & Litwinienko, 2013). Dopamine contains a protonated amine group at physiological pH, which can interact with the negatively-charged groups of PS, for example, through the formation of salt bridges. Interactions of PS with dopamine have been suggested to decrease the availability of neurotransmitters during apoptosis via accumulation to the membrane-water interface (Jodko-Piorecka & Litwinienko, 2013). Calcium may prevent this extensive accumulation to the inner leaflet of the presynaptic vesicle membranes (Mokkila et al., 2017), while in the postsynaptic cell membrane, PS-induced impairments could originate from the peroxidation-induced flip-flop of PS to the outer bilayer leaflet (Fadok et al., 1998; Volinsky et al., 2011). In Parkinson's disease, overproduction of the dopamine metabolism-induced lipid peroxidation products can then lead to disruptions in the membrane composition (Shamim et al., 2018), and therefore, lipid homeostasis. Also, the PS-modulated effects on the lateral packing and interfacial hydration (Fig. 5.2C & D) along with interfacial cation accumulation (Jurkiewicz et al., 2012; Petrache et al., 2004) highlight that the effects of these disruptions are numerous. Excess of PS may also induce membrane accumulation of 3-MT, possibly contributing to the dyskinesias during the L-dopa treatment (Sotnikova et al., 2010). In contrast to dopamine and 3-MT, distribution coefficients of the MB-COMT inhibitors tolcapone and entacapone decreased 43 % and 44 %, respectively, attributing

to their negative net charge in physiological pH. Therefore, PS may also function as a modulator of drug action.

Interactions with phosphatidylethanolamine (PE)

Although PC-PE-PS membranes showed lower partitioning for dopamine and 3-MT compared to PC-PS membranes at low concentrations, dopamine had notable binding to the membrane at 80 mM bulk concentration, which was the highest amount of dopamine used. The sterical unprotection of the PE amine group could explain the former finding, making it available for charge repulsion with the neuromodulators having the same positively-charged amine group. Deficiency in PE, which is prevalent in intracellular membranes where also MB-COMT should reside, has been linked to alterations in Parkinsonian α-synuclein homeostasis, leading to, e.g. the inhibition of ER to Golgi vesicle trafficking (Wang et al., 2014). Since the PE-induced defects in the SLB morphology cannot be ruled out, it is unclear whether the finding for the 80 mM bulk concentration is due to the specific interactions with PE or aggregation of the dopamine inside the supported membrane, however. Matam et al. (2016) demonstrated that dopamine permeating the lipid bilayer is indeed possible.

The choice of a ratio (11:15:6) for the PC-PE-PS lipid mixtures in **III** and **IV** was made based on the study of Orłowski et al. (2012), who modeled the endoplasmic reticulum membrane composition with such ratio. Molecular dynamics simulations of Orłowski et al. (2012) and Postila et al. (2016) have shown a notable increase in membrane binding of dopamine and L-dopa for these PC-PE-PS membranes compared to control membranes with PC only. This can be due to the overestimation of the binding of cations to PS, as demonstrated by the recent examination of the MD simulations for lipid bilayers with PS (Antila et al., 2019). Also, the study concluded that simulations fail to reproduce the order parameters from NMR experiments. Therefore, more modest partitioning of the compounds in experiments is plausible in comparison, and the differences between experiments and simulations should rise mainly from the interactions of the compounds with PS. In experiments, further investigations of the SLB morphology would be needed to optimize the PE content in the membrane and the SLB formation conditions for the studies of inner leaflet model membranes (Simonsson & Höök, 2012).

Interactions with sphingomyelin-cholesterol (SM-Chol)

Partitioning of the catechol molecules in PC-SM-Chol decreased when compared to other model membranes. Lateral segregation in the used equimolar composition of PC-SM-Chol might exist as nanodomains (Koukalová et al., 2017). While it is not possible to deduce if the diminished binding is due to the lack of specific interactions with domain structures, the

average percentage ratio of distribution coefficients for all compounds (PC-SM-Chol / PC), 40 % (Table 5.1), is surprisingly close to the relative amount of PC in the membrane. On the other hand, binding constants (K), or affinities, did not differ that much. Thus, it is important to note the difference between the binding affinity and binding capacity. Affinity is related to the amount of analyte which is needed to reach the half-maximal binding capacity. The distribution coefficient is also affected by the binding capacity, i.e. how many molecules per lipid are bound at full saturation (Eq. 4.8). These capacities (n in Table 5.1) were 32–79 % lower for the membranes containing sphingomyelin and cholesterol compared to pure PC membranes. A straightforward implication would then be that the reduced amount of these components in the inner leaflet of the postsynaptic cell membrane and intracellular membranes could contribute to the effective transport of neurotransmitters and their metabolites inside the postsynaptic neurons.

Although the specifics of the lipid compositions in postsynaptic neuron compartments are still unknown (Postila et al., 2016), individual membrane components, such as cholesterol and sphingolipids, are crucial to the synaptogenesis and synaptic function (Hussain et al., 2019). Understanding how these components cooperate with neurotransmitters is also vital in investigating how the synaptic membranes maintain their lateral order and lipid homeostasis (Tulodziecka et al., 2016) and how aging and neuropathological conditions are linked to lipid dyshomeostasis (Isacson et al., 2019). A comprehensive lipidomic analysis of the raft and nonraft fractions for both healthy brain and brain tissues showing PD-related pathological lesions did reveal a slight decrease in sphingomyelin and cholesterol content in the PD raft extracts (Fabelo et al., 2011); however, this difference was inferred as statistically insignificant. Similar findings exist for Alzheimer's disease lipidomics (Kawatsuki et al., 2019). Therefore, cell biological, lipidomic and biophysical insight to CNS pathologies is needed for a complete picture of the role of individual lipid components in these diseases, keeping in mind the uncertainties regarding SM-Chol-dependent asymmetrical organization in biological membranes (Levental et al., 2020). In the future, interaction studies with varying cholesterol and sphingomyelin content, along with incorporated oxidized lipid components, would elucidate the importance of each factor in the drug and neuromodulatory action.

5.3.3   IMPLICATIONS FOR ENZYME KINETICS

Partitioning of molecules to the membrane

In the traditional Michaelis-Menten kinetics of enzymatic reactions, the Michaelis constant, K_m, and the inhibition constant, K_i, are used in drug research to characterize the potential efficacy of new drugs before *in vivo* pharmacological studies. Higher values of these constants mean that the higher concentrations of the substrate or inhibitor are needed to reach the maximum catalytic rate of the system or inhibit the reaction maximally,

respectively. Therefore, it is plausible that the ratio of these constants in the absence of the membrane (S-COMT) and with the membrane (MB-COMT) could correspond to the ratio of analyte concentrations between the membrane and bulk, i.e. the distribution coefficient D_m. Similarly, lower maximal catalytic rate (V_{max}) for MB-COMT could be explained by the increased turnover time for the ligands resulting from the membrane interactions. This theory is also supported by the findings from the early studies that membrane solubilization using Triton-X effectively abolishes the differences in catalytic properties between the two isoforms (Jeffery & Roth, 1984). An alternative explanation is that substrates can bind to the extra *N*-terminal amino acids present in MB-COMT (Bai et al., 2007).

Based on the results in Table 5.1, the quantitative correlation between the ratio $K_{m/i}^{(S-COMT)}/K_{m/i}^{(MB-COMT)}$ and D_m is present for the substrates (dopamine, L-dopa), but not for the inhibitors (tolcapone, entacapone). Higher membrane affinity of tolcapone compared to entacapone is, however, qualitatively in line with that tolcapone is more specific to MB-COMT, also argued based on the potential of mean force calculations (**III**, Fig. S5). Tolcapone and entacapone are tight-binding inhibitors, with K_i's in the range of nanomoles per liter (Lotta et al., 1995; Nissinen et al., 1992). While inhibitory constants are more reliable than the commonly-used IC_{50}-values, which describe the relative inhibitory potency of compounds at specific experimental conditions, tight-binding nature of an inhibitor makes it challenging to make conclusions regarding the mode of inhibition (competitive or noncompetitive) and relative selectivity between the two isoforms (Borges et al., 1997). Also, if MB-COMT indeed functions as an interfacial enzyme, Michaelis-Menten kinetics could be only seen as a simplification of the underlying kinetics which has complex dependencies on the individual kinetic parameters of the enzyme-ligand and ligand-membrane interactions. Furthermore, molecular crowding in cells potentially makes the diffusion as a rate-limiting step in enzymatic reactions *in vivo* (Zotter et al., 2017).

Orientation of molecules in the membrane

In addition to partitioning between the membrane and water phases, catecholamine and drug action could be sensitive to the orientations of the molecules at the lipid-water interface. MD simulations performed for some of the inhibitors studied by Robinson et al. (2012) showed that inhibitors selective for MB-COMT (lower IC_{50}) would orient in the way that the hydroxyl groups susceptible to catalysis are closer to the membrane normal (**III**, Fig. 1). Tolcapone, which can also be methylated, mostly in the 3*O*-position (Jorga et al., 1999), has its 3*O*-hydroxyl close to parallel to the membrane normal on average (Fig. 5.4). The methylbenzene moiety in the opposing end, corresponding to nonpolar solvent toluene, is hydrophobic. A similar orientation has been previously experimentally proposed for dopamine (Matam et al., 2016), shown in Fig. 5.4. On the other hand, entacapone is
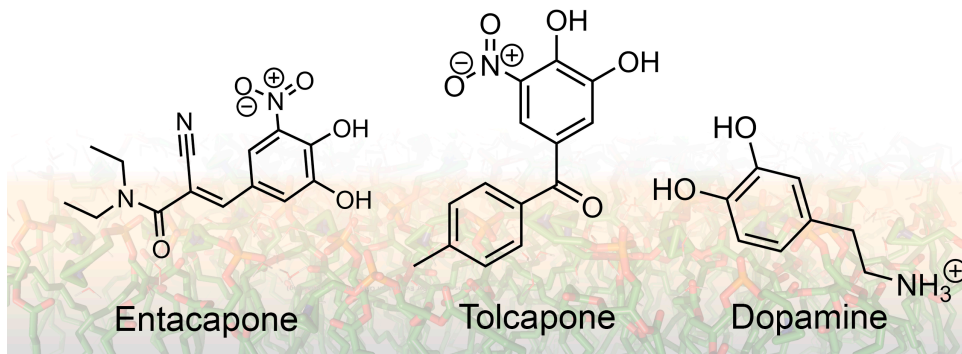
Figure 5.4 Artistic representation of the possible orientations for entacapone, tolcapone (from MD simulations in **II**, Fig. 1A) and dopamine (Matam et al., 2016) at the membrane-water interface.

more likely to orient parallel to the membrane surface, which would make the reactive groups less available for binding with the enzyme.

With these findings in mind, it is of interest to consider the physicochemical features of few potent MB-COMT inhibitors developed during recent years. First, some of the nitrocatechol-based compounds studied by Silva et al. (2016) showed high BBB permeability, lipophilicity and preference towards the rat brain COMT, comparable to tolcapone. Interestingly, molecules that were generally more specific towards total brain COMT contain chemical groups that make parts of the molecule excluding the nitrocatechol ring more lipophilic, and to some extent, have reduced polar surface area. Four most selective molecules had the ratio of IC_{50} values between 17.2 and 27.3, while the ratio of $c \log P$'s between the part excluding the catechol moiety and the entire molecule, is 0.69 to 0.75. For the two least specific molecules with IC_{50} ratios of 0.55 and 1.83, the corresponding ratios are -0.28 and -0.19, respectively. It is then plausible that lipophilicity of the molecule at the opposing end of the nitrocatechol ring would make the molecule orient at the membrane-water interface in the same manner as tolcapone. While $\log P_{\text{oct/w}}$ may not be an accurate predictor of membrane partitioning for charged and polar compounds, as discussed, it can be useful in the presented exploratory comparisons.

Pinheiro et al. (2019) showed later that one of the compounds of their previous study, CNCAPE, inhibited brain MB-COMT (IC_{50} of 2.4 nM) as much as tolcapone, while inhibitory potency in the liver was much lower (27.0 nM for liver MB-COMT and 213.0 nM for liver S-COMT). 8-hydroxyquinolines studied by Buchler et al. (2018) showed notable potency towards human MB-COMT, but the parallels with the theories presented are less clear due to the presence of the quinoline moiety instead of a catechol ring. Nevertheless, nonpolar extensions introduced to the quinoline moiety via a sulfonyl group seem to enhance MB-COMT selectivity, while the polar trifluoromethyl group ($-CF_3$) at the end of a benzene extension diminished it. Optimization of the

physicochemical properties of both the reactive part of a drug and the opposite lipophilic moieties, therefore, offer exciting possibilities for the design of novel MB-COMT selective compounds using *in silico* approaches, much needed for constantly-more expensive drug development pipelines.

6 FUTURE PROSPECTS

This thesis has highlighted the importance of the lipid membrane in integral membrane protein functionality. Despite the outstanding advances in the field of structural biophysics, membrane protein structures remain vastly underrepresented in the structural databases. Cryo-EM and NMR techniques, in particular, have evolved to the point where it is feasible to study integral membrane proteins, relevant drug targets, in their natural lipid environment (Baker et al., 2018; Shiraishi et al., 2018; Yin & Flynn, 2016). Based on the view of the critical role of lipids in the protein functionality, structures derived using detergent-based solubilization methods should be revisited (Chipot et al., 2018) and new detergent-free platforms developed (Lee et al., 2016; Lundgren et al., 2018; Parmar et al., 2018; Simeonov et al., 2013). Also, chemical synthesis and modification methods for the *de novo* production of structurally sensitive membrane proteins have exciting possibilities for proteins that are difficult to purify (Agouridas et al., 2019; Baumruck et al., 2018). Approaches in lipidomics (Bolla et al., 2019; Shamim et al., 2018) and microarray technologies (Saliba et al., 2015) used in tandem with the information gained from structural biology may aid in establishing connections between lipid homeostasis and lipid-assisted dynamical folding of membrane proteins (Dowhan et al., 2019).

Progress in the biophotonic methodologies is essential to the studies of biological processes. Improvement in the spatiotemporal resolution from the current instruments is required to resolve the nanoscale dynamical events in model systems and living organisms. Recently, combinations of different microscopy techniques have demonstrated the importance of the actin cytoskeleton in regulating plasma membrane diffusion (Schneider et al., 2017), and three-dimensional diffusion has been measured in living cells using STED-FCS (Lanzanò et al., 2017). Guo et al. (2018) improved the lateral resolution of TIRF microscopy to 115 nm using instant structured illumination microscopy. Novel holography techniques can provide insight into how cells react to environmental changes due to drugs, for example (Midtvedt et al., 2019). Multi-wavelength (Lakayan et al., 2019) and label-enhanced (Eng et al., 2018, 2016) extensions of the SPR instrumentation increase the capabilities of analysis and sensitivity, respectively. The uncertainties due to the existence of multiple unknown system parameters are also reduced. Localized SPR (Lee et al., 2018; Olaru et al., 2015) and time-resolved surface-enhanced Raman scattering spectroscopy (Kögler et al., 2020) are examples of label-free biophotonic techniques which have improved sensing capabilities compared to their predecessors (Wang et al., 2017). Molecular dynamics simulations and computational analysis workflows are useful tools to complement experiments in the investigations of drug action (Fantin et al., 2019; Riedlová et al., 2017; Rodríguez-Espigares et al., 2018) and cellular functions (Bocharov et al., 2019; Enkavi et al., 2019; Postila et al., 2016). In

this regime, the efforts to improve the correlation between the simulations and experiments (Antila et al., 2019; Javanainen et al., 2018) are continuing. All methodologies above accompany each other in the investigations of the interactions between lipid environment, membrane proteins and drug compounds related to biological function and states of disease.

Kinetics of the chemical reactions at the lipid-water interface (Bondar & Keller, 2018; Bondar & Lemieux, 2019) and the mechanisms driving heterogeneity of the membranes still need further clarification, especially concerning membrane curvature and lipid asymmetry (Cebecauer et al., 2018; Sezgin et al., 2017). Drug delivery strategies for currently untreatable diseases both in CNS and periphery benefit from comprehensive characterization studies on extracellular vesicles (Maeki et al., 2018; Rupert et al., 2018, 2016; Saari et al., 2015), also concerning the role of lipids in their functionality (Holopainen et al., 2019). The presence of membrane-bound catechol-*O*-methyltransferase (MB-COMT) activity in EVs and microsomes from rat hepatocytes (Casal et al., 2016) and the role of EVs in neurodegenerative diseases (Quek & Hill, 2017) have particularly interesting parallels to the topics of this thesis. The formation of protein corona structures on the surfaces of natural and endogenous vesicle carriers in bodily fluids have important implications for both drug delivery applications (Giulimondi et al., 2019; Zhang et al., 2019) and understanding processes involved in complex diseases such as cancer (Caracciolo et al., 2019) and Alzheimer's disease (Nandakumar et al., 2020). For example, the viral protein corona of herpes simplex virus type 1 can modulate the amyloid β-peptide aggregation relevant in amyloid plaque pathologies (Ezzat et al., 2019).

Apo- and holo-structures of the entire MB-COMT protein in the presence of the lipid membrane should provide more insight into its catalytic mechanism; however, previous efforts to purify MB-COMT in its catalytically active form (Pedro et al., 2018, 2015) suggest the protein is inherently unstable outside its natural environment. Meanwhile, biophysical tools combined with protein expression and peptide chemistry techniques can elucidate the functionality of individual protein segments of MB-COMT, such as the linker region with a putative location in the membrane-water interface. These studies can explicate the function of catalytic membrane proteins with similar topological properties, abundant in the human proteome. Finally, the development of novel COMT inhibitors for CNS targeting continues, with an increasing focus on the BBB permeability and selectivity for the membrane-bound isoform (Buchler et al., 2018; Pinheiro et al., 2019; Silva et al., 2016).

7 CONCLUSIONS

Various biophysical techniques were utilized in this thesis for studying model lipid membranes. For the first time, *fluorescence correlation spectroscopy* was combined with a *Langmuir monolayer trough* to investigate the dynamics of domain-forming model membranes (**I**). The main challenge was that multiple fluorescence intensity time traces had to be recorded by scanning along the optical axis. After the autocorrelation analysis of the time traces, the minimum diffusion times corresponding to the positions of the monolayer could be extracted, and these diffusion times were then related to the surface pressures measured simultaneously. As a principal method in the thesis, multi-parametric *surface plasmon resonance* in a dual-wavelength format was employed, allowing nanoscale characterization of supported lipid bilayers and quantitative analysis of analyte-lipid interactions. While Fresnel-layer analysis in a proprietary software was used in the characterization of the SLBs (**II**), the Jung model was later adopted in a home-made Python workflow for the bulk effect correction and data analysis (**IV**). As a complementary technique, impedance-based *quartz crystal microbalance* provided information regarding the sensor-coupled water to find the exact solutions for the biophysical properties of the SLBs (**II**). In the studies of the binding of catechol analytes to the SLBs (**IV**), significant differences in the surface-mass densities calculated for SPR and QCM techniques suggest that the frequency and energy dissipation shifts in QCM can be strongly influenced by factors not related to the actual analyte binding. After the analyte binding, the viscoelastic modeling of the SLBs resulted in vast mass variations between membrane formulations, even after taking into account the changes in bulk properties due to the high concentrations of analytes. Finally, *isothermal titration calorimetry* was used to study the thermodynamics of the S-COMT–vesicle interactions (**III**). The non-sigmoidal decrease in the heights of the enthalpy peaks upon the titration of vesicles may have resulted in a high error of the modeled thermodynamical parameters, probably because concentrations of the interaction constituents were not optimized in the binding assay. The results are qualitatively in line with the SPR and QCM measurements, however, which showed irreversible membrane binding of S-COMT together with the AdoMet cofactor.

Drug action can be understood as a delicate interplay between the essential molecular constituents composing the local environment of the drug target. These targets may be membrane proteins which function directly at the lipid-water interface, demonstrated in this thesis by the proposed action of membrane-bound catechol-*O*-methyltransferase, an essential target for many anti-Parkinson agents (**III**). Sufficient local concentration and proper orientation of a drug in the interface could be a requirement for the drug-target binding (**III**, **IV**). Consequently, since the changes in the membrane composition and morphology may modulate drug action (**IV**), the

characterization of lipid membranes and the development of tools for their analysis is critical (**I, II**). Peroxidation-induced acyl chain truncation of the lipid tails may influence the dynamics of domain structures enriched with sphingomyelin and cholesterol (**I**). These results suggest that these modifications might compromise the intrinsic physical properties maintained in the membranes, despite that the correspondence of these structures to the heterogeneities in biological membranes is still under debate. Phosphatidylserine can modulate the drug action via electrostatic interactions, and the inclusion of sphingomyelin and cholesterol in model membranes with phosphatidylcholine effectively diminishes the interaction of catechol compounds with the membrane (**IV**). Therefore, deviations from the natural prevalence and distribution of the membrane constituents might be detrimental for neuronal function. In conclusion, the results of this thesis highlight the relationships between lipid membranes and the action of drugs and other small molecular compounds with membrane protein targets. The thesis also describes the analysis and modeling protocols for surface-sensitive analytical technologies, which can aid future drug screening efforts and studies of biological interactions using model lipid membranes.

REFERENCES

Abadian P.N., Kelley C.P. & Goluch E.D. Cellular analysis and detection using surface plasmon resonance techniques. Analytical Chemistry, 2014. 86(6): 2799–2812.

Abdiche Y.N. & Myszka D.G. Probing the mechanism of drug/lipid membrane interactions using Biacore. Analytical Biochemistry, 2004. 328(2): 233–243.

Ackerman D.G. & Feigenson G.W. Lipid Bilayers: Clusters, Domains and Phases. Essays in biochemistry, 2015. 57: 33–42.

Agouridas V., El Mahdi O., Diemer V., Cargoët M., Monbaliu J.C.M. & Melnyk O. Native Chemical Ligation and Extended Methods: Mechanisms, Catalysis, Scope, and Limitations. Chemical Reviews, 2019. 119(12): 7328–7443.

Amaro M., Filipe H.A., Prates Ramalho J.P., Hof M. & Loura L.M. Fluorescence of nitrobenzoxadiazole (NBD)-labeled lipids in model membranes is connected not to lipid mobility but to probe location. Physical Chemistry Chemical Physics, 2016. 18(10): 7042–7054.

Anderson T.H., Min Y., Weirich K.L., Zeng H., Fygenson D. & Israelachvili J.N. Formation of supported bilayers on silica substrates. Langmuir, 2009. 25(12): 6997–7005.

Andrecka J., Spillane K.M., Ortega-Arroyo J. & Kukura P. Direct observation and control of supported lipid bilayer formation with interferometric scattering microscopy. ACS Nano, 2013. 7(12): 10662–10670.

Antila H., Buslaev P., Favela-Rosales F., Ferreira T.M., Gushchin I., Javanainen M., Kav B., Madsen J.J., Melcr J., Miettinen M.S., Määttä J., Nencini R., Ollila O.H.S. & Piggot T.J. Headgroup Structure and Cation Binding in Phosphatidylserine Lipid Bilayers. Journal of Physical Chemistry B, 2019. 123(43): 9066–9079.

Atanasov V., Knorr N., Duran R.S., Ingebrandt S., Offenhäusser A., Knoll W. & Köper I. Membrane on a chip: A functional tethered lipid bilayer membrane on silicon oxide surfaces. Biophysical Journal, 2005. 89(3): 1780–1788.

Atkinson J., Epand R.F. & Epand R.M. Tocopherols and tocotrienols in membranes: A critical review. Free Radical Biology and Medicine, 2008. 44(5): 739–764.

Auluck P.K., Caraveo G. & Lindquist S. α-Synuclein: Membrane Interactions and Toxicity in Parkinson's Disease. Annual Review of Cell and Developmental Biology, 2010. 26(1): 211–233.

Ayola R., Condorelli D.F., Ragusa N., Renis M., Alberghina M., Stella A.M. & Lajtha A. Protein synthesis rates in rat brain regions and subcellular fractions during aging. Neurochemical Research, 1988. 13(4): 337–342.

Bai H.W., Shim J.Y., Yu J. & Bao T.Z. Biochemical and molecular modeling studies of the O-methylation of various endogenous and exogenous catechol substrates catalyzed by recombinant human soluble and membrane-bound catechol-O-methyltransferases. Chemical Research in Toxicology, 2007. 20(10): 1409–1425.

Baker L.A., Sinnige T., Schellenberger P., de Keyzer J., Siebert C.A., Driessen A.J., Baldus M. & Grünewald K. Combined 1H-Detected Solid-State NMR Spectroscopy and Electron Cryotomography to Study Membrane Proteins across Resolutions in Native Environments. Structure, 2018. 26(1): 161–170.

Barchet T.M. & Amiji M.M. Challenges and opportunities in CNS delivery of therapeutics for neurodegenerative diseases. Expert Opinion on Drug Delivery, 2009. 6(3): 211–225.

Baumgart T., Hess S.T. & Webb W.W. Imaging coexisting fluid domains in biomembrane models coupling curvature and line tension. Nature, 2003. 425(6960): 821–824.

Baumruck A.C., Tietze D., Steinacker L.K. & Tietze A.A. Chemical synthesis of membrane proteins: A model study on the influenza virus B proton channel. Chemical Science, 2018. 9(8): 2365–2375.

Beranova L., Cwiklik L., Jurkiewicz P., Hof M. & Jungwirth P. Oxidation changes physical properties of phospholipid bilayers: Fluorescence spectroscopy and molecular simulations. Langmuir, 2010. 26(9): 6140–6144.

Berg O.G., Gelb M.H., Tsai M.D. & Jain M.K. Interfacial enzymology: The secreted phospholipase A2-paradigm. Chemical Reviews, 2001. 101(9): 2613–2653.

Berg O.G., Yu B.Z., Rogers J. & Jain M.K. Interfacial Catalysis by Phospholipase A2: Determination of the Interfacial Kinetic Rate Constants. Biochemistry, 1991. 30(29): 7283–7297.

Binder W.H., Barragan V. & Menger F.M. Domains and Rafts in Lipid Membranes. Angewandte Chemie - International Edition, 2003. 42(47): 5802–5827.

Bocharov E.V., Nadezhdin K.D., Urban A.S., Volynsky P.E., Pavlov K.V., Efremov R.G., Arseniev A.S. & Bocharova O.V. Familial L723P Mutation Can Shift the Distribution between the Alternative APP Transmembrane Domain Cleavage Cascades by Local Unfolding of the η-Cleavage Site Suggesting a Straightforward Mechanism of Alzheimer's Disease Pathogenesis. ACS Chemical Biology, 2019. 14(7): 1573–1582.

Bolla J.R., Agasid M.T., Mehmood S. & Robinson C.V. Membrane Protein–Lipid Interactions Probed Using Mass Spectrometry. Annual Review of Biochemistry, 2019. 88(1): 85–111.

Bondar A.N. & Keller S. Lipid Membranes and Reactions at Lipid Interfaces: Theory, Experiments, and Applications. Journal of Membrane Biology, 2018. 251(3): 295–298.

Bondar A.N. & Lemieux M.J. Reactions at Biomembrane Interfaces. Chemical Reviews, 2019. 119(9): 6162–6183.

Bonifácio M.J., Palma P.N., Almeida L. & Soares-da Silva P. Catechol-O-methyltransferase and Its Inhibitors in Parkinson's Disease. CNS Drug Reviews, 2007. 13(3): 352–379.

Borges N., Vieira-Coelho M.a., Parada A. & Soares-da Silva P. Studies on the tight-binding nature of tolcapone inhibition of soluble and membrane-bound rat brain catechol-O-methyltransferase. The Journal of pharmacology and experimental therapeutics, 1997. 282(2): 812–7.

Borst J.W., Visser N.V., Kouptsova O. & Visser A.J. Oxidation of unsaturated phospholipids in membrane bilayer mixtures is accompanied by membrane fluidity changes. Biochimica et Biophysica Acta - Molecular and Cell Biology of Lipids, 2000. 1487(1): 61–73.

Brameshuber M., Sevcsik E., Rossboth B.K., Manner C., Deigner H.P., Peksel B., Péter M., Török Z., Hermetter A. & Schütz G.J. Oxidized Phospholipids Inhibit the Formation of Cholesterol-Dependent Plasma Membrane Nanoplatforms. Biophysical Journal, 2016. 110(1): 205–213.

Brown M.F. Modulation of rhodopsin function by properties of the membrane bilayer. Chemistry and Physics of Lipids, 1994. 73(1-2): 159–180.

Buchler I., Akuma D., Au V., Carr G., De León P., Depasquale M., Ernst G., Huang Y., Kimos M., Kolobova A., Poslusney M., Wei H., Swinnen D., Montel F., Moureau F., Jigorel E., Schulze M.S.E., Wood M. & Barrow J.C. Optimization of 8-Hydroxyquinolines as Inhibitors of Catechol O-Methyltransferase. Journal of Medicinal Chemistry, 2018. 61(21): 9647–9665.

Bunker A., Magarkar A. & Viitala T. Rational design of liposomal drug delivery systems, a review: Combined experimental and computational studies of lipid membranes, liposomes and their PEGylation. Biochimica et Biophysica Acta (BBA) - Biomembranes, 2016. 1858(10): 2334–2352.

Burré J., Sharma M., Tsetsenis T., Buchman V., Etherton M.R. & Südhof T.C. α-Synuclein promotes SNARE-complex assembly in vivo and in vitro. Science, 2010. 329(5999): 1663–1667.

Calafat B.J., Kuijpers T.W., Janssen H., Borregaard N., Verhoeven A.J., Roos D., Calafat J., Kuijpers T.W., Janssen H., Borregaard N., Verhoeven A.J. & Roos D. Evidence for small intracellular vesicles in human blood phagocytes containing cytochrome b558 and the adhesion molecule CD11b/CD18. Blood, 1993. 81(11): 3122–3129.

Cantor R.S. Lipid composition and the lateral pressure profile in bilayers. Biophysical Journal, 1999. 76(5): 2625–2639.

Caracciolo G., Safavi-Sohi R., Malekzadeh R., Poustchi H., Vasighi M., Zenezini Chiozzi R., Capriotti A.L., Laganà A., Hajipour M., Di Domenico M., Di Carlo A., Caputo D., Aghaverdi H., Papi M., Palmieri V., Santoni A., Palchetti S., Digiacomo L., Pozzi D., Suslick K.S. & Mahmoudi M. Disease-specific protein corona sensor arrays may have disease detection capacity. Nanoscale Horizons, 2019. 4(5): 1063–1076.

Casal E., Palomo L., Cabrera D. & Falcon-Perez J.M. A novel sensitive method to measure catechol-O-methyltransferase activity unravels the presence of this activity in extracellular vesicles released by rat hepatocytes. Frontiers in Pharmacology, 2016. 7: 501.

Cebecauer M., Amaro M., Jurkiewicz P., Sarmento M.J., Šachl R., Cwiklik L. & Hof M. Membrane Lipid Nanodomains. Chemical Reviews, 2018. 118(23): 11259–11297.

Cerione R.A., Strulovici B., Benovic J.L., Strader C.D., Caron M.G. & Lefkowitz R.J. Reconstitution of β-adrenergic receptors in lipid vesicles: Affinity chromatography-purified receptors confer catecholamine responsiveness on a heterologous adenylate cyclase system. Proceedings of the National Academy of Sciences, 1983. 80(16): 4899–4903.

Chan Y.H.M. & Boxer S.G. Model membrane systems and their applications. Current Opinion in Chemical Biology, 2007. 11(6): 581–587.

Chen J., Song J., Yuan P., Tian Q., Ji Y., Ren-Patterson R., Liu G., Sei Y. & Weinberger D.R. Orientation and cellular distribution of membrane-bound catechol-O-methyltransferase in cortical neurons: Implications for drug development. Journal of Biological Chemistry, 2011. 286(40): 34752–34760.

Chen M., Borlak J. & Tong W. High lipophilicity and high daily dose of oral medications are associated with significant risk for drug-induced liver injury. Hepatology, 2013. 58(1): 388–396.

Cheng F., Liu C., Jiang J., Lu W., Li W., Liu G., Zhou W., Huang J. & Tang Y. Prediction of drug-target interactions and drug repositioning via network-based inference. PLoS Computational Biology, 2012. 8(5).

Cherepanov D.A., Junge W. & Mulkidjanian A.Y. Proton Transfer Dynamics at the Membrane/Water Interface: Dependence on the Fixed and Mobile pH

Buffers, on the Size and Form of Membrane Particles, and on the Interfacial Potential Barrier. Biophysical Journal, 2004. 86(2): 665–680.

Cherezov V., Rosenbaum D.M., Hanson M.A., Rasmussen S.G., Foon S.T., Kobilka T.S., Choi H.J., Kuhn P., Weis W.I., Kobilka B.K. & Stevens R.C. High-resolution crystal structure of an engineered human β2-adrenergic G protein-coupled receptor. Science, 2007. 318(5854): 1258–1265.

Chipot C., Dehez F., Schnell J.R., Zitzmann N., Pebay-Peyroula E., Catoire L.J., Miroux B., Kunji E.R., Veglia G., Cross T.A. & Schanda P. Perturbations of Native Membrane Protein Structure in Alkyl Phosphocholine Detergents: A Critical Assessment of NMR and Biophysical Studies. Chemical Reviews, 2018. 118(7): 3559–3607.

Chiu S.W. & Leake M.C. Functioning nanomachines seen in real-time in living bacteria using single-molecule and super-resolution fluorescence imaging. International journal of molecular sciences, 2011. 12(4): 2518–2542.

Cho N.J., Frank C.W., Kasemo B. & Höök F. Quartz crystal microbalance with dissipation monitoring of supported lipid bilayers on various substrates. Nature Protocols, 2010. 5(6): 1096–106.

Cho N.J., Wang G., Edvardsson M., Glenn J.S., Hook F. & Frank C.W. Alpha-helical peptide-induced vesicle rupture revealing new insight into the vesicle fusion process as monitored in situ by quartz crystal microbalance-dissipation and reflectometry. Analytical Chemistry, 2009. 81(12): 4752–4761.

Chong C.S. & Colbow K. Light scattering and turbidity measurements on lipid vesicles. Biochimica et Biophysica Acta (BBA) - Biomembranes, 1976. 436(2): 260–282.

Christiaens B., Symoens S., Vanderheyden S., Engelborghs Y., Joliot A., Prochiantz A., Vandekerckhove J., Rosseneu M. & Vanloo B. Tryptophan fluorescence study of the interaction of penetratin peptides with model membranes. European Journal of Biochemistry, 2002. 269(12): 2918–2926.

Chung C.Y., Koprich J.B., Siddiqi H. & Isacson O. Dynamic changes in presynaptic and axonal transport proteins combined with striatal neuroinflammation precede dopaminergic neuronal loss in a rat model of AAV α-synucleinopathy. Journal of Neuroscience, 2009. 29(11): 3365–3373.

Conrad M. Molecular computing: the lock-key paradigm. Computer, 1992. 25(11): 11–20.

Cotton N.J., Stoddard B. & Parson W.W. Oxidative inhibition of human soluble catechol-o-methyltransferase. Journal of Biological Chemistry, 2004. 279(22): 23710–23718.

Cuypers P.A., Corsel J.W., Janssen M.P., Kop J.M., Hermens W.T. & Hemker H.C. The adsorption of prothrombin to phosphatidylserine multilayers quantitated by ellipsometry. Journal of Biological Chemistry, 1983. 258(4): 2426–2431.

Danielli J. The biological action of ions and the concentration of ions at surfaces. Journal of Experimental Biology, 1944. 20(2): 167–176.

de Kruijff B. Lipids beyond the bilayer. Nature, 1997. 386(6621): 129–130.

de Lau L.M., Verbaan D., Marinus J., Heutink P. & Van Hilten J.J. Catechol-O-methyltransferase Val158Met and the risk of dyskinesias in Parkinson's disease. Movement Disorders, 2012. 27(1): 132–135.

del Amo E.M., Urtti A. & Yliperttula M. Pharmacokinetic role of L-type amino acid transporters LAT1 and LAT2. European Journal of Pharmaceutical Sciences, 2008. 35(3): 161–174.

Dexter D.T., Carter C.J., Wells F.R., Javoy-Agid F., Agid Y., Lees A., Jenner P. & Marsden C.D. Basal Lipid Peroxidation in Substantia Nigra Is Increased in Parkinson's Disease. Journal of Neurochemistry, 1989. 52(2): 381–389.

Di Paolo G. & Kim T.W. Linking lipids to Alzheimer's disease: Cholesterol and beyond. Nature Reviews Neuroscience, 2011. 12(5): 284–296.

Dodd C.E., Johnson B.R.G., Jeuken L.J.C., Bugg T.D.H., Bushby R.J. & Evans S.D. Native E. coli inner membrane incorporation in solid-supported lipid bilayer membranes. Biointerphases, 2009. 3(2): FA59–FA67.

Dowhan W., Vitrac H. & Bogdanov M. Lipid-Assisted Membrane Protein Folding and Topogenesis. Protein Journal, 2019. 38(3): 274–288.

Dror R.O., Dirks R.M., Grossman J., Xu H. & Shaw D.E. Biomolecular Simulation: A Computational Microscope for Molecular Biology. Annual Review of Biophysics, 2012. 41(1): 429–452.

East J.M. & Lee A.G. Lipid Selectivity of the Calcium and Magnesium Ion Dependent Adenosinetriphosphatase, Studied with Fluorescence Quenching by a Brominated Phospholipid. Biochemistry, 1982. 21(17): 4144–4151.

Egan M.F., Goldberg T.E., Kolachana B.S., Callicott J.H., Mazzanti C.M., Straub R.E., Goldman D. & Weinberger D.R. Effect of COMT Val108/158 Met genotype on frontal lobe function and risk for schizophrenia. Proceedings of the National Academy of Sciences, 2001. 98(12): 6917–6922.

Eggeling C., Ringemann C., Medda R., Schwarzmann G., Sandhoff K., Polyakova S., Belov V.N., Hein B., Von Middendorff C., Schönle A. & Hell S.W. Direct observation of the nanoscale dynamics of membrane lipids in a living cell. Nature, 2009. 457(7233): 1159–1162.

Ehrig J., Petrov E.P. & Schwille P. Near-critical fluctuations and cytoskeleton-assisted phase separation lead to subdiffusion in cell membranes. Biophysical Journal, 2011. 100(1): 80–89.

Ellison D.W., Beal M.F. & Martin J.B. Phosphoethanolamine and ethanolamine are decreased in Alzheimer's disease and Huntington's disease. Brain Research, 1987. 417(2): 389–392.

Emamzadeh F.N. Role of Apolipoproteins and α-Synuclein in Parkinson's Disease. Journal of Molecular Neuroscience, 2017. 62(3-4): 344–355.

Enderlein J., Gregor I., Patra D., Dertinger T. & Kaupp U.B. Performance of fluorescence correlation spectroscopy for measuring diffusion and concentration. ChemPhysChem, 2005. 6(11): 2324–2336.

Eng L., Garcia B.L., Geisbrecht B.V. & Hanning A. Quantitative monitoring of two simultaneously binding species using Label-Enhanced surface plasmon resonance. Biochemical and Biophysical Research Communications, 2018. 497(1): 133–138.

Eng L., Nygren-Babol L. & Hanning A. Label-enhanced surface plasmon resonance applied to label-free interaction analysis of small molecules and fragments. Analytical Biochemistry, 2016. 510: 79–87.

Enkavi G., Javanainen M., Kulig W., Róg T. & Vattulainen I. Multiscale Simulations of Biological Membranes: The Challenge To Understand Biological Phenomena in a Living Substance. Chemical Reviews, 2019. 119(9): 5607–5774.

Erwin N., Sperlich B., Garivet G., Waldmann H., Weise K. & Winter R. Lipoprotein insertion into membranes of various complexity: Lipid sorting, interfacial adsorption and protein clustering. Physical Chemistry Chemical Physics, 2016. 18(13): 8954–8962.

Ezzat K., Pernemalm M., Pålsson S., Roberts T.C., Järver P., Dondalska A., Bestas B., Sobkowiak M.J., Levänen B., Sköld M., Thompson E.A., Saher O., Kari O.K., Lajunen T., Sverremark Ekström E., Nilsson C., Ishchenko Y., Malm T., Wood M.J., Power U.F., Masich S., Lindén A., Sandberg J.K., Lehtiö J., Spetz A.L. & EL Andaloussi S. The viral protein corona directs viral pathogenesis and amyloid aggregation. Nature Communications, 2019. 10(1): 1–16.

Fabelo N., Martín V., Santpere G., Raquel M., Torrent L., Ferrer I. & Díaz M. Severe Alterations in Lipid Composition of Frontal Cortex Lipid Rafts From Parkinson's Disease and Incidental Parkinson's Disease. Molecular Medicine, 2011. 17(9-10): 1107–1118.

Fadok V.A., Bratton D.L., Frasch S.C., Warner M.L. & Henson P.M. The role of phosphatidylserine in recognition of apoptotic cells by phagocytes. Cell Death and Differentiation, 1998. 5(7): 551–562.

Fanning S., Selkoe D. & Dettmer U. Parkinson's disease: proteinopathy or lipidopathy? npj Parkinson's Disease, 2020. 6(1): 1–9.

Fantin S.M., Parson K.F., Niu S., Liu J., Polasky D.A., Dixit S.M., Ferguson-Miller S.M. & Ruotolo B.T. Collision induced unfolding classifies ligands bound to the integral membrane translocator protein. Analytical Chemistry, 2019. 91(24): 15469–15476.

Ferreira T.M., Coreta-Gomes F., Ollila O.H.S., Moreno M.J., Vaz W.L. & Topgaard D. Cholesterol and POPC segmental order parameters in lipid membranes: Solid state 1H-13C NMR and MD simulation studies. Physical Chemistry Chemical Physics, 2013. 15(6): 1976–1989.

Fields C.R., Bengoa-Vergniory N. & Wade-Martins R. Targeting Alpha-Synuclein as a Therapy for Parkinson's Disease. Frontiers in Molecular Neuroscience, 2019. 12.

Figueira T.N., Freire J.M., Cunha-Santos C., Heras M., Gonçalves J., Moscona A., Porotto M., Salomé Veiga A. & Castanho M.A. Quantitative analysis of molecular partition towards lipid membranes using surface plasmon resonance. Scientific Reports, 2017. 7: 45647.

Fillerup D.L. & Mead J.F. The Lipids of the Aging Human Brain. Lipids, 1967. 2(4): 295–298.

Forsberg M.M., Huotari M., Savolainen J. & Männistö P.T. The role of physicochemical properties of entacapone and tolcapone on their efficacy during local intrastriatal administration. European Journal of Pharmaceutical Sciences, 2005. 24(5): 503–511.

Francis A., Whittemore R., Jeffery D.R., Pearce L.B. & Roth J.A. Catecholamine-metabolizing enzyme activity in the nigrostriatal system. Biochemical Pharmacology, 1987. 36(13): 2229–2231.

Gelb M.H., Min J.H. & Jain M.K. Do membrane-bound enzymes access their substrates from the membrane or aqueous phase: Interfacial versus non-interfacial enzymes. Biochimica et Biophysica Acta (BBA) - Molecular and Cell Biology of Lipids, 2000. 1488(1-2): 20–27.

Giess F., Friedrich M.G., Heberle J., Naumann R.L. & Knoll W. The protein-tethered lipid bilayer: A novel mimic of the biological membrane. Biophysical Journal, 2004. 87(5): 3213–3220.

Giulimondi F., Digiacomo L., Pozzi D., Palchetti S., Vulpis E., Capriotti A.L., Chiozzi R.Z., Laganà A., Amenitsch H., Masuelli L., Mahmoudi M., Screpanti I., Zingoni A. & Caracciolo G. Interplay of protein corona and immune cells controls blood residency of liposomes. Nature Communications, 2019. 10(1): 1–11.

Gorbenko G.P. & Kinnunen P.K. The role of lipid-protein interactions in amyloid-type protein fibril formation. Chemistry and Physics of Lipids, 2006. 141(1-2): 72–82.

Granqvist N., Liang H., Laurila T., Sadowski J., Yliperttula M. & Viitala T. Characterizing ultrathin and thick organic layers by surface plasmon resonance three-wavelength and waveguide mode analysis. Langmuir, 2013. 29(27): 8561–8571.

Granqvist N., Yliperttula M., Välimäki S., Pulkkinen P., Tenhu H. & Viitala T. Control of the morphology of lipid layers by substrate surface chemistry. Langmuir, 2014. 30(10): 2799–2809.

Grauby-Heywang C., Moroté F., Mathelié-Guinlet M., Gammoudi I., Faye N.R. & Cohen-Bouhacina T. Influence of oxidized lipids on palmitoyl-oleoyl-phosphatidylcholine organization, contribution of Langmuir monolayers and Langmuir–Blodgett films. Chemistry and Physics of Lipids, 2016. 200: 74–82.

Gray E., Karslake J., Machta B.B. & Veatch S.L. Liquid general anesthetics lower critical temperatures in plasma membrane vesicles. Biophysical Journal, 2013. 105(12): 2751–2759.

Greenberg M.E., Li X.M., Gugiu B.G., Gu X., Qin J., Salomon R.G. & Hazen S.L. The lipid whisker model of the structure of oxidized cell membranes. Journal of Biological Chemistry, 2008. 283(4): 2385–2396.

Grimm M.O., Grimm H.S. & Hartmann T. Amyloid beta as a regulator of lipid homeostasis. Trends in Molecular Medicine, 2007. 13(8): 337–344.

Guigas G. & Weiss M. Effects of protein crowding on membrane systems. Biochimica et Biophysica Acta (BBA) - Biomembranes, 2016. 1858(10): 2441–2450.

Gunnarsson A., Snijder A., Hicks J., Gunnarsson J., Höök F. & Geschwindner S. Drug discovery at the single molecule level: Inhibition-in-solution assay of membrane-reconstituted β-secretase using single-molecule imaging. Analytical Chemistry, 2015. 87(8): 4100–4103.

Guo M., Chandris P., Giannini J.P., Trexler A.J., Fischer R., Chen J., Vishwasrao H.D., Rey-Suarez I., Wu Y., Wu X., Waterman C.M., Patterson G.H., Upadhyaya A., Taraska J.W. & Shroff H. Single-shot super-resolution total internal reflection fluorescence microscopy. Nature Methods, 2018. 15(6): 425–428.

Han X., Holtzman D.M., McKeel D.W., Kelley J. & Morris J.C. Substantial sulfatide deficiency and ceramide elevation in very early Alzheimer's disease: Potential role in disease pathogenesis. Journal of Neurochemistry, 2002. 82(4): 809–818.

Hanson M.A., Cherezov V., Griffith M.T., Roth C.B., Jaakola V.P., Chien E.Y., Velasquez J., Kuhn P. & Stevens R.C. A Specific Cholesterol Binding Site Is Established by the 2.8 Å Structure of the Human β2-Adrenergic Receptor. Structure, 2008. 16(6): 897–905.

Hardy G.J., Nayak R., Munir Alam S., Shapter J.G., Heinrich F. & Zauscher S. Biomimetic supported lipid bilayers with high cholesterol content formed by α-helical peptide-induced vesicle fusion. Journal of Materials Chemistry, 2012. 22(37): 19506–19513.

Hermansson M., Hokynar K. & Somerharju P. Mechanisms of glycerophospholipid homeostasis in mammalian cells. Progress in Lipid Research, 2011. 50(3): 240–257.

Hernandez-Borrell J., Mas F. & Puy J. A theoretical approach to describe monolayer-liposome lipid interaction. Biophysical Chemistry, 1990. 36(1): 47–55.

Heyse S., Vogel H., Sänger M. & Sigrist H. Covalent attachment of functionalized lipid bilayers to planar waveguides for measuring protein binding to biomimetic membranes. Protein Science, 1995. 4(12): 2532–2544.

Higley M.J. & Sabatini B.L. Calcium signaling in dendritic spines. Cold Spring Harbor Perspectives in Biology, 2012. 4(4): a005686.

Hillery A.M., Lloyd A.W. & Swarbrick J. Drug delivery and targeting: for pharmacists and pharmaceutical scientists. CRC press, 2002.

Holopainen M., Colas R.A., Valkonen S., Tigistu-Sahle F., Hyvärinen K., Mazzacuva F., Lehenkari P., Käkelä R., Dalli J., Kerkelä E. & Laitinen S. Polyunsaturated fatty acids modify the extracellular vesicle membranes and increase the production of proresolving lipid mediators of human mesenchymal stromal cells. Biochimica et Biophysica Acta (BBA) - Molecular and Cell Biology of Lipids, 2019. 1864(10): 1350–1362.

Homan R., Esmaeil N., Mendelsohn L. & Kato G.J. A Fluorescence Method to Detect and Quantitate Sterol Esterification by Lecithin: Cholesterol Acyltransferase. Analytical Biochemistry, 2012. 441(1): 80–86.

Homouz D., Perham M., Samiotakis A., Cheung M.S. & Wittung-Stafshede P. Crowded, cell-like environment induces shape changes in aspherical protein. Proceedings of the National Academy of Sciences, 2008. 105(33): 11754–11759.

Honigmann A., Mueller V., Ta H., Schoenle A., Sezgin E., Hell S.W. & Eggeling C. Scanning STED-FCS reveals spatiotemporal heterogeneity of lipid interaction in the plasma membrane of living cells. Nature Communications, 2014. 5(1): 1–12.

Hornykiewicz O. A brief history of levodopa. Journal of Neurology, 2010. 257(2): 249–252.

Howland M.C., Szmodis A.W., Sanii B. & Parikh A.N. Characterization of physical properties of supported phospholipid membranes using imaging ellipsometry at optical wavelengths. Biophysical Journal, 2007. 92(4): 1306–1317.

Huang W. & Levitt D.G. Theoretical calculation of the dielectric constant of a bilayer membrane. Biophysical Journal, 1977. 17(2): 111–128.

Huber W. & Mueller F. Biomolecular interaction analysis in drug discovery using surface plasmon resonance technology. Current Pharmaceutical Design, 2006. 12(31): 3999–4021.

Humpolíčková J., Gielen E., Benda A., Fagulova V., Vercammen J., VandeVen M., Hof M., Ameloot M. & Engelborghs Y. Probing diffusion laws within cellular membranes by Z-scan fluorescence correlation spectroscopy. Biophysical Journal, 2006. 91(3): 23–25.

Hung S.Y. & Fu W.M. Drug candidates in clinical trials for Alzheimer's disease. Journal of Biomedical Science, 2017. 24(1): 1–12.

Hunte C. & Richers S. Lipids and membrane protein structures. Current Opinion in Structural Biology, 2008. 18(4): 406–411.

Hussain G., Wang J., Rasul A., Anwar H., Imran A., Qasim M., Zafar S., Kamran S.K.S., Razzaq A., Aziz N., Ahmad W., Shabbir A., Iqbal J., Baig S.M. & Sun T. Role of cholesterol and sphingolipids in brain development and neurological diseases. Lipids in Health and Disease, 2019. 18(1): 1–12.

Ikonen M., Murtomäki L. & Kontturi K. Microcalorimetric and zeta potential study on binding of drugs on liposomes. Colloids and Surfaces B: Biointerfaces, 2010. 78(2): 275–282.

Isacson O., Brekk O.R. & Hallett P.J. Novel Results and Concepts Emerging From Lipid Cell Biology Relevant to Degenerative Brain Aging and Disease. Frontiers in Neurology, 2019. 10: 1053.

Jackman J.A., Choi J.h., Zhdanov V.P. & Cho N.j. Influence of Osmotic Pressure on Adhesion of Lipid Vesicles to Solid Supports. Langmuir, 2013. 29: 11375–11384.

Jacobson K., Mouritsen O.G. & Anderson R.G. Lipid rafts: At a crossroad between cell biology and physics. Nature Cell Biology, 2007. 9(1): 7–14.

Jafurulla M. & Chattopadhyay A. Membrane Lipids in the Function of Serotonin and Adrenergic Receptors. Current Medicinal Chemistry, 2012. 20(1): 47–55.

Jain M.K. & White H.B. Long-range order in biomembranes. In Advances in lipid research, volume 15, pp. 1–60. Elsevier, 1977.

Javanainen M., Lamberg A., Cwiklik L., Vattulainen I. & Ollila O.S. Atomistic Model for Nearly Quantitative Simulations of Langmuir Monolayers. Langmuir, 2018. 34(7): 2565–2572.

Jeffery D.R. & Roth J.A. Characterization of Membrane-Bound and Soluble Catechol-O-Methyltransferase from Human Frontal Cortex. Journal of Neurochemistry, 1984. 42(3): 826–832.

Jodko-Piorecka K. & Litwinienko G. First experimental evidence of dopamine interactions with negatively charged model biomembranes. ACS Chemical Neuroscience, 2013. 4(7): 1114–1122.

Johnston K.S., Karlsen S.R., Jung C.C. & Yee S.S. New analytical technique for characterization of thin films using surface plasmon resonance. Materials Chemistry & Physics, 1995. 42(4): 242–246.

Jorga K., Fotteler B., Heizmann P. & Gasser R. Metabolism and excretion of tolcapone, a novel inhibitor of catechol-O-methyltransferase. British Journal of Clinical Pharmacology, 1999. 48(4): 513–520.

Jung L.S., Campbell C.T., Chinowsky T.M., Mar M.N. & Yee S.S. Quantitative Interpretation of the Response of Surface Plasmon Resonance Sensors to Adsorbed Films. Langmuir, 1998. 14(17): 5636–5648.

Jurkiewicz P., Cwiklik L., Vojtíšková A., Jungwirth P. & Hof M. Structure, dynamics, and hydration of POPC/POPS bilayers suspended in NaCl, KCl, and CsCl solutions. Biochimica et Biophysica Acta (BBA) - Biomembranes, 2012. 1818(3): 609–616.

Kawatsuki A., ya Morita S., Watanabe N., Hibino E., Mitsuishi Y., Sugi T., Murayama S. & Nishimura M. Lipid class composition of membrane and raft fractions from brains of individuals with Alzheimer's disease. Biochemistry and Biophysics Reports, 2019. 20: 100704.

Kedem O. & Katchalsky A. Thermodynamic analysis of the permeability of biological membranes to non-electrolytes. Biochimica et Biophysica Acta, 1958. 27: 229–246.

Keller C.A., Glasmästar K., Zhdanov V.P. & Kasemo B. Formation of Supported Membranes from Vesicles. Physical Review Letters, 2000. 84(23): 5443–5446.

Keller C.A. & Kasemo B. Surface specific kinetics of lipid vesicle adsorption measured with a quartz crystal microbalance. Biophysical Journal, 1998. 75(3): 1397–1402.

Khabiri M., Roeselova M. & Cwiklik L. Properties of oxidized phospholipid monolayers: An atomistic molecular dynamics study. Chemical Physics Letters, 2012. 519-520: 93–99.

Khandelia H. & Mouritsen O.G. Lipid gymnastics: Evidence of complete acyl chain reversal in oxidized phospholipids from molecular simulations. Biophysical Journal, 2009. 96(7): 2734–2743.

Kinnunen P.K. On the principles of functional ordering in biological membranes. Chemistry and Physics of Lipids, 1991. 57(2-3): 375–399.

Kinnunen P.K., Kaarniranta K. & Mahalka A.K. Protein-oxidized phospholipid interactions in cellular signaling for cell death: From biophysics to clinical correlations. Biochimica et Biophysica Acta - Biomembranes, 2012. 1818(10): 2446–2455.

Kögler M., Itkonen J., Viitala T. & Casteleijn M.G. Assessment of recombinant protein production in E. coli with Time-Gated Surface Enhanced Raman Spectroscopy (TG-SERS). Scientific Reports, 2020. 10(1): 1–11.

Kooyman R.P. Physics of Surface Plasmon Resonance. In Handbook of Surface Plasmon Resonance, chapter 2. Royal Society of Chemistry, 2008.

Koukalová A., Amaro M., Aydogan G., Gröbner G., Williamson P.T., Mikhalyov I., Hof M. & Šachl R. Lipid Driven Nanodomains in Giant Lipid Vesicles are Fluid and Disordered. Scientific Reports, 2017. 7(1): 1–12.

Kučerka N., Gallová J., Uhríková D., Balgavý P., Bulacu M., Marrink S.J. & Katsaras J. Areas of monounsaturated diacylphosphatidylcholines. Biophysical Journal, 2009. 97(7): 1926–1932.

Kučerka N., Heberle F.A., Pan J. & Katsaras J. Structural significance of lipid diversity as studied by small angle neutron and X-ray scattering. Membranes, 2015. 5(3): 454–472.

Kučerka N., Nieh M.P. & Katsaras J. Fluid phase lipid areas and bilayer thicknesses of commonly used phosphatidylcholines as a function of temperature. Biochimica et Biophysica Acta (BBA) - Biomembranes, 2011. 1808(11): 2761–2771.

Kulovesi P., Telenius J., Koivuniemi A., Brezesinski G., Rantamäki A., Viitala T., Puukilainen E., Ritala M., Wiedmer S.K., Vattulainen I. & Holopainen J.M. Molecular organization of the tear fluid lipid layer. Biophysical Journal, 2010. 99(8): 2559–2567.

Lakayan D., Tuppurainen J., Suutari T.E., van Iperen D.J., Somsen G.W. & Kool J. Design and evaluation of a multiplexed angular-scanning surface plasmon resonance system employing line-laser optics and CCD detection in combination with multi-ligand sensor chips. Sensors and Actuators, B: Chemical, 2019. 282: 243–250.

Lane R.M. & Farlow M.R. Lipid homeostasis and apolipoprotein E in the development and progression of Alzheimer's disease. Journal of Lipid Research, 2005. 46(5): 949–968.

Lanzanò L., Scipioni L., Di Bona M., Bianchini P., Bizzarri R., Cardarelli F., Diaspro A. & Vicidomini G. Measurement of nanoscale three-dimensional diffusion in the interior of living cells by STED-FCS. Nature Communications, 2017. 8(1): 1–9.

Lapinski M.M., Castro-Forero A., Greiner A.J., Ofoli R.Y. & Blanchard G.J. Comparison of liposomes formed by sonication and extrusion: Rotational and translational diffusion of an embedded chromophore. Langmuir, 2007. 23(23): 11677–11683.

Lee D.W., Min Y., Dhar P., Ramachandran A., Israelachvili J.N. & Zasadzinski J.A. Relating domain size distribution to line tension and molecular dipole density in model cytoplasmic myelin lipid monolayers. Proceedings of the National Academy of Sciences, 2011. 108(23): 9425–9430.

Lee S.C., Knowles T.J., Postis V.L.G., Jamshad M., Parslow R.A., Lin Y.p., Goldman A., Sridhar P., Overduin M., Muench S.P. & Dafforn T.R. A Method for Detergent-free isolation of Membrane Protein. Nature Protocols, 2016. 11: 1149–1162.

Lee T.H., Heng C., Swann M.J., Gehman J.D., Separovic F. & Aguilar M.I. Real-time quantitative analysis of lipid disordering by aurein 1.2 during membrane adsorption, destabilisation and lysis. Biochimica et Biophysica Acta (BBA) - Biomembranes, 2010. 1798(10): 1977–1986.

Lee T.H., Hirst D.J. & Aguilar M.I. New insights into the molecular mechanisms of biomembrane structural changes and interactions by optical biosensor technology. Biochimica et Biophysica Acta (BBA) - Biomembranes, 2015. 1848(9): 1868–1885.

Lee T.H., Hirst D.J., Kulkarni K., Del Borgo M.P. & Aguilar M.I. Exploring Molecular-Biomembrane Interactions with Surface Plasmon Resonance and Dual Polarization Interferometry Technology: Expanding the Spotlight onto Biomembrane Structure. Chemical Reviews, 2018. 118(11): 5392–5487.

Levental I., Levental K.R. & Heberle F.A. Lipid Rafts: Controversies Resolved, Mysteries Remain. Trends in Cell Biology, 2020. 30(5): 341–353.

Levental K.R. & Levental I. Giant Plasma Membrane Vesicles: Models for Understanding Membrane Organization, volume 75. Elsevier Ltd, 2015.

Liang H., Miranto H., Granqvist N., Sadowski J.W., Viitala T., Wang B. & Yliperttula M. Surface plasmon resonance instrument as a refractometer for liquids and ultrathin films. Sensors and Actuators, B: Chemical, 2010. 149(1): 212–220.

Limbird L.E. & Lefkowitz R.J. Adenylate cyclase-coupled beta adrenergic receptors: effect of membrane lipid-perturbing agents on receptor binding and enzyme stimulation by catecholamines. Molecular Pharmacology, 1976. 12(4): 559–567.

Lipinski C.A., Dominy B.W. & Feeney P.J. Experimental and computational approaches to estimate solubility and permeability in drug discovery and development settings. Advanced Drug Delivery Reviews, 1997. 23(1-3): 3–25.

Liu J.J., Green P., John Mann J., Rapoport S.I. & Sublette M.E. Pathways of polyunsaturated fatty acid utilization: Implications for brain function in neuropsychiatric health and disease. Brain Research, 2015. 1597: 220–246.

London E. Membrane fusion: A new role for lipid domains? Nature Chemical Biology, 2015. 11(6): 383–384.

Longo D.M., Yang Y., Watkins P.B., Howell B.A. & Siler S.Q. Elucidating differences in the hepatotoxic potential of tolcapone and entacapone with DILIsym®, a mechanistic model of drug-induced liver injury. CPT: Pharmacometrics and Systems Pharmacology, 2016. 5(1): 31–39.

Lopes S. & Castanho M. Overview of Common Spectroscopic Methods to Determine the Orientation/Alignment of Membrane Probes and Drugs in Lipidic Bilayers. Current Organic Chemistry, 2005. 9(9): 889–898.

Lotta T., Vidgren J., Tilgmann C., Ulmanen I., Melén K., Julkunen I. & Taskinen J. Kinetics of Human Soluble and Membrane-Bound Catechol O-Methyltransferase: A Revised Mechanism and Description of the Thermolabile Variant of the Enzyme. Biochemistry, 1995. 34(13): 4202–4210.

Lundgren A., Fast B.J., Block S., Agnarsson B., Reimhult E., Gunnarsson A. & Höök F. Affinity Purification and Single-Molecule Analysis of Integral Membrane Proteins from Crude Cell-Membrane Preparations. Nano Letters, 2018. 18(1): 381–385.

Ma Z., Liu H. & Wu B. Structure-based drug design of catechol-O-methyltransferase inhibitors for CNS disorders. British Journal of Clinical Pharmacology, 2014. 77(3): 410–420.

MacGillavry H.D. & Blanpied T.A. Single-Molecule Tracking Photoactivated Localization Microscopy to Map Nano-Scale Structure and Dynamics in Living Spines. Current protocols in neuroscience, 2013. 65(1): 2–20.

Mack F. & Bönisch H. Dissociation constants and lipophilicity of catecholamines and related compounds. Naunyn-Schmiedeberg's Archives of Pharmacology, 1979. 310: 1–9.

Maeki M., Kimura N., Sato Y., Harashima H. & Tokeshi M. Advances in microfluidics for lipid nanoparticles and extracellular vesicles and applications in drug delivery systems. Advanced Drug Delivery Reviews, 2018. 128: 84–100.

Maherani B., Arab-Tehrany E., Rogalska E., Korchowiec B., Kheirolomoom A. & Linder M. Vibrational, calorimetric, and molecular conformational study on calcein interaction with model lipid membrane. Journal of Nanoparticle Research, 2013. 15(7).

Mälkiä A., Murtomäki L., Urtti A. & Kontturi K. Drug permeation in biomembranes. European Journal of Pharmaceutical Sciences, 2004. 23(1): 13–47.

Männistö P.T. & Kaakkola S. Catechol-O-methyltransferase (COMT): biochemistry, molecular biology, pharmacology, and clinical efficacy of the new selective COMT inhibitors. Pharmacological reviews, 1999. 51(4): 593–628.

Mapar M., Jõemetsa S., Pace H., Zhdanov V.P., Agnarsson B. & Höök F. Spatiotemporal Kinetics of Supported Lipid Bilayer Formation on Glass via Vesicle Adsorption and Rupture. Journal of Physical Chemistry Letters, 2018. 9(17): 5143–5149.

Marius P., Alvis S.J., East J.M. & Lee A.G. The interfacial lipid binding site on the potassium channel KcsA is specific for anionic phospholipids. Biophysical Journal, 2005. 89(6): 4081–4089.

Marsh D. Lateral pressure in membranes. Biochimica et Biophysica Acta - Reviews on Biomembranes, 1996. 1286(3): 183–223.

Maser T., Rich M., Hayes D., Zhao P., Nagulapally A.B., Bond J. & Saulnier Sholler G. Tolcapone induces oxidative stress leading to apoptosis and inhibition of tumor growth in Neuroblastoma. Cancer Medicine, 2017. 6(6): 1341–1352.

Mashaghi A., Swann M., Popplewell J., Textor M. & Reimhult E. Optical anisotropy of supported lipid structures probed by waveguide spectroscopy and its application to study of supported lipid bilayer formation kinetics. Analytical Chemistry, 2008. 80(10): 3666–3676.

Mason R.P., Walter M.F. & Mason P.E. Effect of oxidative stress on membrane structure: Small-angle x-ray diffraction analysis. Free Radical Biology and Medicine, 1997. 23(3): 419–425.

Matam Y., Ray B.D. & Petrache H.I. Direct affinity of dopamine to lipid membranes investigated by Nuclear Magnetic Resonance spectroscopy. Neuroscience Letters, 2016. 618: 104–109.

Matos P.M., Franquelim H.G., Castanho M.A. & Santos N.C. Quantitative assessment of peptide-lipid interactions. Ubiquitous fluorescence methodologies. Biochimica et Biophysica Acta (BBA) - Biomembranes, 2010. 1798(11): 1999–2012.

McMahon H.T. & Gallop J.L. Membrane curvature and mechanisms of dynamic cell membrane remodelling. Nature, 2005. 438(7068): 590–596.

McNaught A. & Wilkinson A. (editors). IUPAC. Compendium of Chemical Terminology. Blackwell Scientific Publications, Oxford, Online version (2019-) created by S. J. Chalk, 2. edition, 1997.

Midtvedt D., Olsén E., Höök F. & Jeffries G.D. Label-free spatio-temporal monitoring of cytosolic mass, osmolarity, and volume in living cells. Nature Communications, 2019. 10(1): 1–9.

Miermont A., Waharte F., Hu S., McClean M.N., Bottani S., Léon S. & Hersen P. Severe osmotic compression triggers a slowdown of intracellular signaling, which can be explained by molecular crowding. Proceedings of the National Academy of Sciences, 2013. 110(14): 5725–5730.

Mokkila S., Postila P.A., Rissanen S., Juhola H., Vattulainen I. & Róg T. Calcium Assists Dopamine Release by Preventing Aggregation on the Inner Leaflet of Presynaptic Vesicles. ACS Chemical Neuroscience, 2017. 8(6): 1242–1250.

Monk B.C., Tomasiak T.M., Keniya M.V., Huschmann F.U., Tyndall J.D.A., O'Connell J.D., Cannon R.D., McDonald J.G., Rodriguez A., Finer-Moore J.S. & Stroud R.M. Architecture of a single membrane spanning cytochrome P450 suggests constraints that orient the catalytic domain relative to a bilayer. Proceedings of the National Academy of Sciences, 2014. 111(10): 3865–3870.

Mosca M., Ceglie A. & Ambrosone L. Effect of membrane composition on lipid oxidation in liposomes. Chemistry and Physics of Lipids, 2011. 164(2): 158–165.

Müller T. Catechol-O-methyltransferase inhibitors in Parkinson's disease. Drugs, 2015. 75(2): 157–174.

Myöhänen T.T. & Männistö P.T. Distribution and functions of catechol-O-methyltransferase proteins. Do recent findings change the picture? In International Review of Neurobiology, volume 95, pp. 29–47. Academic Press, 2010.

Nalam P.C., Daikhin L., Espinosa-Marzal R.M., Clasohm J., Urbakh M. & Spencer N.D. Two-Fluid Model for the Interpretation of Quartz Crystal Microbalance Response: Tuning Properties of Polymer Brushes with Solvent Mixtures. The Journal of Physical Chemistry C, 2013. 117(9): 4533–4543.

Nandakumar A., Xing Y., Aranha R.R., Faridi A., Kakinen A., Javed I., Koppel K., Pilkington E.H., Purcell A.W., Davis T.P., Faridi P., Ding F. & Ke P.C. Human Plasma Protein Corona of Aβ Amyloid and Its Impact on Islet Amyloid Polypeptide Cross-Seeding. Biomacromolecules, 2020. 21(2): 988–998.

Nicolson G.L. The Fluid - Mosaic Model of Membrane Structure: Still relevant to understanding the structure, function and dynamics of biological membranes after more than 40 years. Biochimica et Biophysica Acta (BBA) - Biomembranes, 2014. 1838(6): 1451–1466.

Niemelä P.S., Ollila S., Hyvönen M.T., Karttunen M. & Vattulainen I. Assessing the Nature of Lipid Raft Membranes. PLoS computational biology, 2007. 3(2).

Nissinen E., Linden I.B., Schultz E. & Pohto P. Biochemical and pharmacological properties of a peripherally acting catechol-O-methyltransferase inhibitor entacapone. Naunyn-Schmiedeberg's Archives of Pharmacology, 1992. 346(3): 262–266.

O'Brien J.S. & Sampson E.L. Lipid composition of the normal human brain: gray matter, white matter, and myelin. Journal of lipid research, 1965. 6(4): 537–44.

Olanow C.W. & Watkins P.B. Tolcapone: An efficacy and safety review (2007). Clinical Neuropharmacology, 2007. 30(5): 287–294.

Olaru A., Bala C., Jaffrezic-Renault N. & Aboul-Enein H.Y. Surface Plasmon Resonance (SPR) Biosensors in Pharmaceutical Analysis. Critical Reviews in Analytical Chemistry, 2015. 45(2): 97–105.

Oldendorf W.H., Hyman S., Braun L. & Oldendorf S.Z. Blood-brain barrier: penetration of morphine, codeine, heroin, and methadone after carotid injection. Science, 1972. 178(4064): 984–986.

Olsson T., Zhdanov V.P. & Höök F. Total internal reflection fluorescence microscopy for determination of size of individual immobilized vesicles: Theory and experiment. Journal of Applied Physics, 2015. 118(6): 064702.

Orłowski A., Grzybek M., Bunker A., Pasenkiewicz-Gierula M., Vattulainen I., Männistö P.T. & Rõg T. Strong preferences of dopamine and L-dopa towards lipid head group: Importance of lipid composition and implication for neurotransmitter metabolism. Journal of Neurochemistry, 2012. 122(4): 681–690.

Orłowski A., St-Pierre J.F., Magarkar A., Bunker A., Pasenkiewicz-Gierula M., Vattulainen I. & Róg T. Properties of the membrane binding component of catechol-O-methyltransferase revealed by atomistic molecular dynamics simulations. Journal of Physical Chemistry B, 2011. 115(46): 13541–13550.

Osanai H., Ikehara T., Miyauchi S., Shimono K., Tamogami J., Toshifumi N. & Kamo N. A study of the Interaction of drugs with liposomes with isothermal titration calorimetry. Journal of Biophysical Chemistry, 2013. 4(1): 11–21.

Ouberai M.M., Wang J., Swann M.J., Galvagnion C., Guilliams T., Dobson C.M. & Welland M.E. α-Synuclein senses lipid packing defects and induces lateral expansion of lipids leading to membrane remodeling. Journal of Biological Chemistry, 2013. 288(29): 20883–20895.

Pace H., Simonsson Nyström L., Gunnarsson A., Eck E., Monson C., Geschwindner S., Snijder A. & Höök F. Preserved Transmembrane Protein Mobility in Polymer-Supported Lipid Bilayers Derived from Cell Membranes. Analytical Chemistry, 2015. 87(18): 9194–9203.

Palsdottir H. & Hunte C. Lipids in membrane protein structures. Biochimica et Biophysica Acta (BBA) - Biomembranes, 2004. 1666(1-2): 2–18.

Pan J., Cheng X., Sharp M., Ho C.S., Khadka N. & Katsaras J. Structural and mechanical properties of cardiolipin lipid bilayers determined using neutron spin echo, small angle neutron and X-ray scattering, and molecular dynamics simulations. Soft Matter, 2015. 11(1): 130–138.

Pardridge W.M. Blood-brain barrier delivery. Drug Discovery Today, 2007. 12(1-2): 54–61.

Parmar M., Rawson S., Scarff C.A., Goldman A., Dafforn T.R., Muench S.P. & Postis V.L. Using a SMALP platform to determine a sub-nm single particle cryo-EM membrane protein structure. Biochimica et Biophysica Acta (BBA) - Biomembranes, 2018. 1860(2): 378–383.

Parra-Ortiz E., Browning K.L., Damgaard L.S., Nordström R., Micciulla S., Bucciarelli S. & Malmsten M. Effects of oxidation on the physicochemical properties of polyunsaturated lipid membranes. Journal of Colloid and Interface Science, 2019. 538: 404–419.

Patel M.M. & Patel B.M. Crossing the Blood–Brain Barrier: Recent Advances in Drug Delivery to the Brain. CNS Drugs, 2017. 31(2): 109–133.

Pathak P. & London E. Measurement of lipid nanodomain (Raft) formation and size in sphingomyelin/POPC/cholesterol vesicles shows TX-100 and transmembrane helices increase domain size by coalescing preexisting nanodomains but do not induce domain formation. Biophysical Journal, 2011. 101(10): 2417–2425.

Pedro A.Q., Gonçalves A.M., Queiroz J.A. & Passarinha L.A. Purification of Histidine-Tagged Membrane-Bound Catechol-O-Methyltransferase from Detergent-Solubilized Pichia pastoris Membranes. Chromatographia, 2018. 81(3): 425–434.

Pedro A.Q., Pereira P., Bonifácio M.J., Queiroz J.A. & Passarinha L.A. Purification of Membrane-Bound Catechol-O-Methyltransferase by Arginine-Affinity Chromatography. Chromatographia, 2015. 78(21-22): 1339–1348.

Peetla C., Stine A. & Labhasetwar V. Biophysical interactions with model lipid membranes: applications in drug discovery and drug delivery. Molecular Pharmaceutics, 2011. 6(5): 1264–1276.

Peitzsch M., Prejbisz A., Kroiß M., Beuschlein F., Arlt W., Januszewicz A., Siegert G. & Eisenhofer G. Analysis of plasma 3-methoxytyramine, normetanephrine and metanephrine by ultraperformance liquid chromatography-tandem mass spectrometry: Utility for diagnosis of dopamineproducing metastatic phaeochromocytoma. Annals of Clinical Biochemistry, 2013. 50(2): 147–155.

Peterlinz K. & Georgiadis R. Two-color approach for determination of thickness and dielectric constant of thin films using surface plasmon resonance spectroscopy. Optics Communications, 1996. 130(4-6): 260–266.

Petrache H.I., Tristram-Nagle S., Gawrisch K., Harries D., Parsegian V.A. & Nagle J.F. Structure and Fluctuations of Charged Phosphatidylserine Bilayers in the Absence of Salt. Biophysical Journal, 2004. 86(3): 1574–1586.

Petrany M.J. & Millay D.P. Cell Fusion: Merging Membranes and Making Muscle. Trends in Cell Biology, 2019. 29(12): 964–973.

Picconi B., Centonze D., Håkansson K., Bernardi G., Greengard P., Fisone G., Cenci M.A. & Calabresi P. Loss of bidirectional striatal synaptic plasticity in L-DOPA-induced dyskinesia. Nature Neuroscience, 2003. 6(5): 501–506.

Pincet F., Adrien V., Yang R., Delacotte J., Rothman J.E., Urbach W. & Tareste D. FRAP to characterize molecular diffusion and interaction in various membrane environments. PLoS ONE, 2016. 11(7): 1–19.

Pinheiro S.D., Serrão M.P., Silva T., Borges F. & Soares-da Silva P. Pharmacodynamic evaluation of novel Catechol-O-methyltransferase inhibitors. European Journal of Pharmacology, 2019. 847: 53–60.

Posada I.M.D., Busto J.V., Goñi F.M. & Alonso A. Membrane binding and insertion of the predicted transmembrane domain of human scramblase 1. Biochimica et Biophysica Acta (BBA) - Biomembranes, 2014. 1838(1): 388–397.

Postila P.A., Vattulainen I. & Róg T. Selective effect of cell membrane on synaptic neurotransmission. Scientific Reports, 2016. 6: 19345.

Powers J.M., Tummons R.C., Moser A.B., Moser H.W., Huff D.S. & Kelley R.I. Neuronal lipidosis and neuroaxonal dystrophy in cerebro-hepato-renal (Zellweger) syndrome. Acta Neuropathologica, 1987. 73(4): 333–343.

Przybylo M., Sýkora J., Humpolíčová J., Benda A., Zan A. & Hof M. Lipid diffusion in giant unilamellar vesicles is more than 2 times faster than in supported phospholipid bilayers under identical conditions. Langmuir, 2006. 22(22): 9096–9099.

Quek C. & Hill A.F. The role of extracellular vesicles in neurodegenerative diseases. Biochemical and Biophysical Research Communications, 2017. 483(4): 1178–1186.

Raimúndez-Rodríguez E.A., Losada-Barreiro S. & Bravo-Díaz C. Enhancing the fraction of antioxidants at the interfaces of oil-in-water emulsions: A kinetic and thermodynamic analysis of their partitioning. Journal of Colloid and Interface Science, 2019. 555: 224–233.

Rasmussen S.G., Choi H.J., Rosenbaum D.M., Kobilka T.S., Thian F.S., Edwards P.C., Burghammer M., Ratnala V.R., Sanishvili R., Fischetti R.F., Schertler G.F., Weis W.I. & Kobilka B.K. Crystal structure of the human β2 adrenergic G-protein-coupled receptor. Nature, 2007. 450(7168): 383–387.

Rauch C. & Farge E. Endocytosis switch controlled by transmembrane osmotic pressure and phospholipid number asymmetry. Biophysical Journal, 2000. 78(6): 3036–3047.

Ravenstijn P.G., Drenth H.J., O'Neill M.J., Danhof M. & de Lange E.C. Evaluation of blood-brain barrier transport and CNS drug metabolism in diseased and control brain after intravenous L-DOPA in a unilateral rat model of Parkinson's disease. Fluids and Barriers of the CNS, 2012. 9(1): 4.

Rawicz W., Olbrich K.C., McIntosh T., Needham D. & Evans E.A. Effect of chain length and unsaturation on elasticity of lipid bilayers. Biophysical Journal, 2000. 79(1): 328–339.

Reimhult E., Larsson C., Kasemo B. & Höök F. Simultaneous surface plasmon resonance and quartz crystal microbalance with dissipation monitoring measurements of biomolecular adsorption events involving structural transformations and variations in coupled water. Analytical Chemistry, 2004. 76(24): 7211–7220.

Reimhult E., Merz C., Ye Q. & Textor M. Novel surface architectures for biomimetic lipid membranes. In NSTI-Nanotech, volume 2, pp. 688–691. The Nano Science and Technology Institute, 2007.

Reimhult E., Zäch M., Höök F. & Kasemo B. A multitechnique study of liposome adsorption on Au and lipid bilayer formation on SiO2. Langmuir, 2006. 22(7): 3313–3319.

Richter R.P. & Brisson A.R. Following the formation of supported lipid bilayers on Mica: A study combining AFM, QCM-D, and ellipsometry. Biophysical Journal, 2005. 88(5): 3422–3433.

Riedlová K., Nekardová M., Kačer P., Syslová K., Vazdar M., Jungwirth P., Kudová E. & Cwiklik L. Distributions of therapeutically promising neurosteroids in cellular membranes. Chemistry and Physics of Lipids, 2017. 203: 78–86.

Rinia H.A., Snel M.M., van der Eerden J.P. & de Kruijff B. Visualizing detergent resistant domains in model membranes with atomic force microscopy. FEBS Letters, 2001. 501(1): 92–96.

Robinson R.G., Smith S.M., Wolkenberg S.E., Kandebo M., Yao L., Gibson C.R., Harrison S.T., Polsky-Fisher S., Barrow J.C., Manley P.J., Mulhearn J.J., Nanda K.K., Schubert J.W., Trotter B.W., Zhao Z., Sanders J.M., Smith R.F., McLoughlin D., Sharma S., Hall D.L., Walker T.L., Kershner J.L., Bhandari

N., Hutson P.H. & Sachs N.A. Characterization of non-nitrocatechol pan and isoform specific catechol-O-methyltransferase inhibitors and substrates. ACS Chemical Neuroscience, 2012. 3(2): 129–140.

Rodahl M. & Kasemo B. Frequency and dissipation-factor responses to localized liquid deposits on a QCM electrode. Sensors and Actuators, B: Chemical, 1996. 37(1-2): 111–116.

Rodríguez-Espigares I., Kaczor A.A., Stepniewski T.M. & Selent J. Computational Methods for GPCR Drug Discovery. Methods in Molecular Biology, 2018. 1705: 321–334.

Rothman J.E., Dawidowicz E.A., Lenard J. & Tsai D.K. Transbilayer Phospholipid Asymmetry and Its Maintenance in the Membrane of Influenza Virus. Biochemistry, 1976. 15(11): 2361–2370.

Rouser G., Galli C. & Kritchevsky G. Lipid class composition of normal human brain and variations in metachromatic leucodystrophy, Tay-Sachs, Niemann-Pick, chronic Gaucher's and Alzheimer's diseases. Journal of the American Oil Chemists' Society, 1965. 42(5): 404–410.

Roux M. & Bloom M. Calcium, magnesium, lithium, sodium, and potassium distributions in the headgroup region of binary membranes of phosphatidylcholine and phosphatidylserine as seen by deuterium NMR. Biochemistry, 2005. 29(30): 7077–7089.

Ruipérez V., Darios F. & Davletov B. Alpha-synuclein, lipids and Parkinson's disease. Progress in Lipid Research, 2010. 49(4): 420–428.

Rupert D.L., Lässer C., Eldh M., Block S., Zhdanov V.P., Lotvall J.O., Bally M. & Höök F. Determination of exosome concentration in solution using surface plasmon resonance spectroscopy. Analytical Chemistry, 2014. 86(12): 5929–5936.

Rupert D.L., Mapar M., Shelke G.V., Norling K., Elmeskog M., Lötvall J.O., Block S., Bally M., Agnarsson B. & Höök F. Effective Refractive Index and Lipid Content of Extracellular Vesicles Revealed Using Optical Waveguide Scattering and Fluorescence Microscopy. Langmuir, 2018. 34(29): 8522–8531.

Rupert D.L.M., Shelke G.V., Emilsson G., Claudio V., Block S., Lässer C., Dahlin A., Lötvall J.O., Bally M., Zhdanov V.P. & Höök F. Dual-Wavelength Surface Plasmon Resonance for Determining the Size and Concentration of Sub-Populations of Extracellular Vesicles. Analytical Chemistry, 2016. 88(20): 9980–9988.

Rusu E.D. Mass transport with enzyme reactions. Acta Mechanica, 1998. 127(1-4): 183–191.

Rutherford K., Alphandéry E., McMillan A., Daggett V. & Parson W.W. The V108M mutation decreases the structural stability of catechol O-methyltransferase. Biochimica et Biophysica Acta (BBA) - Proteins and Proteomics, 2008. 1784(7-8): 1098–1105.

Saari H., Lázaro-Ibáñez E., Viitala T., Vuorimaa-Laukkanen E., Siljander P. & Yliperttula M. Microvesicle- and exosome-mediated drug delivery enhances the cytotoxicity of Paclitaxel in autologous prostate cancer cells. Journal of Controlled Release, 2015. 220: 727–737.

Sakai H., Sou K., Horinouchi H., Kobayashi K. & Tsuchida E. Review of hemoglobin-vesicles as artificial oxygen carriers. Artificial Organs, 2009. 33(2): 139–145.

Salamon Z., Brown M.F. & Tollin G. Plasmon resonance spectroscopy: probing molecular interactions within membranes. Trends in biochemical sciences, 1999. 24(6): 213–219.

Salamon Z. & Tollin G. Optical anisotropy in lipid bilayer membranes: Coupled plasmon-waveguide resonance measurements of molecular orientation, polarizability, and shape. Biophysical Journal, 2001. 80(3): 1557–1567.

Salamon Z., Wang Y., Soulages J.L., Brown M.F. & Tollin G. Surface plasmon resonance spectroscopy studies of membrane proteins: Transducin binding and activation by rhodopsin monitored in thin membrane films. Biophysical Journal, 1996. 71(1): 283–294.

Saliba A.E., Vonkova I. & Gavin A.C. The systematic analysis of protein–lipid interactions comes of age. Nature Reviews Molecular Cell Biology, 2015. 16(12): 753–761.

Schneider F., Waithe D., Clausen M.P., Galiani S., Koller T., Ozhan G., Eggeling C. & Sezgin E. Diffusion of lipids and GPI-anchored proteins in actin-free plasma membrane vesicles measured by STED-FCS. Molecular Biology of the Cell, 2017. 28(11): 1507–1518.

Schott B.H., Frischknecht R., Debska-Vielhaber G., John N., Behnisch G., Düzel E., Gundelfinger E.D. & Seidenbecher C.I. Membrane-bound catechol-O-methyl transferase in cortical neurons and glial cells is intracellularly oriented. Frontiers in Psychiatry, 2010. 1: 142.

Seddon A.M., Casey D., Law R.V., Gee A., Templer R.H. & Ces O. Drug interactions with lipid membranes. Chemical Society Reviews, 2009. 38(9): 2509–2519.

Seddon A.M., Curnow P. & Booth P.J. Membrane proteins, lipids and detergents: not just a soap opera. Biochimica et Biophysica Acta, 2004. 1666: 105–117.

Seelig J. Thermodynamics of lipid-peptide interactions. Biochimica et Biophysica Acta (BBA) - Biomembranes, 2004. 1666(1-2): 40–50.

Seu K.J., Pandey A.P., Haque F., Proctor E.A., Ribbe A.E. & Hovis J.S. Effect of surface treatment on diffusion and domain formation in supported lipid bilayers. Biophysical Journal, 2007. 92(7): 2445–2450.

Sezgin E., Levental I., Mayor S. & Eggeling C. The mystery of membrane organization: Composition, regulation and roles of lipid rafts. Nature Reviews Molecular Cell Biology, 2017. 18(6): 361–374.

Sezgin E., Schneider F., Galiani S., Urbančič I., Waithe D., Lagerholm B.C. & Eggeling C. Measuring nanoscale diffusion dynamics in cellular membranes with super-resolution STED–FCS. Nature Protocols, 2019. 14(4): 1054–1083.

Shamim A., Mahmood T., Ahsan F., Kumar A. & Bagga P. Lipids: An insight into the neurodegenerative disorders. Clinical Nutrition Experimental, 2018. 20: 1–19.

Sharon R., Bar-Joseph I., Frosch M.P., Walsh D.M., Hamilton J.A. & Selkoe D.J. The formation of highly soluble oligomers of α-synuclein is regulated by fatty acids and enhanced in Parkinson's disease. Neuron, 2003. 37(4): 583–595.

Shiraishi Y., Natsume M., Kofuku Y., Imai S., Nakata K., Mizukoshi T., Ueda T., Iwaï H. & Shimada I. Phosphorylation-induced conformation of β2-adrenoceptor related to arrestin recruitment revealed by NMR. Nature Communications, 2018. 9(1): 1–10.

Silva T., Mohamed T., Shakeri A., Rao P.P., Martínez-Gonzalez L., Pérez D.I., Martínez A., Valente M.J., Garrido J., Uriarte E., Serrão P., Soares-Da-silva P., Remião F. & Borges F. Development of blood-brain barrier permeable nitrocatechol-based catechol O-methyltransferase inhibitors with reduced potential for hepatotoxicity. Journal of Medicinal Chemistry, 2016. 59(16): 7584–7597.

Simeonov A. & Davis M.I. Interference with Fluorescence and Absorbance. In Assay Guidance Manual, pp. 1–13. Eli Lilly & Company and the National Center for Advancing Translational Sciences, 2015.

Simeonov P., Werner S., Haupt C., Tanabe M. & Bacia K. Membrane protein reconstitution into liposomes guided by dual-color fluorescence cross-correlation spectroscopy. Biophysical Chemistry, 2013. 184: 37–43.

Simons K. & Ikonen E. Functional rafts in cell membranes. Nature, 1997. 387(6633): 569–572.

Simonsson L. & Höök F. Formation and diffusivity characterization of supported lipid bilayers with complex lipid compositions. Langmuir, 2012. 28(28): 10528–10533.

Singer S. & Nicolson G.L. The fluid mosaic model of the structure of cell membranes. Journal of Chemical Information and Modeling, 1972. 175(4023): 720–731.

Söderlund T., Alakoskela J.M.I., Pakkanen A.L. & Kinnunen P.K. Comparison of the effects of surface tension and osmotic pressure on the interfacial hydration of a fluid phospholipid bilayer. Biophysical Journal, 2003. 85(4): 2333–2341.

Somerharju P., Virtanen J.A., Cheng K.H. & Hermansson M. The superlattice model of lateral organization of membranes and its implications on membrane lipid homeostasis. Biochimica et Biophysica Acta (BBA) - Biomembranes, 2009. 1788(1): 12–23.

Sotnikova T.D., Beaulieu J.M., Espinoza S., Masri B., Zhang X., Salahpour A., Barak L.S., Caron M.G. & Gainetdinov R.R. The dopamine metabolite 3-methoxytyramine is a neuromodulator. PLoS ONE, 2010. 5(10).

Štefl M., Šachl R., Olzyńska A., Amaro M., Savchenko D., Deyneka A., Hermetter A., Cwiklik L., Humpolíčková J. & Hof M. Comprehensive portrait of cholesterol containing oxidized membrane. Biochimica et Biophysica Acta (BBA) - Biomembranes, 2014. 1838(7): 1769–1776.

Sterling S.M., Allgeyer E.S., Fick J., Prudovsky I., Mason M.D. & Neivandt D.J. Phospholipid Diffusion Coefficients of Cushioned Model Membranes determined via Z-Scan Fluorescence Correlation Spectroscopy. Langmuir, 2013. 29(25): 7966–7974.

Stone M.B., Shelby S.A., Núñez M.F., Wisser K. & Veatch S.L. Protein sorting by lipid phase-like domains supports emergent signaling function in B lymphocyte plasma membranes. eLife, 2017. 6: 1–33.

Svarcbahs R., Julku U.H. & Myöhänen T.T. Inhibition of prolyl oligopeptidase restores spontaneous motor behavior in the α-synuclein virus vector-based Parkinson's disease mouse model by decreasing α-synuclein oligomeric species in mouse brain. Journal of Neuroscience, 2016. 36(49): 12485–12497.

Swaminath G., Deupi X., Lee T.W., Zhu W., Thian F.S., Kobilka T.S. & Kobilka B. Probing the $\beta 2$ adrenoceptor binding site with catechol reveals differences in binding and activation by agonists and partial agonists. Journal of Biological Chemistry, 2005. 280(23): 22165–22171.

Swann M.J., Peel L.L., Carrington S. & Freeman N.J. Dual-polarization interferometry: An analytical technique to measure changes in protein structure in real time, to determine the stoichiometry of binding events, and to differentiate between specific and nonspecific interactions. Analytical Biochemistry, 2004. 329(2): 190–198.

Swanson P.D., Harvey F.H. & Stahl W.L. Subcellular Fractionation of Postmortem Brain. Journal of Neurochemistry, 1973. 20(2): 465–475.

Szoka Jr. F. & Papahadjopoulos D. Comparative properties and methods of preparation of lipid vesicles (liposomes). Annual review of biophysics and bioengineering, 1980. 9(1): 467–508.

Tamm L.K. & McConnell H.M. Supported Phospholipid Bilayers. Biophysical Journal, 1985. 47(1): 105–113.

Tang C.Y. & Allen H.C. Ionic binding of Na+ versus K+ to the carboxylic acid headgroup of palmitic acid monolayers studied by vibrational sum frequency generation spectroscopy. Journal of Physical Chemistry A, 2009. 113(26): 7383–7393.

The Uniprot Consortium. UniProtKB - P21964 (COMT_HUMAN). https://www.uniprot.org/uniprot/P21964 (Date accessed 24.5.2020), 2020.

Tulodziecka K., Diaz-Rohrer B.B., Farley M.M., Chan R.B., Paolo G.D., Levental K.R., Neal Waxham M. & Levental I. Remodeling of the postsynaptic plasma membrane during neural development. Molecular Biology of the Cell, 2016. 27(22): 3480–3489.

Ullrich S.J., Hellmich U.A., Ullrich S. & Glaubitz C. Interfacial enzyme kinetics of a membrane bound kinase analyzed by real-time MAS-NMR. Nature Chemical Biology, 2011. 7(5): 263–270.

van de Weert M. & Stella L. Fluorescence quenching and ligand binding: A critical discussion of a popular methodology. Journal of Molecular Structure, 2011. 998(1-3): 144–150.

van der Pol E., Böing A.N., Harrison P., Sturk A. & Nieuwland R. Classification, functions, and clinical relevance of extracellular vesicles. Pharmacological Reviews, 2012. 64(3): 676–705.

van Meer G. Cellular lipidomics. EMBO Journal, 2005. 24(18): 3159–3165.

van Meer G., Voelker D.R. & Feigenson G.W. Membrane lipids: where they are and how they behave. Nature Reviews Molecular Cell Biology, 2008. 9(2): 112–124.

Vance D.E. & Vance J.E. Physiological consequences of disruption of mammalian phospholipid biosynthetic genes. Journal of Lipid Research, 2009. 50(Supplement): S132–S137.

Veatch S.L., Cicuta P., Sengupta P., Honerkamp-Smith A., Holowka D. & Baird B. Critical fluctuations in plasma membrane vesicles. ACS Chemical Biology, 2008. 3(5): 287–293.

Verger R., Mieras M.C.E. & De Haas G.H. Action of phospholipase A at interfaces. Journal of Biological Chemistry, 1973. 248(11): 4023–4034.

Viitala T., Liang H., Gupta M., Zwinger T., Yliperttula M. & Bunker A. Fluid dynamics modeling for synchronizing surface plasmon resonance and quartz crystal microbalance as tools for biomolecular and targeted drug delivery studies. Journal of Colloid and Interface Science, 2012. 378(1): 251–259.

Vinklárek I.S., Vel'As L., Riegerová P., Skála K., Mikhalyov I., Gretskaya N., Hof M. & Šachl R. Experimental Evidence of the Existence of Interleaflet Coupled Nanodomains: An MC-FRET Study. Journal of Physical Chemistry Letters, 2019. 10(9): 2024–2030.

Voinova M.V., Rodahl M., Jonson M. & Kasemo B. Viscoelastic acoustic response of layered polymer films at fluid-solid interfaces: Continuum mechanics approach. Physica Scripta, 1998. 59(5): 391.

Volinsky R., Cwiklik L., Jurkiewicz P., Hof M., Jungwirth P. & Kinnunen P.K. Oxidized phosphatidylcholines facilitate phospholipid flip-flop in liposomes. Biophysical Journal, 2011. 101(6): 1376–1384.

Volinsky R. & Kinnunen P.K. Oxidized phosphatidylcholines in membrane-level cellular signaling: From biophysics to physiology and molecular pathology. FEBS Journal, 2013. 280(12): 2806–2816.

Volinsky R., Paananen R. & Kinnunen P.K. Oxidized phosphatidylcholines promote phase separation of cholesterol-sphingomyelin domains. Biophysical Journal, 2012. 103(2): 247–254.

Wallgren M., Beranova L., Pham Q.D., Linh K., Lidman M., Procek J., Cyprych K., Kinnunen P.K., Hof M. & Gröbner G. Impact of oxidized phospholipids on the structural and dynamic organization of phospholipid membranes: A combined DSC and solid state NMR study. Faraday Discussions, 2012. 161: 499–513.

Wang J., Lin W., Cao E., Xu X., Liang W. & Zhang X. Surface plasmon resonance sensors on Raman and fluorescence spectroscopy. Sensors, 2017. 17(12): 1–19.

Wang S., Zhang S., Liou L.C., Ren Q., Zhang Z., Caldwell G.A., Caldwell K.A. & Witt S.N. Phosphatidylethanolamine deficiency disrupts α-synuclein homeostasis in yeast and worm models of Parkinson disease. Proceedings of the National Academy of Sciences, 2014. 111(38): E3976–E3985.

Wang X. & Quinn P.J. The location and function of vitamin E in membranes (Review). Molecular Membrane Biology, 2000. 17(3): 143–156.

Watts A. Solid-state NMR in drug design and discovery for membrane-embedded targets. Nature Reviews Drug Discovery, 2005. 4(7): 555–568.

Wenstrup D., Ehman W.D. & Markesbery W.R. Trace element imbalances in isolated subcellular fractions of Alzheimer's disease brains. Brain Research, 1990. 533(1): 125–131.

Widengren J., Mets Ü. & Rigler R. Fluorescence correlation spectroscopy of triplet states in solution: A theoretical and experimental study. Journal of Physical Chemistry, 1995. 99(36): 13368–13379.

Wiedmann T.S., Pates R.D., Beach J.M., Salmon A. & Brown M.F. Lipid-Protein Interactions Mediate the Photochemical Function of Rhodopsin. Biochemistry, 1988. 27(17): 6469–6474.

Williams-Gray C.H., Hampshire A., Barker R.A. & Owen A.M. Attentional control in Parkinson's disease is dependent on COMT val158met genotype. Brain, 2008. 131(2): 397–408.

Wong-ekkabut J., Xu Z., Triampo W., Tang I.M., Tieleman D.P. & Monticelli L. Effect of lipid peroxidation on the properties of lipid bilayers: A molecular dynamics study. Biophysical Journal, 2007. 93(12): 4225–4236.

Wood P.L. Lipidomics of Alzheimer's disease: Current status. Alzheimer's Research and Therapy, 2012. 4(1): 1–10.

Yamamoto E., Akimoto T., Kalli A.C., Yasuoka K. & Sansom M.S. Dynamic interactions between a membrane binding protein and lipids induce fluctuating diffusivity. Science Advances, 2017. 3(1): 1–7.

Yang S.T.T., Kiessling V., Simmons J.A., White J.M. & Tamm L.K. HIV gp41-mediated membrane fusion occurs at edges of cholesterol-rich lipid domains. Nature Chemical Biology, 2015. 11(6): 424–431.

Ye Q., Konradi R., Textor M. & Reimhult E. Liposomes tethered to omega-functional PEG brushes and induced formation of PEG brush supported planar lipid bilayers. Langmuir, 2009. 25(23): 13534–13539.

Yin H. & Flynn A.D. Drugging Membrane Protein Interactions. Annual Review of Biomedical Engineering, 2016. 18(1): 51–76.

Yıldırım M.A., Goh K.I., Cusick M.E., Barabási A.L. & Vidal M. Drug—target network. Nature Biotechnology, 2007. 25(10): 1119–1126.

Yonkunas M. & Kurnikova M. The Hydrophobic Effect Contributes to the Closed State of a Simplified Ion Channel through a Conserved Hydrophobic Patch at the Pore-Helix Crossing. Frontiers in Pharmacology, 2015. 6: 284.

Zhang Z., Guan J., Jiang Z., Yang Y., Liu J., Hua W., Mao Y., Li C., Lu W., Qian J. & Zhan C. Brain-targeted drug delivery by manipulating protein corona functions. Nature Communications, 2019. 10(1).

Zhao Q. & Wu B.L. Ice breaking in GPCR structural biology. Acta Pharmacologica Sinica, 2012. 33(3): 324–334.

Zhou M., Otomo A., Yokoyama S. & Mashiko S. Estimation of organic molecular film structures using surface-plasmon resonance spectroscopy. Thin Solid Films, 2001. 393(1-2): 114–118.

Zotter A., Bäuerle F., Dey D., Kiss V. & Schreiber G. Quantifying enzyme activity in living cells. Journal of Biological Chemistry, 2017. 292(38): 15838–15848.